

University of Alberta

**Accelerated Dewatering of Oil Sands Tailings by Microbially Induced
Chemical Changes**

by

Nicholas Patrick Arkell

A thesis submitted to the Faculty of Graduate Studies and Research
in partial fulfillment of the requirements for the degree of

Master of Science

in

Land Reclamation and Remediation

Department of Renewable Resources

©Nicholas Patrick Arkell

Fall 2012

Edmonton, Alberta

Permission is hereby granted to the University of Alberta Libraries to reproduce single copies of this thesis and to lend or sell such copies for private, scholarly or scientific research purposes only. Where the thesis is converted to, or otherwise made available in digital form, the University of Alberta will advise potential users of the thesis of these terms.

The author reserves all other publication and other rights in association with the copyright in the thesis and, except as herein before provided, neither the thesis nor any substantial portion thereof may be printed or otherwise reproduced in any material form whatsoever without the author's prior written permission.

Abstract

Processing of oil sands ores to extract bitumen generates large volumes of tailings which are deposited into large settling basins, where the solids settle by gravity over 3-4 years to become mature fine tailings (MFT). Methanogenesis has been correlated with increased water recovery from and densification of MFT. This phenomenon offers potential tailings management options, including biodensification, an accelerated dewatering process where the microbial community is stimulated by amending MFT with carbon-substrates. The chemistry of methanogenic accelerated dewatering was investigated with 2L and 50L settling columns of MFT amended with carbon-substrates to infer possible mechanisms. It was found that enhanced biogenic gas production induced chemical changes in MFT. The carbon-amended MFT had increased pore-water concentrations of HCO_3^- , Ca^{2+} , Mg^{2+} and a lower pH. The pore-water chemistry affects the colloidal properties of the suspended clays in the MFT which leads to the accelerated settling of clay particles and dewatering of MFT.

Acknowledgements

I would like to thank Dr. Tariq Siddique for his time and patience with me along with Dr. Alsu Kuznetsova and Dr. Petr Kuznetsov for their support and insight. Thank you to AWRI Biodensification group, Dr. Julia Foght, Dr. Selma Guigard, Dr. Rajender Gupta, Carmen Li, Rozlyn Young, Saba Roozbahani, Kathy Semple, Arun Samanta, Eleisha Underwood and Dr. Abroise Itika. Thank you to support staff which made this work possible, Jela Burkus, Jim Skarok, Allan Harms and Jean Xi.

Table of Contents

1	Introduction.....	1
1.1	Rationale.....	1
1.2	Statement Of Objectives.....	3
2	Background.....	5
2.1	Oil Sands Industry.....	5
2.1.1	Introduction.....	5
2.1.2	Oil Sands Processing.....	5
2.1.3	Oil Sands Tailings.....	7
2.1.4	Management of Tailings.....	8
2.2	Properties of MFT.....	9
2.2.1	Composition of MFT.....	9
2.2.2	Mineralogy of MFT.....	9
2.2.2.1	Cation Exchange Capacity.....	12
2.2.2.2	Exchangeable Cations.....	12
2.2.2.3	Diffuse Double Layer.....	13
2.2.3	Pore-Water Chemistry of MFT.....	15
2.2.4	Microbial Communities In MFT and Methanogenesis.....	16
2.3	Methanogenic Accelerated Dewatering.....	20
2.4	Chemical Pathway For Accelerated Dewatering.....	24
3	Materials And Methods.....	26
3.1	Summary of Experiments.....	26
3.1.1	Processing of MFT Samples.....	26
3.2	Experiment 1: 2L Settling Columns.....	26
3.2.1	Experimental Design.....	26
3.2.2	MFT Preparation and Time Zero Analysis.....	27
3.2.3	Procedure for Filling Columns.....	28

3.2.4	Incubation and Monitoring	28
3.2.5	Column Sacrificing and Sampling	29
3.2.6	2L Columns: Methods of Physical and Chemical Analysis.....	31
3.2.6.1	Measuring Water Release and Settling of Tailings.....	31
3.2.6.2	MFT Moisture Percentage and Density	32
3.2.6.3	<i>In Situ</i> Measurement of pH.....	33
3.2.6.4	Separation of Pore-Water from MFT.....	33
3.2.6.5	Measurement of Eh.....	33
3.2.6.6	Elemental Analyses By ICP-MS.....	33
3.2.6.7	Determination of Anions By Ion Chromatography And Colorimetry	34
3.2.6.8	Determination of Pore-Water HCO_3^-	35
3.2.6.9	Determination of Exchangeable Cations	35
3.3	Experiment 1: 50L Settling Columns	37
3.3.1	Experimental Design.....	37
3.3.2	Constructions of the Columns	38
3.3.3	MFT Preparation, Filling Procedure and Final Assembly.....	39
3.3.4	Incubation and Monitoring	40
3.3.5	Procedure for MFT Sampling	41
3.3.6	45l Columns: Methods of Physical and Chemical Analysis	41
3.3.6.1	Oil-Water-Solid Content by Dean-Stark Method	41
3.3.6.2	Particle Size Distribution	42
3.3.6.3	<i>In Situ</i> Measurement of pH.....	43
3.3.6.4	Determination of Cations By Atomic Absorption Spectroscopy.....	43
3.3.6.5	Determination of Headspace Gases in 50L Columns	43
3.3.6.6	Determination of Carbonate Minerals in MFT	45
4	Results.....	46
4.1	2L Settling Columns	46
4.1.1	Water Release, Settling and Densification of MFT	46
4.1.2	pH Change in 2L Columns	49

4.1.3	Eh Change in 2L Columns.....	52
4.1.4	Pore-Water HCO_3^- in 2L Columns.....	53
4.1.5	Pore-Water Cations in 2L Columns.....	54
4.1.6	Exchangeable Cations in 2L Columns.....	58
4.1.7	Chemical Analysis of Release Cap-Water in 2L Columns.....	62
4.2	50L Settling Columns.....	62
4.2.1	Gas Production In 50L Columns.....	63
4.2.2	Water Release And Settling Of MFT In 50L Columns.....	64
4.2.3	Ph Change In 50L Columns.....	67
4.2.3	HCO_3^- , SO_4^{2-} And Cl^- In 50L Columns.....	68
4.2.5	Pore-Water Cations In 50L Columns.....	70
4.2.6	MFT Solids Carbonate Content In 50L Columns.....	73
5	Discussion.....	74
5.1	Water Release and Settling.....	74
5.2	Chemical Changes.....	75
5.2.1	Biogenic Gas Production.....	75
5.2.2	Pore-Water HCO_3^- And pH.....	77
5.2.3	Pore-Water Cations and Carbonate Minerals.....	79
5.2.4	Exchangeable Cations.....	80
5.2.5	Double Diffuse Layer and Water Release.....	83
5.3	Evaluation of Chemical Pathway to Accelerated Dewatering.....	88
6	Conclusion.....	91
7	References.....	94
	Appendix A.....	99
	Appendix B.....	102
	Appendix C.....	120

LIST OF TABLES

Table 2-1. Composition of clay minerals in Syncrude MFT clay fractions (<2.0 μm).	10
Table 2-2. Structure and properties of clay groups important in MFT, adapted from (Kaminski 2008) and (Mitchel 1976)	11
Table 3-1. Summary of settling column experiment	26
Table 3-2. Experimental layout of 2L settling columns filled with Syncrude MFT. Seven columns for each treatment U1-U7 and A1-A7 were established. Treatments comprised of ~1400 mg L ⁻¹ sodium acetate and unamended control. Incubation times for the different columns are indicated in the table..	27

List of Figures

Figure 2-1. Simplified Diagram of reactions performed by bacteria depending on redox potential of the environment in marine sediments (Burdige 1993).....	16
Figure 2-2. Proposed methanogenic hydrocarbon degradation pathway in oil sands tailing. (Adopted from Siddique et al. 2011).....	19
Figure 2-3. Water released from amended and unamended MFT in 2L settling columns. Water release is given in percentage of initial pore-water. MFT are from Syncrude, Shell Albian and Suncor tailings ponds. Unpublished data from group study.	22
Figure 2-4. Bicarbonate concentrations in MFT in 2L settling columns. MFT are from Syncrude, Shell Albian and Suncor. Error bars are calculated using S.E., n=3. Analysis of Syncrude samples provided by Syncrude. There was no Whey column performed for Shell Albian MFT. Unpublished data from group study	23
Figure 2-5. Hypothesized chemical pathway for accelerated dewatering during methanogenesis.	24
Figure 3-1. Sampling locations of 2L settling columns at time of decommissioning.....	30
Figure 3-2. Final setup of the 50L columns, UM (right) and C (left). Features of apparatus are labeled: (A) pH ports, (B) GS-MS. (C) gas trap, (D) pressure transducers. (E) pressure reading unit, (F) Measuring Tape, and (G) Containment tub.	39
Figure 4-1. Water release from 2L settling columns of Syncrude MFT. Water release is calculated in volumetric percentage of the initial pore-water contents. Error bars show standard error (S.E.); days 0-21 n=5, days 22-42 n=4, days 43-82 n=3.....	47
Figure 4-2. Settling of 2L settling columns of Syncrude MFT. Settling is reported as a decrease in solids-cap water interface in cm from initial height. Error bars represent S.E.; days 0-21 n=5, days 22-42 n=4, days 43-82 n=3.....	48
Figure 4-3. 2L settling columns of Syncrude MFT after 82 days of incubation. Unamended (left) Acetate amended (right).....	49
Figure 4-4. pH of 2L settling columns of Syncrude MFT by treatment during 82 days of incubation. Error bars show S.E., n=2.....	50

Figure 4-5. pH of 2L settling columns of Syncrude MFT by treatment and incubation time. Error bars show S.E.; n=2 for Initial, 21 d and 42 d, and n=6 for 82 d. (A) signifies a significant difference between the treatments (B), (b) signifies a significant difference within a treatment from initial values (a), and (*) signifies a significant difference between top and bottom values.	51
Figure 4-6. Eh of 2L settling columns of Syncrude MFT by treatment and incubation time. Error bars show S.E.; n=2 for Initial, 21 d and 42 d, and n=6 for 82 d. (A) signifies a significant difference between the treatments (B), (b) signifies a significant difference within a treatment from initial values (a), and (*) signifies a significant difference between top and bottom values..	52
Figure 4-7. Pore-water HCO_3^- of 2L settling columns of Syncrude MFT by treatment and incubation time. Error bars show S.E.; n=2 for Initial, 21 d, and 42 d, and n=6 for 82 d. (A) signifies a significant difference between the treatments (B), (b) signifies a significant difference within a treatment from initial values (a), and (*) signifies a significant difference between top and bottom values.	53
Figure 4-8. Pore-water Ca^{2+} of 2L settling columns of Syncrude MFT by treatment and incubation time. Error bars show S.E.; n=2 for Initial, 21 d, and 42 d, and n=6 for 82 d. (A) signifies a significant difference between the treatments (B), (b) signifies a significant difference within a treatment from initial values (a), and (*) signifies a significant difference between top and bottom values.	55
Figure 4-9. Pore-water Mg^{2+} of 2L settling columns of Syncrude MFT by treatment and incubation time. Error bars indicate S.E.; n=2 for Initial, 21 d, and 42 d, and n=6 for 82 d. (A) signifies a significant difference between the treatments (B), (b) signifies a significant difference within a treatment from initial values (a), and (*) signifies a significant difference between top and bottom values.	56
Figure 4-10. Pore-water Na^+ of 2L settling columns of Syncrude MFT by treatment and incubation time. Error bars represent S.E.; n=2 for Initial, 21 d, and 42 d, and n=6 for 82 d. (A) signifies a significant difference between the treatments (B), (b) signifies a significant difference within a treatment from initial values (a), and (*) signifies a significant difference between top and bottom values.	57

Figure 4-11. Pore-water K^+ of 2L settling columns of Syncrude MFT by treatment and incubation time. Error bars represent S.E.; n=2 for Initial, 21 d, and 42 d, and n=6 for 82 d. (A) signifies a significant difference between the treatments (B), (b) signifies a significant difference within a treatment from initial values (a), and (*) signifies a significant difference between top and bottom values.	58
Figure 4-12. Exchangeable Ca of 2L settling columns of Syncrude MFT by treatment and incubation time. Error bars show S.E.; n=2 for Initial, 21 d, and 42 d, and n=6 for 82 d. (A) signifies a significant difference between the treatments (B), (b) signifies a significant difference within a treatment from initial values (a), and (*) signifies a significant difference between top and bottom values.	59
Figure 4-13. Exchangeable Mg of 2L settling columns of Syncrude MFT by treatment and incubation time. Error bars show S.E.; n=2 for Initial, 21 d, and 42 d, and n=6 for 82 d. (A) signifies a significant difference between the treatments (B), (b) signifies a significant difference within a treatment from initial values (a), and (*) signifies a significant difference between top and bottom values.	60
Figure 4-14. Exchangeable Na of 2L settling columns of Syncrude MFT by treatment and incubation time. Error bars show S.E.; n=2 for Initial, 21 d, and 42 d, and n=6 for 82 d. (A) signifies a significant difference between the treatments (B), (b) signifies a significant difference within a treatment from initial values (a), and (*) signifies a significant difference between top and bottom values.	61
Figure 4-15. Exchangeable K of 2L settling columns of Syncrude MFT by treatment and incubation time. Error bars show S.E.; n=2 for Initial, 21 d, and 42 d, and n=6 for 82 d. (A) signifies a significant difference between the treatments (B), (b) signifies a significant difference within a treatment from initial values (a), and (*) signifies a significant difference between top and bottom values.	62
Figure 4-16. Volume of biogenic gases produced over 213 d of incubation in 50L Syncrude MFT settling columns: canola amended and unamended control.....	63
Figure 4-17. Composition of biogenic gases produced over 213 d of incubation in 50L Syncrude MFT settling columns: canola amended and unamended control.	64
Figure 4-18. Water Release during 213 d incubation from 50L Syncrude MFT settling columns: canola amended and unamended control. Release water is reported in volumetric percentage of initial pore-water	65

Figure 4-19. Settling of 50 L Syncrude MFT settling columns: canola amended and unamended control. Settling reported as a decrease in solids-cap water interface in cm from initial height	66
Figure 4-20. Formation of a large biogas bubble after 46 d of incubation in the 50L settling column amended with canola meal.	66
Figure 4-21. Appearance of lighter coloured MFT material marbled throughout the 50L settling column amended with canola meal after 62 d of incubation.	67
Figure 4-22. pH of 50L Syncrude MFT settling columns: canola amended and unamended control. Values are mean pH of middle and bottom ports. Errors bars show S.E. with n=2.....	68
Figure 4-23. HCO ₃ ⁻ concentrations in the cap-water and MFT pore-water collected from top, middle and bottom ports, respectively at canola amended and unamended control 50L settling columns. Incubation time was 213 at time of sampling. Error bars show S.E. with n=2. (A) Signifies a significant difference between the treatments.	69
Figure 4-24. Ca ²⁺ and Mg ²⁺ concentrations of MFT pore-water and cap-water samples collected from top, middle and bottom ports of canola amended and unamended control 50 L MFT settling columns. Incubation time was 213 at time of sampling. Error bars show S.E., n=2. (A) Signifies a significant difference between the treatments	71
Figure 4-25. Na ⁺ and K ⁺ concentrations of MFT pore-water and cap-water samples collected from top, middle and bottom ports of canola amended and unamended control 50 L MFT settling columns. Incubation time was 213 at time of sampling. Error bars show S.E., n=2. (A) Signifies a significant difference between the treatments.	72
Figure 4-26. Carbonate contents of MFT solid fraction in samples collected from middle and bottom ports of canola amended and unamended control 50 L MFT settling columns. Incubation time was 213 at time of sampling. Error bars show S.E., n=2.....	73
Figure 5-1. Ionic Strength (<i>I</i>) of 2L settling columns of Syncrude MFT by treatment and time. Error bars show S.E., n=2 for Initial, 21 d, and 42 d, and n=6 for 82 d. (A) signifies a significant difference between the treatments (B), (b) signifies a significant difference within a treatment from initial values (a), and (*) signifies a significant difference between top and bottom values.	84

Figure 5-2. Exchangeable cations' mean charge on clays in the MFT of 2L settling columns by treatment and time. Error bars show S.E.; n=2 for Initial, 21 d, and 42 d and n=6 for 82 d. (A) signifies a significant difference between the treatments (B), (b) signifies a significant difference within a treatment from initial values (a), and (*) signifies a significant difference between top and bottom values.	85
Figure 5-3. Estimated DDL thickness of clays in the MFT of 2L settling columns by treatment and time. Error bars indicate S.E.; n=2 for Initial, 21 d, and 42 d, and n=6 for 82 d. (A) signifies a significant difference between the treatments (B), (b) signifies a significant difference within a treatment from initial values (a), and (*) signifies a significant difference between top and bottom DDL	86
Figure 5-4. Water release versus estimated diffuse double layer thickness of clay in the MFT of 2L settling columns. Error bars indicate S.E., n=4.	87
Figure 5-5. Water release versus square root of pore-water ionic strength in the MFT of 2L settling columns. Error bars show S.E., n=4.	87

List of Abbreviations

A	2L Acetate Amended Settling Column
ADW	Accelerated Dewatering
AENV	Alberta Environment
AWRI	Alberta Water Research Institute
BTEX	Benzene, Toluene, Ethyl-Benzene, and Cylene
C 50	L Canola Colum
c	Concentration
C	Molar Concentration
CEC	Cation Exchange Capacity
CECe	Cation Exchange Capacity Effective
cmol _c	Centimol Charge Equivilant
°C	Degrees Celcius
CT	Consolidated Tailings
d	Days
D	Density
DDL	Diffuse Double Layer
Eh	Redox Potential
ERCB	Energy Resource Conservation Board
Eq	Equation
F	Faraday Constant
FFT	Fluid Fines Tailings
GC	Gas Chromatography
H	Height
ICP-MS	Induction Coupled Plasma
I	Ionic Strength
K	Equilibrium Constant
L	Litre
M	Mass
m	Molar Mass
mol	Moles
M	Molarity
MCF	Moisture Correction Factor
MFT	Mature Fines Tailings
MBI	Methyl Blue Index
mg	Milligram
MLSB	Mildred Lake Settling Basin
kg	Kilogram
NRAL	Natural Resources Analytical Laboratory
R	Gas Constant
r	Radius
r ²	Co-efficient of Determination
S.E.	Standard Error
SCL	Syncrude
Spp.	Species

SRB	Sulfate Reducing Bacteria
ST	Sand Tailings
T	Temperature
TET	Total Extracted Tailings
TFT	Thin Fines Tailings
U	2L Unamended Control Settling Column
UM	50L Unamended Control Column
V	Volume
WIP	West In Pit
WR	Water Release
x	Distance
XC	Exchangeable Cation Concentration
y	Year
Z	Charge
B	Boltzmann Constant
μ_s	Gravimetric Solids Content
μ_w	Gravimetric Water Content
μ	Mean
Ψ	Electric Potential
k^{-1}	Diffuse Double Layer Characteristic Length
e	Permittivity
X	Mole Fraction

1. Introduction

1.1. Rationale

The oil sands deposits are a vast reserve of bitumen, which are mined by several companies in northern Alberta, Canada to produce crude oil. The process of extracting bitumen from the oil sands ore requires large volumes of water which are withdrawn from the Athabasca River; 107 million m³ of water was used in 2009 alone (Alberta Energy 2011). The caustic-based Clark Hot Water Extraction process produces large quantities of aqueous slurry waste, called extracted tailings (Chalaturnyk et al. 2002). The tailings are composed of sands, silts, clays, process affected water, unrecovered bitumen, residual organic solvents and chemicals used in the extraction process. The extracted tailings are not released into the environment because oil sands companies operate under zero discharge policy; but tailings are deposited into large settling basins (also termed tailings ponds).

Once diverted into the settling basin, the coarse sand fraction of the tailings quickly settles out on the beaches. The remaining fines tailings, which consists of the slow settling silts, clays, residual bitumen, process extractants and water, is deposited in to the tailings ponds. During the first 3-4 years, the fine tailings undergoes rapid dewatering and densification which produces released water, which is recycled back into the extraction process, and mature fines tailings (MFT). MFT has a solids content of ~30 %, by weight, and further dewatering and densification under natural conditions is very slow. Consolidation into a trafficable consistency is estimated to take 125-150 years (Eckert et al. 1996).

This large inventory of fine tailings poses a challenge for oil sands companies. The tailings ponds are an environmental liability. Two goals for tailings' management are to de-water the tailings to recycle the entrained pore-water for reuse in the bitumen extraction process and to densify the tailings for reclamation activities (List and Lord 1997). Several technologies including chemical and physical treatments have been developed and employed to improve

consolidation of oil sands tailings (BGC Engineering Inc. 2010) but they are either not economical or their environmental fates are unknown.

Oil sands tailings are biologically active and contain complex communities of microorganisms (Penner and Foght 2010; Siddique et al. 2011). Syncrude Canada Ltd. (SCL)'s Mildred Lake Settling Basin (MLSB), the largest tailings pond in Alberta, began producing biogenic methane (CH₄) in the early 1990s. The nearly 10 km² MLSB is estimated to produce in excess of 40 million L d⁻¹ of biogenic methane (Holowenko et al. 2000; Siddique et al. 2008). The hydrocarbon-degrading microbial community in Syncrude's tailings includes nitrate-, iron-, and sulfate-reducing bacteria as well as methanogenic bacteria and archaea (Penner and Foght 2010). The source of the CH₄ is naphtha, a diluent used in the bitumen extraction process, which is anaerobically degraded by the bacteria into simpler organic compounds that are further converted to methane and carbon dioxide (CO₂) by the archaea (methanogens). Naphtha is a mixture of *n*-alkanes, BTEX (benzene, toluene, ethylbenzene and xylenes), branched alkanes and cycloalkanes. Siddique et al. (2006; 2007) demonstrated that microbes in Syncrude tailings can biodegrade *n*-alkanes and BTEX components of naphtha under methanogenic conditions.

Fedorak et al. (2003) found that densification rates of methanogenic tailings were faster than non-methanogenic tailings, suggesting that microbial activity in the tailings might enhance densification. Bordenave et al. (2010) confirmed that oil sand tailings densification increased with methanogenic activity. Exploiting this phenomenon by amending MFT with readily biodegradable carbon substrates to encourage methanogenesis, creating enhanced densification and accelerated water release, may present a desirable process for tailings management. The enhanced densification achieved by this process is termed as biodensification and the water recovery as accelerated dewatering.

A large collaborative research work entitled "Accelerated Dewatering of Oil Sands Fine Tailings through Biological Densification" at the University of Alberta was initiated with the support of the Alberta Water Research Institute,

now within the Alberta Innovates-Energy and Environmental Solutions-Water Resources, to better understand biodensification and to test its feasibility as a tailings management option. Three different approaches were used to investigate this phenomena (1) abiotic, (2) biotic and (3) chemical changes induced by microbial activity. The abiotic approach considers only the physical effects of the gas production, such as channelization that could increase hydraulic conductivity. The biotic approach investigates direct microbial interactions with the suspended solids, such as the formation of a biofilm that could act as a surfactant. The chemical changes induced by microbial activity are of interest because: they may contribute to a mechanism that explains biodensification, give insight into the geochemistry of oil sands tailings ponds and can be used to assess the quality of recycled water released by biodensification.

Previous work using settling columns has shown changes in pore-water pH and bicarbonate (HCO_3^-) concentrations in methanogenic MFT. Fedorak et al. (2003) found that Syncrude MFT undergoing methanogenesis and sedimentation had an increase in HCO_3^- . Similarly, Salloum et al. (2002) found an increase in pore-water HCO_3^- in MFT with enhanced microbial activity. Li (2010) found decreased pH and increased HCO_3^- in Albian Sands MFT undergoing methanogenesis and sedimentation.

1.2. Statement of Objectives

This thesis is a portion of a larger research project which aimed at understanding physical, chemical, and microbiological processes occurring in MFT under methanogenic conditions that affected settling and dewatering of oil sands tailings. The focus of this thesis was to investigate microbially induced chemical processes involved in biodensification of tailings.

The specific goals of this thesis project were to:

1. Observe the changes in pore-water chemistry in MFT during methanogenic microbial activities accelerating settling of oil sands

tailings, in particular, changes in pH, Eh, concentrations of soluble cations and anions were investigated.

2. Observe the changes in clay surface chemistry, and to measure the exchangeable cations and see how the composition changed during methanogenesis.
3. Identify the sink and sources of the various species of anions and cations.
4. Infer possible mechanisms of biodensification.

To achieve these goals, bench-scale 2-L and meso-scale 50-L static settling columns were set up to investigate MFT undergoing methanogenic accelerated dewatering.

A chemical mechanism was envisaged to develop the following pathway as a hypothesis. As the methanogenic microbial community produces CH_4 and CO_2 from the metabolism of carbon substrates, the CO_2 will dissolve in water and lower the pH of the pore-water. The lowering pH will cause Ca^{2+} and Mg^{2+} bearing minerals, such as calcite (CaCO_3) and or dolomite ($\text{CaMg}[\text{CO}_3]_2$), to dissolve releasing Ca^{2+} and Mg^{2+} into the MFT pore-water. The released Ca^{2+} and Mg^{2+} will displace Na^+ on the exchanger surfaces of the clay. Increased soluble cations and anions can also increase ionic strength of the pore-water. Increased ionic strength and divalent cations on exchanger surface can shrink the diffuse double layer (DDL). This leads to flocculation and settling of clay particles in the MFT and resulting in an increased water release and densification of tailings.

2. Background

2.1. Oil Sands Industry

2.1.1. Introduction

Canada has the third largest oil reserves in the world, and 97% of these reserves are located in the Alberta oil sands deposits (Alberta Energy 2011). The Alberta oil sands are geological units that consist of a mixture of bitumen, water, coarse sands and fines. The deposits contain an estimated 1.7 trillion barrels of bitumen, of which 175 billion barrels are recoverable with current technologies (Alberta Energy 2011). There are four major reserves, Athabasca, Peace River, Wabasca and Cold Lake Reserves. The Athabasca Reserve is the single largest petroleum reserve in the world. Currently these reserves supply over 50% of Canadian oil production. This is predicted to grow to over 70 % by 2025 (Canadian Association of Petroleum Producers 2010).

Exploration activity in the oil sands region began in the early 1920s by the Alberta Government and over time, various companies explored the commercial and technical aspects of exploiting the vast oil sands reserves. In 1967, Suncor Energy Inc. opened its first commercial scale surface oil sands processing facility. Located 30 km north of Fort McMurray, the facility included a strip mining operation, extraction plant and an upgrading facility. In the same area, Syncrude Canada Ltd. began production operations in 1978. Shell Albian Sands began mining operations along the Muskeg River in 1999. Canadian Natural Resources Limited (CNRL) began operation of its Horizon Sands Project in 2009. These are the four major operators in the Athabasca Deposit (Alberta Energy 2011).

2.1.2. Oil Sands Processing

Oil sands surface mining operations in the Athabasca oil sands use similar processes for recovering bitumen. The overburden is removed by truck and shovel, then the oil sands ores are mined using draglines, or truck and shovel, and conveyed to extraction plants. The extraction plants remove the bitumen from the

oil sands using the Clark Hot Water Extraction Process, developed in the 1920s by Dr. Karl Clark (Chalaturnyk et al. 2002).

Athabasca oil sands are water-wet, meaning the bitumen is not directly in contact with the sediment surfaces and a thin layer of water separates them. The bitumen contains organic compounds with complex chemical structures including asphaltic acids, which are partly aromatic and contain phenolic, carboxylic and sulphonic functional groups. The Clark Hot Water Extraction Process extracts the bitumen by mixing disaggregated oil sands with water containing NaOH, heating to 85°C, and buffering to a pH of 8 to 9 in a horizontal tumbler (Chalaturnyk et al. 2002). This treatment causes interactions with functional groups on the bitumen and makes the bitumen more water-soluble and surfactant-like (Chalaturnyk et al. 2002). This reduces surface and interfacial tensions allowing the bitumen to be freed from the sediments.

The slurry from the extraction process is transported to a primary separation vessel. The bitumen is separated from the sediments via froth flotation. Aeration promotes the flotation of bitumen to the surface, and coarse particles settle to the bottom. The froth is skimmed off the top and pumped for further processing. The middlings, the material found in the middle of the separator, and the settled material are pumped to a secondary separation vessel. In the secondary vessel, diluents, such as naphtha, are added to enhance the recovery of bitumen (Schramm et al. 2000).

The froth stream is deaerated and treated in the froth treatment plant. Naphtha is added to the froth stream enhance separation of the bitumen from water and clays to remove water, prior to being pumped to the upgraders. In the upgrader the bitumen is converted from a tar-like material to a low-sulfur synthetic crude oil. This crude oil is transported by pipeline to conventional refineries where it is refined into jet fuels, gasoline, heating fuel and other petroleum products (Canadian Association of Petroleum Producers 2010).

The waste materials collected from the separation vessels and froth treatments consist of sands, clays, water, residual bitumen, and solvents that are deposited in tailings ponds.

2.1.3. Oil Sands Tailings

In oil sands processing, generally producing 1 m³ of bitumen requires 7.1 m³ of recycled water and 2.1 m³ make-up water withdrawn from the Athabasca River Basin (Flint 2005). Bitumen extraction results in a tailings stream which occupies a volume of more than 2.5 times the original oil sands. The total inventory of oil sands tailings in 2010 was 840 million m³ and is projected to reach 8.2 billion m³ by 2065 (Alberta Energy 2011).

The tailings first discharged from the plant are total extraction tailings (TET), and have a solids content between 40 and 55 %. This material is deposited in a settling basin where 95% of the coarse (>44µm) and 50% of the fine (<44µm) sediments settle. The fines settling during this period is caused by interactions between the fine particles and the fast settling coarse particles. The tailings are segregated into sand tailings (ST) and thin fines tailings (TFT). ST is used as a construction material for building geotechnical structures such as dykes. TFT consists of slow settling fine particles, residual bitumen and water. TFT has a solids content of 3 to 8% and is transferred to a settling pond. There, it rapidly settles to a solids content of 20 %, then slowly settles over several years to 30% (Eckert et al. 1996). Once the solids content is over 30%, it is termed as mature fine tailings (MFT) (Fine Tailings Fundamentals Consortium 1995). Further settling of fines can take decades (Eckert et al. 1996). If some form of treatment process, such as centrifugation, is used to densify the tailings to the same solids levels as MFT, the term fluid fine tailings (FFT) is used (Alberta Energy 2001). MFT and FFT basically describe the same material; in this thesis the term MFT is used.

2.1.5. Management of Tailings

There are two primary goals for managing tailings in the oil sands industry. The first is to prepare the tailings for final disposal and land reclamation and the second is to recycle the water to be reused in processing. The Energy Resource Conservation Board (ERCB) regulates and sets goals for tailings disposal. Alberta Environment (ANEV) regulates pollution control, water allocation and land reclamation. Tailings management must meet ERCB directive 074 which states that 50 % of fines must be captured from TFT to reduce the total volume of tailings by 2013; and that TFT must be prepared for reclamation activity by densification so it can be “trafficable”, which is defined by shear stress of >5 kPa. ANEV issues permits for water use for oil sands operators and sets water recycling goals, including accelerated water recovery times (ERCB 2009).

The biggest challenge in tailings management is to meet these goals. The colloidal fines, bitumen and pore-water interactions cause hindered settling (Eckert et al. 1996) that results in slow consolidation of tailings and less release of pore-water. If left to settle by natural conditions, the fines suspended in the water will take over a hundred years to meet the guidelines (Eckert et al. 1996).

Two methods have been proposed for reclamation of the oil sands tailings ponds. The “wet landscape” approach involves covering the MFT basins with a water cap to create a lake ecosystem. The “dry landscape approach” uses dewatered tailings. Here, dewatered tailings are disposed in a basin and capped with a geo-liner. A dry ecosystem is established on this surface through revegetation (List and Lord 1997).

There are several tailings management technologies aimed at preparing MFT for final reclamation. Consolidated tailings (CT) are MFT mixed with ST and gypsum for co-disposal to create nonsegregated tailings (NST) (Mikula et al. 2004). The Ca^{2+} in the gypsum acts as a flocculant. An issue with this method is that the released water is high in SO_4^{2-} and Ca^{2+} (MacKinnon et al. 2001). Accelerated Dewatering (ADW) of tailings uses a flocculant to densify the MFT

and release water. Flocculants could include gypsum or polymers (BGC Engineering Inc. 2010). The issue with using flocculants is that the recovered water is not suitable for recycling in the bitumen extraction process; and the environmental consequences of these chemical amendments are still unknown. Another option being explored is the use of centrifuges to separate the water from solids, however this method is quite cost intensive (BGC Engineering Inc. 2010).

Thin layer disposal involves the spreading of a thin layer of MFT on an evaporation surface and allowing the water to evaporate. The dry solids are collected for disposal. The issue with this is that the water is lost to evaporation and not available to be recycled (BGC Engineering Inc. 2010).

There is currently no single solution that meets the goals for disposal of MFT as set by the ERCB and AENV, and a mix of technologies have been used to solve the tailings management challenges.

2.2. Properties of MFT

2.2.1. MFT Composition

MFT is a slurry composed of fine mineral solids, alkaline water and residual bitumen. Typical MFT has a solids content of 30% by mass, and a bitumen content of 5%. Typically the particle size distribution is 65% clay, 30% silt and 5% sand (ERCB 2011).

2.2.2. Mineralogy of MFT

The mineralogy of the oil sands is complex; to date 90 mineral species have been identified in oil sands deposits or process streams (Kaminsky 2008). The principal minerals in the Athabasca oil sands deposits are quartz (80%), kaolinite (9%), feldspar (2%), calcite (0.2%), dolomite (0.4%), siderite (1%), and illite (4%) (Bayliss and Levison 1976).

Kaminsky et al. (2009) examined the distribution of clay minerals in the various process streams at Syncrude operations. They found that the Syncrude MFT was comprised of interlayered illite-smectite, kaolinite-smectite along with

kaolinite-illite groups (Table A-1). Similarly, unpublished data from the AWRI research group found that Syncrude MFT was comprised of illite-smectite and kaolinite-smectite groups (Table 2-1).

Table 2-1. Composition of clay minerals in Syncrude MFT clay fractions (<2.0 μm).

Clay Mineral	Composition (%)	
	<0.2 μm	0.2-2.0 μm
Chlorite	2	0
Kaolinite-smectite	62 (100 % Kaolinite)	45 (94 % Kaolinite)
Illite-smectite	36 (96 % Illite)	55 (87-93 % illite)

Clay minerals are phyllosilicates comprised of continuous two-dimensional sheets. The sheets are generally silicon (Si^{4+}) tetrahedral with Si^{4+} in coordination with 4 O^{2-} ions, and aluminum (Al^{3+}) or magnesium (Mg^{2+}) in octahedral sheets with coordination number of 6 (surrounded by 6 OH^- and O^{2-}). Based on the ratio of tetrahedral to octahedral sheets, phyllosilicates are classified into three types. An octahedral and a tetrahedral sheet joined as a layer with a gap, or interlayer space, form 1:1 type phyllosilicates. In 2:1 type, two tetrahedral sheets sandwich the octahedral sheets, while in 2:1:1 type phyllosilicates, two tetrahedral sheets sandwich the octahedral sheet and another octahedral sheet occupies the interlayer space between the two layers (Mitchel 1976).

An important feature of clay is isomorphic substitution. Two types of substitution occur: substitution in the octahedral layer and substitution in the tetrahedral layer. Atoms having similar sizes (<15% variation in size) but with different charges can substitute atoms in the tetrahedral and octahedral sheets. For instance, Al^{3+} can substitute for Si^{4+} in the tetrahedral sheet. Since Al^{3+} does not have the same valence as Si^{4+} to satisfy completely the negative charges of ligands (O^{2-} and OH^-), the substitution causes a net negative charge to appear on the sheet.

The properties of the groups of the major clays present in the oil sands are summarized in Table 2-2. These properties are fairly general because they are

given for a group. And within a group, variation in isomorphous substitution creates variation in properties.

Table 2-2. Structure and properties of clay groups important in MFT, adapted from (Kaminski 2008) and (Mitchel 1976).

Name	Structure	Interlayer bond	CEC (cmol _c kg ⁻¹)	Surface Area (m ² g ⁻¹)
Kaolinite	Al ₄ Si ₄ O ₁₀ (OH) ₈	H ⁺ , strong	3-15	10-20
Illite	(K _x)(Al,Fe ³⁺) ₄ (Si _{8-x} ,Al _x)O ₂₀ (OH) ₄	K ⁺ , strong	10-40	65-100
Montmorillonite	(X _x)[(Al,Fe ³⁺) _{4-y} (Mg,Fe ²⁺) _y](Si _{8-x} ,Al _x)O ₂₀ (OH) ₄	O-O, weak	80-150	50-120 external, 700-840 total
Vermiculite	(X _x)(Si _{8-x} ,Al _x)O ₂₀ (OH) ₄	weak	100-150	40-90 external, 870 total
Chlorite	[(Al _{x+y} ,Mg _{6-x-y})(OH) ₁₂][(Mg,Fe ²⁺) _{6-y} (Al,Fe ³⁺) _y](Si _{8-x} ,Al _x)O ₂₀ (OH) ₄	-	10-40	-

MFT also contains a significant amount of mixed layered clays. Mixed layer clay minerals occur when interlayer or layer types differ within a mineral and mixed layer clays are not part of the International Association for the Study of Clays classification. When naming mixed-layer minerals, they are named by the names of both components (types of phyllosilicates). Generally, the properties of mixed layer minerals are similar to a mixture of the two components (Srodon 1999).

Studying the clay mineralogy of MFT is important for understanding the chemical changes occurring during methanogenesis, because the clay reactive surfaces control the cation exchange capacity of the MFT.

2.2.2.1. Cation Exchange Capacity

The isomorphous substitutions in the octahedral sheets and/or tetrahedral sheets of clay minerals create permanent negative charges on the clay surface. For instance, an Al^{3+} can substitute for a Si^{4+} in the tetrahedral layer. The charges are balanced by interlayer or outer surface hydrated cations such as Na^+ , K^+ , Mg^{2+} and Ca^{2+} . Generally, the cations that balance the net negative charges are exchangeable. A notable exception to this occurs in illite and other micas where the charge is balanced by non-exchangeable K^+ in the interlayer space. This is because the radius of the K^+ is the correct size to fit between the O^{2-} atoms that make up the base of the tetrahedral sheet. This, combined with the local charge, causes the K^+ to be tightly bound (Mitchel 1976).

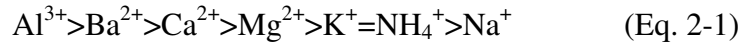
In addition to the permanent charges, clay minerals have pH dependent charges caused by protonation and deprotonation reactions on the broken edges of the clay lattices. Other sources of pH dependent charges in the MFT are due to functional groups on amorphous minerals such as oxides, hydroxides, oxy hydroxides of Fe and Al, organic matter, and bitumen. Exchangeable cations balance these pH dependent charges as well. Because, these charges are pH dependent, increase or decrease in pH changes cation exchange capacity (CEC) of MFT; therefore CEC decreases as pH decreases. The total CEC of the MFT solids is the sum of the permanent charges on clays, pH dependent charges on the clays, amorphous minerals and organic matter. (Mitchel 1976)

The CEC of the MFT is important to the understanding of the chemical changes occurring in the MFT during methanogenesis because of interactions between pore-water (soluble) cations and exchangeable cations on clays surfaces through exchange reactions.

2.2.2.2. Exchangeable Cations

The exchangeable cations are in equilibrium with the soluble (pore-water) cations. Though the composition of the exchangeable cations and pore-water cations are not identical, the clay mineralogy and ionic strength of the pore-water

have an effect on this composition (Kopittike et al. 2006). Increasing ionic strength of pore-water can affect selectivity of cations in adsorption processes. Selectivity refers to how some cations have a high affinity for being adsorbed into the exchange complex. The order of preference is governed by the valence and the hydrated radius of the cation, this lyotropic series is given in Equation 2-1.



Clay mineralogy also affects the composition of exchangeable cations. Some cations have a higher affinity for penetrating into interlayer spaces, such as NH_4^{+} (So et al. 2006). Thus the ratio of interlayer surface to external surface can affect composition of exchangeable cations. The composition of exchangeable cations on the clays in MFT is assumed to be dominated by sodium (Mikula et al. 2004) because NaOH is used with the hot water in the bitumen extraction process. No published research has directly measured the exchangeable cations in the MFT.

Analyzing the exchangeable cations is important to understanding chemical changes occurring in MFT undergoing methanogenesis because the CEC can be a sink and source of cations. Additionally, studying exchangeable cations is important for understanding accelerated dewatering because the exchangeable cations affect the diffuse double layer of the clays.

2.2.2.3. Diffuse Double Layer

The exchangeable cations are held near the surface of the clay. The negative charge on the clay surface and the swarm of positive counter ions make the electric double layer. The first layer is formed by the negative charge on the clay, it is assumed that the charge is uniformly spread across the surface. The second layer is in the solution (pore-water) directly adjacent to the clay. The cations are attracted to the negative surface, but at the same time free to distribute themselves evenly through the liquid. These two processes come to equilibrium, resulting in a distribution zone (Tan 1998).

One model used to describe the electric double layer is the Gouy-Chapman Diffuse Double Layer (DDL). The cations are attracted to the negative surfaces and tend to distribute themselves; so electroneutrality is maintained, which follows the Boltzmann equation (Equation 2-2):

$$C_x = C_B \exp\left(\frac{-ze\Psi_0}{bT}\right) \quad (\text{Eq 2-2})$$

where, C_x is concentration of cations at x distance from the surface, C_B is the concentration of cations in the bulk solution, z is charge, Ψ_0 is the surface electric potential, b is the Boltzmann constant, and T is the absolute temperature. The electric potential in a fluid as a function of distance from the surface is given by equation 2-3:

$$\Psi_x = \Psi_{(o)} \exp(-kx) \quad (\text{Eq 2-3})$$

where, x is the distance from the surface and k is a parameter related to the thickness of the diffuse layer (Equation 2-4):

$$k = ZF \left(\frac{2000I}{\epsilon\epsilon_o RT} \right) \quad (\text{Eq 2-4})$$

where, F is the Faraday's constant, ϵ_o is the permittivity of a vacuum, ϵ_w is the dielectric constant of water, R is the gas constant and I is the ionic strength of the bulk solution.

The inverse of k is often used to characterize the thickness of the DDL, in m (Equation 2-5).

$$k^{-1} = \frac{3.042(10^{10})}{ZI^{0.5}} \quad (\text{Eq 2-5})$$

From Equation 2-5, the thickness of the DDL is controlled by two factors, ionic strength and ion valence. High concentrations of electrolytes result in a suppression of the DDL. A high concentration of cations in the bulk solution reduces the concentration gradient between the bulk solution and the surface. This reduces the tendency for the cations to diffuse away from the surface. Secondly,

the valence of the cations in the DDL affects the thickness of the DDL. Monovalent cations diffuse further away from the surface than divalent cations. Trivalent cations have the smallest DDL (Tan 2010).

MFT can be considered a clay suspension. In clay suspensions, the colloidal nature of clay and pore-water chemistry determine flocculation or dispersion of clay particles. In the slurry, the clay particles are surrounded by the swarm of cations that determine the thickness of DDL. Expanded DDL of clay particles causes dispersion due to repulsion between the particles (Tang 1998). The suspension is then considered stable, and the clays considered to be dispersed. Decreasing the thickness of DDL promotes flocculation. As shown above, increasing the ionic strength of the bulk solution and increasing the concentration of divalent exchangeable cations both decrease the thickness of DDL, promoting flocculation.

2.2.3. Pore-water Chemistry of MFT

The pore-water chemistry of the MFT is a function of source and composition of the oil sands ores, the water used in the extraction process, and the chemicals added during extraction. The composition of pore-water is not static. Water is recycled from the tailings ponds and reused in the extraction process, leading to an accumulation of ions (Mikula et al. 1996).

The major anions (HCO_3^- , SO_4^{2-} , Cl^-) and cations (Na^+ , K^+ , Mg^{2+} and Ca^{2+}) account for almost the entire dissolved fraction in the pore-water (Alberta Energy 2011). Na^+ is the predominant cation and the high Na^+ content comes from the process chemicals. Bicarbonate (HCO_3^-) is the most abundant anion. The pH of the pore-water ranges from 7.0 to 8.3. In this range, dissolved carbonates are mostly in the form of HCO_3^- . Sulphate (SO_4^{2-}) is also present; its concentration is affected by microbial processes. Concentrations of oxygenated nutrients, including nitrite, nitrate and orthophosphate in pore-water is low. Most of the nitrogen is present as ammonia in the range of 2 to 8 mg L⁻¹. The concentrations of dissolved trace metals in MFT pore-water are low relative to

regulatory guidelines. Some notable species such as Al, Ba, B, Fe, Mo, Sr, Zn can have concentrations above 0.1 mg L^{-1} (Alberta Energy 2011). The concentration of dissolved organic carbon ranges from 44 to 86 mg L^{-1} .

MFT is an anaerobic environment, with a redox potential (Eh) in the range of -50 to -200 mV (Lou 2004). Eh characterizes the redox conditions of the medium, in the case of MFT, as it measures the tendency of the medium to either gain or lose electrons when subjected to a new chemical species via redox reactions (Tan 2010). Each chemical species has a different affinity to be oxidized or reduced, resulting in a redox ladder. Microbes utilize the highest energy yield terminal electron acceptor (the most positive Eh), then each species in sequence undergoes redox reactions. In natural marine sediment environments this results in zonation, where as depth increases, conditions become increasingly anaerobic resulting in zones of dominant redox reactions performed by the bacteria (Burdige 1993) (Figure 2-1). The microbial community of MFT is discussed further in the next section.

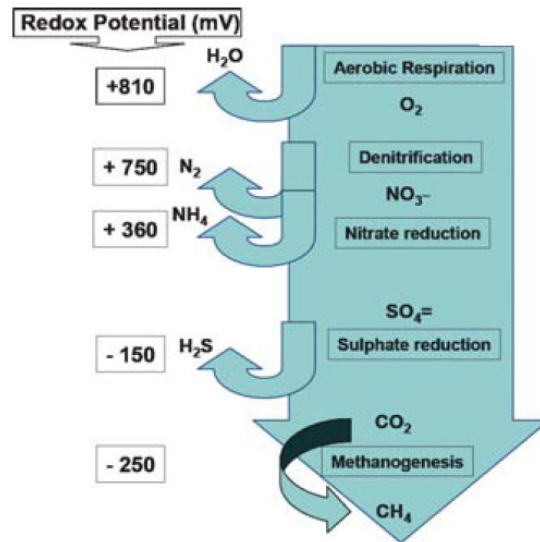


Figure 2-1. Simplified Diagram of reactions performed by bacteria depending on redox potential of the environment in marine sediments (Burdige 1993).

2.2.4. Microbial Communities in MFT and Methanogenesis

MFT supports an active microbial consortium which can affect the chemistry and rheological properties of the MFT. This motivated tailings managers to initiate microbiological investigation. The first study of the microbial community was performed by Foght et al. (1985), which concluded that the level of microbial activity was too low to influence the chemical and rheological properties of the MFT. However, in the coming decades it began apparent that microbial communities developed as evident from methane emissions from the tailings ponds that motivated scientists for further investigations (Holowenko et al. 2000).

Foght and Penner (2010) provided a detailed analysis of the microbial consortia in the MFT collected from the MLSB and West In-Pit (WIP) at SCL, finding the acetoclastic methanogens dominate the archaea in MFT accounting for 86%-100% of the archeal clone sequences. Also, proteobacteria was found to be dominant in the bacteria. The majority of the sequences belonged to betaproteobacteria. This group is associated with sulfate-reducing, nitrate-reducing, iron-reducing and hydrogenotrophic bacteria. Gammaproteobacteria and Deltaproteobacteria were also present in some sample in appreciable quantities. These sequences are associated with sulfate-reducing bacteria. Li (2010) performed a similar microbial community analysis on Albian MFT, finding that archaea DNA was dominated by acetoclastic methanogens. Albian contained some similar bacteria but less diverse species as compared to the SCL.

These consortia of microbes support the production of CH₄ in the tailings ponds. In the early 1990s, the MLSB began to emit CH₄, primarily in the southern section of the basin where the fresh MFT is deposited from the Plant 6 Tailings extraction plants (Lou 2004). In 1995, MFT was started to be deposited in the WIP, and within two years, CH₄ flux was observed from WIP. Current CH₄ release from both ponds is estimated 43 million L day⁻¹ (Holowenko et al. 2000). Similarly, in the early 2000s, the tailings ponds at Albian sands began to produce CH₄, about 5 years after the beginning of deposition of MFT (Li 2010).

The source of CH₄ flux in the tailings ponds is from the biodegradation of residual hydrocarbons in the MFT by the microbial consortia. SCL uses naphtha as a diluent in the extraction of bitumen, as discussed in section 2.1.2. Naphtha is a mixture of aliphatic and aromatic compounds (C₃-C₁₄) containing a significant portion of *n*-alkanes (C₇-C₉) in addition to BTEX compounds (benzene, toluene, ethylbenzene and xylene). Siddique et al. (2006) demonstrated the biodegradation of short chain *n*-alkanes (C₆-C₁₀) in the MFT under methanogenic conditions. In the following year, Siddique et al. (2007) demonstrated the biodegradation of BTEX and naphtha in the MFT under methanogenic conditions. In both of these studies, the biodegradation of naphtha compounds were correlated with CH₄ production.

The biodegradation pathway from naphtha to the release of CH₄ by the microbial consortia in MFT was investigated by Siddique et al. (2011). They proposed a pathway for the biodegradation of naphtha components resulting in CH₄ production (Figure 2-2). First, *n*-alkenes and BTEX compounds are activated and fermented by *Syntrophous* spp. to produce acetate, CO₂ and H₂. The acetate can be directly converted into CH₄ and CO₂ by acetoclastic methanogens, or further metabolized by *Syntrophous* spp. to CO₂ and H₂. The CO₂ in this path is then reduced with H₂ by hydrogenotrophic methanogens to produce CH₄.

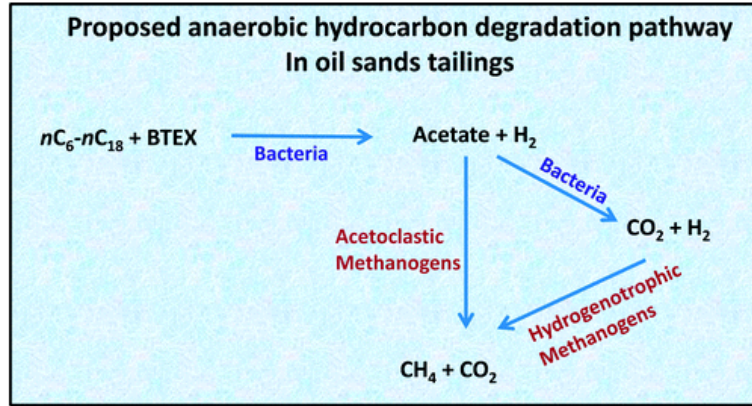
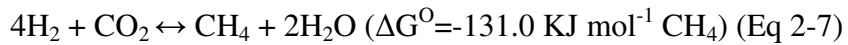
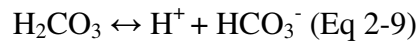
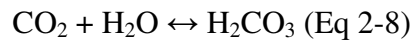


Figure 2-2. Proposed methanogenic hydrocarbon degradation pathway in oil sands tailing. (Adopted from Siddique et al. 2011)

The methanogenesis occurring in the MFT could induce chemical changes as the end products of biodegradation release CH_4 and CO_2 . The acetoclastic methanogens convert acetate into methane and carbon dioxide (Equation 2-6). Hydrogenotrophic methanogens use hydrogen to reduce carbon dioxide into methane (Equation 2-7).



Consequently these products are released into the MFT. The CO_2 dissolves as carbonic acid, into HCO_3^- and CO_3^{2-} , depending on the pH of the MFT (Equations 2-8 to 2-10):



These reactions may alter the pH of the MFT, leading to chemical changes in the MFT. Additionally, the methane produced has an extremely low solubility and forms large gas bubbles causing possible rheological changes in the MFT.

2.3. Methanogenic Accelerated Dewatering of MFT

The production of biogases by the microbial communities in MFT affect the rheological properties of the MFT. Originally, it was thought that the production of biogases would hinder the densification of the MFT by disturbing the settling of the solids and reducing the hydraulic conductivity (Kasperski 1992). However, Fedorak et al. (2003) reported enhanced densification rate in methanogenic MFT compared to non-methanogenic MFT in settling column experiments. Non-methanogenic Syncrude MFT incubated for 6 years showed little densification whereas another methanogenic Syncrude MFT, incubated for 208 days, rapidly settled. This result suggested that microbial activity in MFT enhanced densification which could be beneficial for tailings management.

This discovery presented a possible new treatment for MFT to accelerate densification and dewatering: Amending MFT with a suitable carbon substrate to enhance microbial gas production which encourage settling of the MFT and recovery of more pore-water during densification. This microbially aided settling is termed as biodensification. The mechanism(s) that causes this phenomenon is currently unknown (Foght et al. 2010).

To investigate and optimize the conditions for microbial metabolisms and explore the settling mechanisms linked to microbial activities, this research project was started at the University of Alberta with the support of Alberta Innovates Energy and Environment Solution (formerly Alberta Water Research Institute). A group of six Principle Investigators Dr. Julia Foght from Biological Sciences, Dr. Phil Fedorak from Biological Sciences, Dr. Tariq Siddique from Renewable Resources, Selma Guigard Civil and Environmental Engineering, Dr. Rajender Gutpa from Chemical and Materials Engineering and Dr. David Bressler from Agricultural Food and Nutritional Sciences studied different aspects of biodensification including physical, chemical, and biological factors affecting settling of fines in the oil sands tailings.

Bench-scale 2-L settling column experiments using a variety of carbon substrates were performed on MFT from Syncrude, Shell Albian and Suncor. The carbon sources tested were various agricultural and bioindustrial byproducts: glycerol, bone meal, blood meal, corn DDGS, whey powder, canola meal and stearic acid. Sodium acetate was used as a positive control and unamended baseline controls were also included in the study. The amendments were added on the basis of 40 mg carbon L⁻¹ of MFT. The columns were incubated in the dark at room temperature similar to *in situ* conditions (~20°C). The Syncrude columns were incubated for 168 days, Shell Albian columns for 56 days and Suncor columns for 64 days. The recovery of water and settling of tailings in the columns were measured. Parallel to the 2-L settling columns, triplicate microcosms in sealed serum bottles were set up to measure CH₄ production.

The amended MFT released more pore-water than the unamended controls, except in the case of stearic acid amendment which did not produce any significant result over baseline controls indicating that it is not a suitable substrate for microbial metabolism and hence biodensification (Figure 2-3). The amount of water release differ between the MFT sources, the amended columns had pore-water in the ranges for: Suncor 20.0 to 35.9 %, SCL 13.9 to 20.4 %, and Albian 15.7 to 41.43%. The differences of water release between MFT sources is probably due to the different physical (particle size distribution) and chemical (differing processing chemical) properties which control their settling behaviors. The two best performing substrates were corn DDGS and canola. Some amendments outperformed the positive control, this may occur explained by the fact that amendments also contains other nutrients such as nitrogen and phosphorus, that may stimulate more microbial activity.

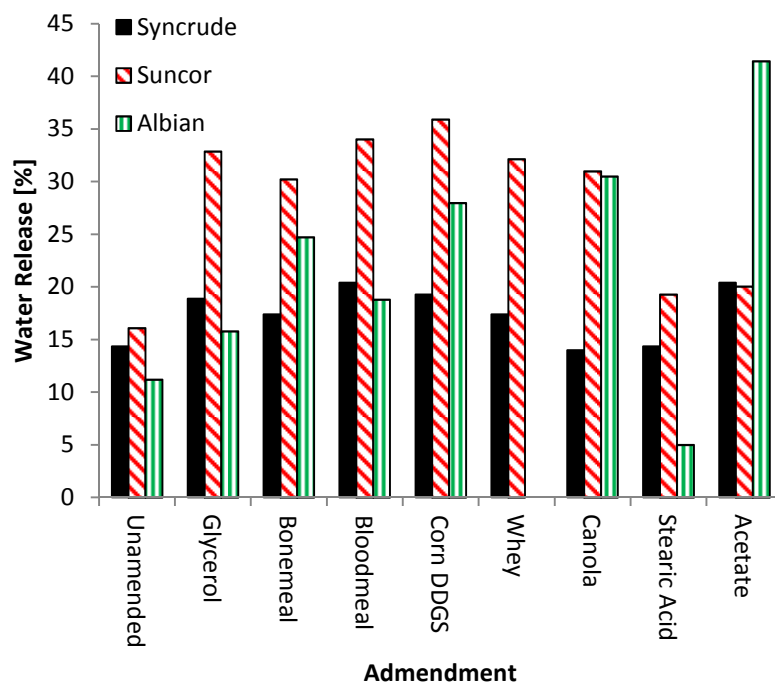


Figure 2-3. Water released from amended and unamended MFT in 2L settling columns. Water release is given in percentage of initial pore-water. MFT are from Syncrude, Shell Albian and Suncor tailings ponds. Unpublished data from group study.

At the end of the incubation period, chemical analyses were performed on the MFT in the columns. The chemical analyses showed that the amended MFT had higher concentrations of bicarbonates, except for MFT amended with stearic acid (Figure 2-4). The major source of the increase in bicarbonates is the dissolution of the CO_2 produced by microbial communities during organic substrates' metabolism (Equations 2-6, 2-18, 2-9).

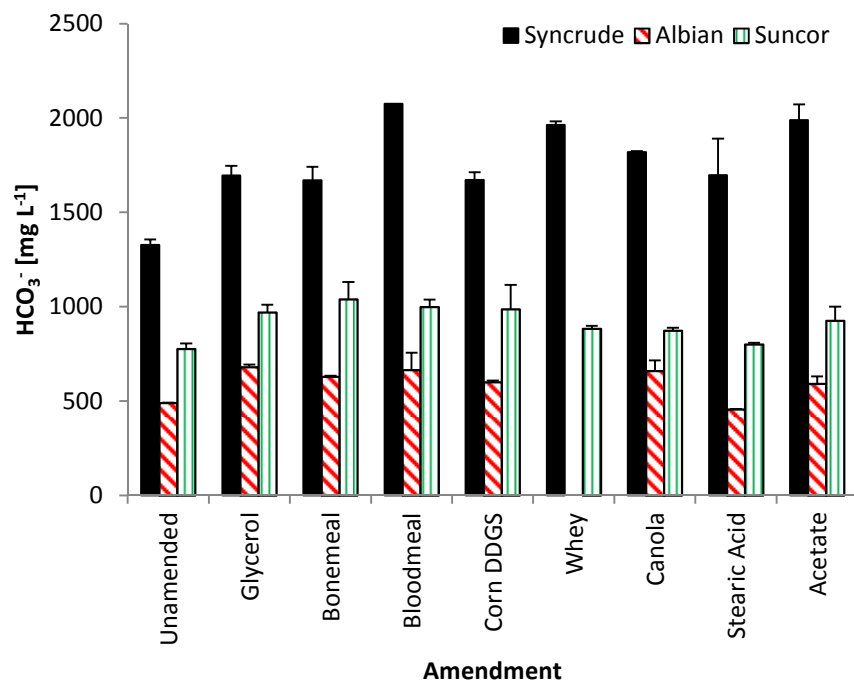


Figure 2-4. Bicarbonate concentrations in MFT in 2L settling columns. MFT are from Syncrude, Shell Albian and Suncor. Error bars are calculated using S.E., n=3. Analysis of Syncrude samples provided by Syncrude. There was no Whey column performed for Shell Albian MFT. Unpublished data from group study.

The pore-water cations for the Syncrude MFT were determined by Syncrude (Figures A-1 - A-4). The pore-water analyses were corrected/adjusted using the chemical analyses of the amendments. There were higher levels of Mg^{2+} and Ca^{2+} in the amended MFT than the unamended control. The concentration of Mg^{2+} was 12.4 mg L^{-1} in the unamended MFT and ranged from 16.0 to 24.8 mg L^{-1} in the amended MFT. The concentration of Ca^{2+} was 21.4 mg L^{-1} in the unamended MFT and ranged from 25.75 to 75.0 mg L^{-1} in the amended MFT. It is hypothesized that the source of these divalent cations is carbonate minerals, calcite ($CaCO_3$) and dolomite ($CaMg[CO_3]_2$). As the biogenic CO_2 dissolves as carbonic acid, it lowers the pH of the MFT. As the pH lowers, $CaCO_3$ and $CaMg[CO_3]_2$ may dissolve into solution.

There are three mechanisms that have been proposed to explain bioremediation (Foght et al. 2010). First, as the microbial community is stimulated, their increasing biomass forms a bio-film that acts as a surfactant,

lowering the interfacial tension leading to densification. Secondly, physical channels caused by the produced CH_4 bubbles increase hydraulic conductivity in the MFT allowing water to escape and fine particles to settle. Thirdly, the chemical changes in the pore-water including lowering of pH and the release of Ca^{2+} and Mg^{2+} lead to the densification of tailings. The chemical mechanism is elaborated in the following section.

2.4. Chemical Pathway for Accelerated Dewatering

The behavior of MFT under methanogenic conditions involves interactions between biological, chemical, mineralogical and geotechnical systems. Hypothetically, the enhanced microbial activity from the addition of carbon caused chemical changes that lead to a pathway resulting in accelerated dewatering/settling of oil sands tailings (Figure 2-5). There are 5 steps in the pathway:

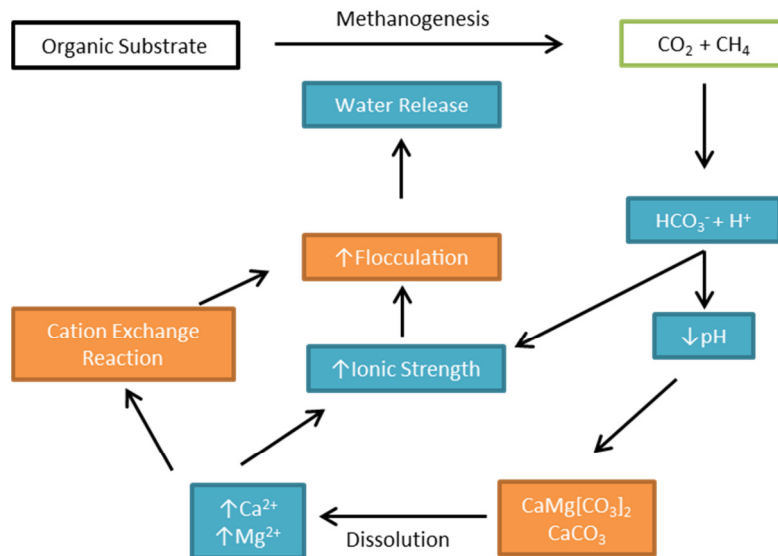


Figure 2-5. Hypothesized chemical pathway for accelerated dewatering during methanogenesis.

- 1) Biodegradation of an organic substrate leading to methanogenesis (production of CH_4 and CO_2).
- 2) Dissolution of the biogenic CO_2 in pore-water as carbonic acid producing HCO_3^- and H^+ lowering the pH of the pore-water and increasing its ionic strength.
- 3) The lower of the pore-water pH, causing dissolution of carbonate minerals such as CaCO_3 and $\text{CaMg}(\text{CO}_3)_2$ releasing Ca^{2+} and Mg^{2+} divalent cations into solution (pore-water).
- 4) Release of Ca^{2+} and Mg^{2+} exchange with Na^+ on the exchange surfaces of clay during cation exchange reaction.
- 5) Altered composition of cations on the exchanger surfaces and the increased ionic strength of the pore-water cause a decrease in the DDL of the suspended clay particles in the MFT leading to flocculation, settling and water release.

3. Materials and Methods

3.1. Summary of Experiments

This research used static settling columns to study and monitor the chemical changes occurring in MFT undergoing methanogenic accelerated dewatering. It consisted of two experiments summarized in Table 3-1.

Table 3-1. Summary of settling column experiments.

Experiment	Scale	Carbon Amendment	# of Columns	Column Names	
				Amended	Control
1	2L	Sodium Acetate	14	A1-A7	U1-U7
2	50L	Canola Waste	2	C	UM

3.1.1. Processing of MFT Samples

For 2 and 50L column experiments, 120 L of MFT was delivered in 20-L plastic pails by Syncrude Canada Ltd (SCL) in May 2011 along with 60 L of cap water in 15 L jerry cans. The MFT originated from Mildred Lake Settling Basin, UTM coordinates 57°4'27"N, 111°38'19"W.

Prior to beginning the experiments, the solids content of MFT was determined by Dean-Stark (detailed in Section 3.3.6.1) and the particle size distribution of MFT (detailed in Section 3.3.6.3) was determined. These analyses were performed to compare this batch MFT to other MFTs used in previous AWRI settling column experiments.

3.2. Experiment 1: 2L Settling Columns

3.2.1. Experimental Design

A bench-scale 2L settling column experiment was performed to monitor the changes in: pH; Eh; soluble anions such as NO_3^- , Cl^- , SO_4^{2-} and HCO_3^- ; major soluble and exchangeable cations such as Ca^{2+} , Mg^{2+} , Na^+ , K^+ .

Sodium acetate was used as a carbon source for the production of biogenic gas in the methanogenic columns. Acetate is readily converted to methane by

methanogens. Acetate conversion to methane normally is the last step in the pathway of methanogenic biodegradation of hydrocarbons in MFT, where more complex carbon compounds are degraded to acetate first. Using acetate speeds up this process. In this experiment, 1000 mg L⁻¹ acetate was added to the amended columns by adding 1310 mg L⁻¹ sodium acetate.

The experiment was performed with a total of 14 settling columns, summarized in Table 3-2. There were 7 acetate amended columns, (A1-A7), and 7 unamended control columns, (U1-U7). The total incubation time for the experiment was 82 days, with some columns being sacrificed for sampling and analysis at days 21 and 42. On day 21, columns U4 and A4 were sacrificed and on day 42, columns U2 and A2 were sacrificed. On day 82, columns U1, U3, U5, A1, A5 and A7 were sacrificed. Columns U6, U7, A3 and A6 were reserved for measuring *in situ* pH regularly.

Table 3-2. Experimental layout of 2L settling columns filled with Syncrude MFT. Seven columns for each treatment U1-U7 and A1-A7 were established. Treatments comprised of ~1400 mg L⁻¹ sodium acetate and unamended control. Incubation times for the different columns are indicated in the table.

Incubation Time (d)	Treatment	
	Unamended Control	Sodium Acetate
21	U4	A4
42	U2	A2
82	U1, U3, U5	A1, A5, A7
82 (reserved for pH)	U6, U7	A3, A6

When a column was sacrificed, its cap water, top layer of MFT and bottom layer MFT were sampled separately for chemical analyses.

3.2.2. MFT Preparation and Time Zero Analysis

The MFT used in this experiment was prepared in two homogenized pails containing 30 L of MFT at 25 % solids. Two 12 L samples were measured in 15 L N₂ flushed pails and sealed. The first pail was used to fill the unamended

columns. To the second pail, 16.67 g of sodium acetate was added and stirred for 5 minutes; this MFT was used for the acetate amended columns.

Prior to filling the columns, the MFT in the pails were sampled for time zero analysis. The pH was measured (as detailed in Section 3.2.6.3). From each pail, 250 mL of MFT was withdrawn and placed in 5 anaerobic centrifuged tubes (50 mL) with locking caps. The centrifuge tubes were flushed with N₂ prior to being filled, maintaining a N₂ headspace.

For both treatments at time zero, the MFTs were analyzed for Eh (Section 3.2.6.5), pore-water cations (Section 3.2.6.6) and anions (Section 3.2.6.7), HCO₃⁻ (Section 3.2.6.8) and exchangeable cations (Section 3.2.6.9).

3.2.3. Procedure for Filling Columns

After the MFT was prepared, the columns were filled. Two liter Pyrex graduated cylinders were used as settling columns. Prior to filling, the columns were autoclaved to eliminate bacterial contamination. The column was flushed with N₂ for 3-4 minutes, and continued to be flushed during filling to prevent aeration of the MFT. The column was filled to 1.6 L with MFT transferred with a 600 mL beaker. The columns were covered with a latex glove to prevent aeration of the MFT during incubation. The initial height of the MFT was marked with a marker on the column.

3.2.4. Incubation and monitoring

After filling, the columns were moved to the incubation room. The columns were maintained at a temperature of 20 to 22°C, under dark conditions during incubation. All columns were regularly monitored for water release and settling as detailed in Section 3.3.6.1. These measurements were taken every 2 or 3 days. Gas bubble evolution, colour changes in the MFT and other visual changes in the columns were monitored and interesting phenomena were photographed.

The *in situ* pH of columns A3, A6, U6 and U7 was regularly monitored during the incubation period. Measurements were taken after every 3 or 4 days.

During measurement, the glove cap was removed from the column and a N₂ was flushed in to the head space. The pH probe was vertically inserted to a depth of 6 cm from the cap water-MFT interface. The procedure for pH reading is detailed in Section 3.2.6.3. After removing the pH meter, the column was re-covered with a latex glove and the N₂ hose removed.

3.2.5. Column Sacrificing and Sampling

At the end of the planned incubation periods, the columns were sacrificed for sampling and analyses. The main concern while sampling and preparing for samples for chemical analysis was to keep the samples for analyses at the anaerobic conditions under which tailings were incubated for densification study. Because the MFT was collected from tailings ponds where anaerobic (methanogenic) conditions prevail and the MFT was studied under for densification under anaerobic conditions, the material was handled in a glove bag under a nitrogen atmosphere. The samples were stored in polysulfone centrifuge tube with sealing caps (Nalgene, USA), flushed with N₂ and stored at 4°C. Also continuing microbial activity in sample was a concern so samples were prepared and analyzed within days.

For dismantling columns, the latex glove cover was removed and the head space was continuously flushed with N₂ during sampling. First, the pH and Eh of the cap water was measured. Then, two 50 mL samples of cap water were withdrawn with a 25 mL syringe and placed in 50 mL anaerobic centrifuge tubes with air-tight caps (Figure 3-1). The remainder of the cap water was removed with a syringe and discarded.

Next, the top layer of MFT was sampled (Figure 3-1). First, the pH was measured. Then 250 mL of MFT was withdrawn with a 25 mL syringe and placed in five 50 mL anaerobic centrifuged tubes with air-tight caps. The centrifuge tubes were flushed with N₂ prior to being filled.

Afterwards, the bottom layer of the MFT in the column was sampled (Figure 3-1). The pH was measured. To reach the bottom of the column, 1/4 inch plastic

tubing was attached to a 25mL syringe for sampling. A total of 250 mL of MFT was withdrawn and placed in fine 50 mL anaerobic centrifuged tubes with locking caps. The centrifuge tubes were flushed with N₂ prior to being filled. The remainder of the MFT in the column was discarded.

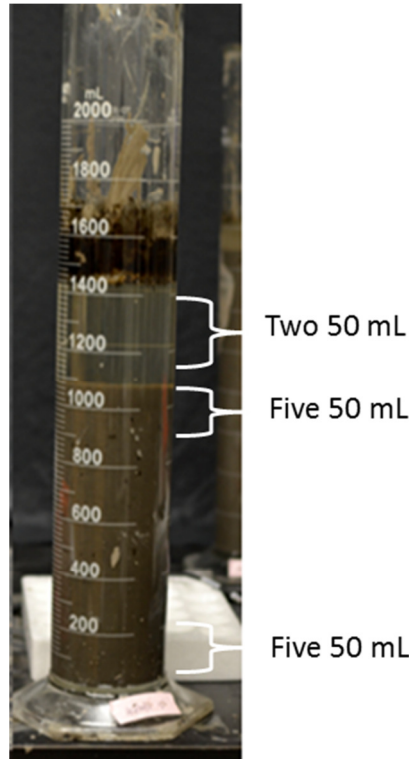


Figure 3-1. Sampling locations of 2L settling columns at time of decommissioning.

For each MFT sampling location, two 50 mL samples were withdrawn for the replicated analysis of pore-water cations (Section 3.2.6.6), exchangeable cations (Section 3.2.6.9) and gravimetric moisture content (Section 3.2.6.2.). Two additional 50 mL samples were withdrawn for the replicated analysis of Eh (Section 3.2.6.5), anions (Section 3.2.6.7), HCO₃⁻ (Section 3.2.6.7) and NH₄⁺ (Section 3.3.6.4). The fifth sample was reserved for possible future analysis.

For the cap-water samples, two 50 mL samples were withdrawn for the replicated analysis of cations (Section 3.2.6.6), anions (Section 3.2.6.7), HCO₃⁻ (Section 3.2.6.7) and NH₄⁺ (Section 3.3.6.4).

3.2.6. 2L Columns: Methods of Physical and Chemical Analysis

3.2.6.1. Measuring Water Release and Settling of Tailings

The rate of densification and water release during densification were monitored by measuring the height of the MFT solid phase-cap water interface (solid-liquid interface) and height of the cap water above solid-liquid interface in each column. The initial height of the solid-liquid interface was marked on the exterior of the column. Settling of tailings and recovery of water were calculated comparing the initial height of the solid-liquid interface and the height of cap water to the measurements taken at the end of incubations. The amount of water released during settling of MFT in a column was measured by the height between solid-liquid interface and surface of the cap water. The measured height of released water was converted to volume using Equation 3-1.

$$WR_{vol} = \pi r^2 h_{cap\ water} \quad (\text{Eq. 3-1})$$

where WR_{vol} is volume of water released, r is the inner radius of the column and $h_{cap\ water}$ is the height of the cap water.

Water release is reported as a volumetric percent ($WR_{\%}$) of the pore-water at time zero using equation 3-2.

$$WR_{\%} = \frac{WR_{vol}}{V_{MFT,i} \theta_w} \quad (\text{Eq. 3-2})$$

where $V_{MFT,i}$ is the initial volume of the MFT, and θ_w is the volumetric fraction of water in MFT.

3.2.6.2. MFT Moisture Percentage and Density

The gravimetric moisture percentage of samples (μ_w) was determined by oven drying the samples. In triplicate, approximately 5 mL of MFT was withdrawn via macropipette and transferred to a pre-weighed aluminum tray. The tray was weighed and then placed in an 110°C oven for at least 24 h. The sample was dried until constant mass was reached. The moisture percentage was calculated by Equation 3-3 (Kasperski 1992):

$$\mu_w = 100 \cdot \frac{m_{wet} - m_{dry}}{m_{wet}} \quad (\text{Eq. 3-3})$$

where m_{wet} is the mass of wet MFT and m_{dry} is the mass of oven dried MFT.

The solid percentage (μ_s) was calculated from the moisture content by Equation 3-4 (Kasperski 1992):

$$\mu_s = 100 - \mu_w \quad (\text{Eq. 3-4})$$

The density of the MFT was determined by pipetting 5 mL of sample into a pre-weighed 10 mL graduated cylinder. Since MFT was viscous, it was found that pipetting did not transfer an accurate volume thus the graduated cylinder was topped up to 5 mL and weighed. Density was calculated using equation 3-5:

$$D = \frac{m}{V} \quad (\text{Eq. 3-5})$$

where, m is mass and V is volume.

3.2.6.3. *In situ* Measurement of pH

In situ pH measurements of the MFT were taken with a Hach H170g Multi hand-held pH/conductivity meter equipped with an ISFET pH17-SS micro probe (Hach, USA). *In situ* measurements of pH in MFT are difficult with glass pH-electrode, because bitumen binds to the glass bulb of electrode, and can permanently damage the ion-exchange function of the glass. ISFET pH electrodes use an ion-sensitive field-effect transistor to measure pH. This transistor can be gently cleaned of bitumen, and thus can be reused in the MFT.

For pH measurements, first the pH probe was checked and calibrated against standards. Then pH probe was inserted into the MFT sample and the reading was taken. After the measurement, the probe was well rinsed with DI water.

3.2.6.4. Separation of Pore-water from MFT

Pore-water was separated from the MFT by centrifugation. Taking a 50 mL MFT sample in a polysulfone centrifuge tube with sealing caps (Nalgene, USA) flushed with N₂, the sample was centrifuged at 12,100 g at 4°C for 30 minutes in a Sorvall RC 5B Superspeed centrifuge using a SS-34 rotor to separate the pore - water. The supernatant was collected under a N₂ stream using a 25 mL syringe, filtered using a 0.45 µm syringe tip filter, and transferred to an anaerobic centrifuge tube.

3.2.6.5. Measurement of Eh

Eh was measured with TX-100 pH/mV 2-Wire Transmitter equipped with a S651 ORP Submersible Electrode (Sensorex, USA). This is a platinum electrode and was calibrated against a standard ORP redox solution prior and after Eh measurements. For Eh measurements, cap water was analyzed directly and Eh of pore-water was measured after separating the pore-water from the MFT as detailed in Section 3.2.6.4. After removing the locking cap from the centrifuge tube, the Eh probe was inserted into the supernatant under an atmosphere of N₂. In some samples, the Eh required a long time (20 minutes) to reach a stable point. The measurements were taken twice.

3.2.6.6. Elemental Analyses by ICP-MS

Inductively Coupled Plasma Mass Spectrometry (ICP-MS) was used to determine major cations and trace metals in cap water samples, separated MFT pore-water and extracts from cation exchange reactions. A challenge in performing analytical chemistry on MFT was that the concentration range of Na⁺ was high (1000 mg L⁻¹ range) and caused interference in some instrumentation,

e.g. in ion chromatography the large peak Na^+ can mask the other elements. In this application, ICP-MS was useful and was the preferred method of instrumentation because it had a high dynamic range of detection. ICP-MS was used to determine soluble: Na, Mg, Al, Si, K, Ca, Cr, Fe, Mn, Ni, Co, Cu, Zn, Se, Sr, Mo, Cs, Ba, Pb and U.

One mL of sample (cap-water, pore-water, or exchangeable cation extract) was filtered through 0.45 μm filter and diluted to 50 mL with 1 % trace metal grade nitric acid in a 50 mL volumetric flask and spiked with 250 μL of grade multi-element internal standard (CLMS-1, SPEX CeriPerp Inc). Approximately, 10 mL of this solution was transferred to a sampling tube and placed on the autosampler. After every ten samples, a rinse cycling was run followed by two external standards of 2 ppb and 20 ppb for quality control. Analysis was performed on a PerkinElmer SCIEX ELAN 9000 ICP-MS with argon as the ionizing gas. The conditions for the ICP-MS were: a vacuum of $9.2 \cdot 10^{-6}$ torr, nebulizer gas flow of 1L min^{-1} , ICP RF power of 1200W, lens voltage of 8.75 V, analog stage voltage 1750 V and the pulse stage voltage at 1300 V.

Ionized argon can form complexes with Cl^- and Ca^{2+} as these ions complexes have the same mass to charge ratio as other elements causing interference (Wu et al. 1997). Since MFT pore-water has high levels of Cl^- and Ca^{2+} , ICP-MS is not appropriate for the determination of As or V and the readings for As and V were ignored.

3.2.6.7. Determination of Anions by Ion Chromatography and Colorimetry

The concentration of anions such as Cl^- , NO_3^- and SO_4^{2-} were determined by ion chromatography and PO_4^{-3} by colorimetry in the Natural Resources Analytical Laboratory (NRAL) in the Department of Renewable Resources. The pore-water was separated from the MFT by centrifugation as detailed in section 3.2.6.4. The samples were submitted to NRAL for analysis.

The Cl^- , NO_3^- and SO_4^{2-} were analyzed on a Dionex Ion Chromatograph DX 600 equipped with an AS9-HC 4 mm analytical column, CD25 detector and an AS50 autosampler. A volume of 25 μL of sample was injected by the autosampler into the system that used Na_2CO_3 as an eluent, and the separated anions were detected and quantified by the conductivity detector. PO_4^{-3} was analyzed on a SmartChem Discrete Wet Chemistry Analyzer 200. The sample was reacted with Molybdate in an acidic solution, the PO_4^{-3} reacted with the Molybdate which produced a blue anionic colloidal solution. The absorption of the 880 nm λ was measured to determine the concentration.

3.2.6.8. Determination of Pore-Water HCO_3^-

The alkalinity as carbonates in water was determined by using the methyl orange indicator method in Natural Resources Analytical Laboratory (NRAL) in the Department of Renewable Resources. The pore-water was separated by centrifugation as detailed in Section 3.2.6.4. Samples were submitted to NRAL where they were analyzed on a Smartchem Discrete Wet Chemistry Analyzer 200. The method used methyl methacrylate orange indicator in a potassium acid phthalate buffer of pH 3.1. When a sample is added to this buffer solution, the alkalinity causes a loss of colour directly related to the concentration of alkalinity. The endpoint pH of this solution determines which species are present. The results are reported as $\text{HCO}_3^- \text{ mg L}^{-1}$.

3.2.6.9. Determination of Exchangeable Cations

The exchangeable cations in MFT were determined by the different methods (Rayment and Lyons 2011) to find more appropriate method for the determination of exchangeable cations under anaerobic conditions.

In soils and sediments, the cation exchange capacity is comprised of permanent and pH dependent charges (Tan 2008). The permanent charge is an electrostatic charge that originates during isomorphous substitutions in the lattices of phyllosilicate minerals. The pH dependent charge originates from protonation and deprotonation reactions on the broken edges of phyllosilicate lattices, oxides,

hydroxides, oxyhydroxides and organic matter. MFT contains all of these, thus it is important to keep the pH under anaerobic conditions to get an accurate representation of the CEC.

The composition of the exchangeable cations is also affected by the ionic strength of the pore-water (Kopittke et al., 2006). As ionic strength increases, it increases the selectivity of the cations in exchange. Thus the ionic strength of the extractant should be similar to that of the pore-water. In saline soils, salts can cause errors in determining exchangeable cations. They can be dissolved during extraction causing an over estimation of exchangeable cations (Tucker, 1985). Since MFT is saline and solid phase contains carbonates minerals such as calcite and dolomite, there is a concern of dissolution of these minerals. The different methods for correction of total extractable cations for soluble cations address these issues to give an accurate measure of exchangeable cations in saline condition (Raymond and Layent, 2011).

For the determination of exchangeable cations, from a 50 mL sample of MFT, a 2 g subsample was taken and placed in a weighed anaerobic centrifuge tube under a N₂ atmosphere. The exact mass of the sample was determined. Then 20 mL of 0.1 M BaCl₂/0.1 M NH₄Cl extractant was added and the tube was shaken in a reciprocal shaker for 2 h. The extractant was separated from the solids by centrifugation as detailed in Section 3.2.6.4. To preserve the metals, 1 mL trace metal grade nitric acid was added to supernatant. This extraction solution was analyzed by ICP-MS as in Section 3.2.6.6.

Two grams of MFT from another subsample from the 50 mL sample was taken to determine the moisture content of the sample using the method in Section 3.2.6.2. The remainder of the sample was used to analyze the pore-water. The pore-water was separated from solid using the procedure described in Section 3.2.6.6.

Using Equation 3-6, the amount of exchangeable cations for each species was calculated (Raymond and Layent, 2011):

$$XC = \frac{(a-b) \cdot 20 \text{ mL} \cdot MCF}{10 \cdot (m/Z) \cdot s} \quad (\text{Eq. 3-6})$$

where XC is the concentration of the exchangeable cation [$\text{cmol}_c \text{ kg}^{-1}$ solids], 'a' is the concentration of the cation in the extraction solution [mg L^{-1}], 'b' is the concentration of the cation in the pore-water [mg L^{-1}], 'm' is the molar mass, Z is the charge, s is the mass of the sample [g], 20 mL is the volume of extractant, 10 corrects the mol g^{-1} to cmol kg^{-1} , MCF is the moisture correction factor which is given in Equation 3-7:

$$MCF = \frac{100 + \mu_w}{100} \quad (\text{Eq. 3-7})$$

Where, μ_w is the moisture content of the MFT slurry.

3.3. Experiment 2: 50 L Mesocosms

3.3.1. Experimental Design

Based on previous bench scale-settling experiments, the ARWI research group designed a scale-up 50 L settling column experiment to demonstrate and further validate biodensification process in oil sands tailings. Hydrolyzed canola meal, was shown to be a suitable substrate for microbial metabolism in our previous columns experiments and was used as a carbon source to amend the column in this work.

This experiment consisted of two settling columns filled with 50 L of MFT each to be incubated for ~210 days. One was amended with 400 mg carbon L^{-1} (1.42 g hydrolyzed canola L^{-1}) and the other was an unamended control.

For the chemistry aspect of this experiment, the primary objectives were to measure, under methanogenic conditions, *in situ* changes in pH, pore-water cations, pore-water HCO_3^- , carbonate minerals content of the solid phase and biogenic gas production.

3.3.2. Construction of the Columns

The columns were constructed of 0.635 cm thick x 30.48 cm outer diameter acrylic pipe (Johnson Industrial Plastics). The height of the columns was 195.58 cm. The bottom of the columns was covered with a 45.5 x 45.5 x 2.5 cm acrylic plate, and the top of the columns were sealed with a 35.5 x 35.5 x 1.27 cm acrylic plate. The parts for the sampling ports and tubings were acquired from Swaglock.

The columns were assembled by the Biological Sciences Workshop, at the University of Alberta. The designs of the parts are detailed below.

Beveled into the bottom plate was 1.27 cm grooves the same diameter of the columns to fit the bottom of the tubes into. Acrylic glue was placed in the groove and the columns place in. Four triangular support pieces were used to reinforce the seal between the bottom plate and the column.

Into the top plate, two bore-through fitting for 1/16 inch stainless steel tubes were installed for the GC and gas trap. A third bore-through fitting was installed for sampling cap water or possible vertical sampling of the MFT. The top plate was installed after the columns were filled.

Into the side of the column, three ports for measuring pH of the MFT were installed at heights 35 cm, 92 cm and 150 cm. The ports were constructed of a 3/8 inch bore-through fitting screwed into the column. An 1/8 inch reducer fitting was attached followed by a 1/8 inch valve and finally another 3/8 inch bore-through fitting. The pH probe has a diameter of 1/8 inch, so when inserts through the port it seals and prevents leakage.

Installed parallel with pH ports were ports for measuring pore pressure. An 1/4 inch brass bore-through was screwed into the column. The fitting was attached with a, 1/4 inch brass valve with another 1/4 inch brass t-junction with a bleeder and a 75 μ m sieve filter. Pressure transducers were attached to these ports, but were not used for this thesis.

After construction, the columns were transported to the incubation room in Earth Sciences Building where they were placed in plastic containment tubs and strapped to a bench surface. The final apparatus is shown in Figure 3-2.

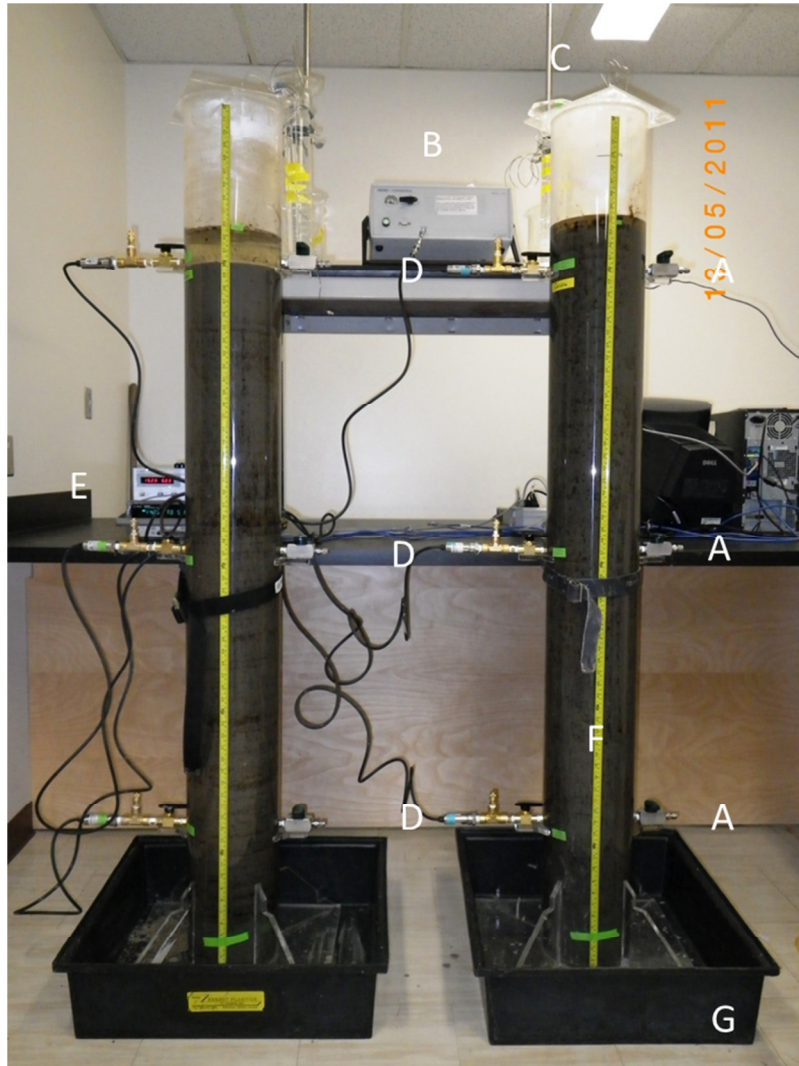


Figure 3-2. Final setup of the 50L columns, UM (right) and C (left). Features of apparatus are labeled: (A) pH ports, (B) GC. (C) gas trap, (D) pressure transducers. (E) pressure reading unit, (F) Measuring Tape, and (G) Containment tub.

3.3.3. MFT Preparation, Filling Procedure and Final Assembly

Six 20 L pails, each containing 10 L homogenized Syncrude MFT at 36 % solids content, were used for this experiment. For the unamended column, 5.15 L

of cap water was added to each of 3 pails to make a total volume of 45.45 L MFT with 25 % solid content. For the canola-amended column, 21.4 g of hydrolyzed canola was added to 5.15 L of cap water which was added to each of the remaining 3 pails to make a total of 45.45 L at 25 % solid content in MFT.

The columns were flushed with N₂, and the headspace continued to be flushed while the column was filled with 45 L of MFT. The MFT was transferred with 4 L beakers and a transfer tray to pour the MFT down the side of the columns to avoid aeration. After filling, the lid plate was attached. To ensure an airtight seal, acrylic glue was applied to the top of the column and the lid plate was tightly pressed and held. After 24 h, the seal was tested by slightly pressurizing the column through the gas trap port. Once the seal passed the inspection, a bead of silicon was calked around the seal. After the lid plates were sealed on, the gas traps were attached to the columns.

3.3.4. Incubation and Monitoring

After filling the columns were incubated in a dark room at temperature of 20 to 22°C for 213 days undisturbed except when measuring pH through designated ports. On day 213, the columns were sampled through the pH ports for chemical analyses.

During incubation of the column, the columns were regularly monitored for settling of tailings, water release, gas production, gas composition and pH. Also visual changes in the MFT were observed and photographed.

Settling and water release were measured with an attached measuring tape (Section 3.2.6.1). Measurements were taken every other day for the first 3 months, then weekly until day 213. Gas produced in the columns was measured by gas trap and the composition was quantitatively determined by GC (Section 3.3.6.5). The pH was measured twice a week for each column through the three pH ports. To take a reading, the pH probe was inserted into the valve housing on the port. Then simultaneously the valve was opened and the pH probe was inserted into the column. The measurement of pH is detailed in Section 3.3.6.3. Once the reading

was taken, the probe was withdrawn from the valve housing and the valve was closed. In this manner, the probe could be inserted into the column without disturbing the MFT. The valve housing was cleaned with distilled water. At first, the top ports were in MFT, eventually the solid-liquid interface settled below the top port; then the pH was recorded as cap water pH from the top port.

3.3.5. Procedure for MFT Sampling

On day 213 of incubation, the columns were sampled for physical and chemical analyses. Samples were withdrawn from the pH ports, giving three sample locations in each column: cap water, middle MFT, and bottom MFT. The heights of the water and solid-liquid interface were recorded before and after sampling.

To withdraw a sample, a 1/8 inch stainless steel tube was attached to a 25 mL plastic syringe and the tube was inserted into the port. The port valve was opened and the tube was inserted into the column. The sample was taken and tube was withdrawn from the valve housing and the valve was closed. The sample was transferred to a 50 mL anaerobic centrifuged tube with locking caps, and flushed with N₂. Two samplings would be taken to fill one bottle. Five 50 mL of MFT samples were taken from the middle and lower ports. Similarly, two 50 mL samples cap water was sampled from the top ports.

The MFT samples were analyzed for cations (Section 3.3.6.4), anions (Section 3.2.6.7), HCO₃⁻ (Section 3.2.6.8) and carbonates minerals (Section 3.3.6.6). The cap water samples were analyzed for cations (Section 3.3.6.4), anions (Section 3.2.6.7) and HCO₃⁻ (Section 3.2.6.9).

3.3.6. 50L Columns: Methods of Physical and Chemical Analysis

3.3.6.1. Oil-Water-Solid Content by Dean-Stark Method

The oil-water-solid content of the bulk MFT received from Syncrude was determined in the Department of Civil and Environmental Engineering using Dean-Stark extraction (Dean and Stark, 1920). Fifty g of MFT was taken in a

cellulose extraction thimble that was placed in a 150 mL beaker. The reaction flask was filled with 200 mL of toluene. The flask was attached to the Dean-Stark apparatus. The sample was refluxed until the toluene ran clear and all of the water was collected in the water trap. The mass of the solid was determined by oven drying the thimble. The mass of the water was determined by weighing the water collected in the water trap. And the bitumen content was determined by transferring the toluene extract into a 250 mL volumetric flask and bringing up to volume with toluene. 10 mL of the extractant was pipetted onto pre-weighed filter paper; the paper was dried and weighed. The mass of the bitumen on the filter paper was multiplied by 25 to give the total mass of bitumen in the sample.

3.3.6.2. Particle Size Distribution

The particle size distribution of the bulk MFT received from Syncrude was determined by first isolating the mineral fraction of the MFT, then analyzing by laser diffraction. The objective of this analysis was to compare the PSD of this MFT to the MFT used in previous experiments and characterize the amount of clay-size fines. Scott and Jeeravipoolvarn (2004) evaluated the application of various PSD test methods on MFT and recommended removal of bitumen to avoid any cementing of the mineral fraction. Cementing causes an understating of finest particle sizes. To accomplish this, a low temperature toluene wash was used to remove the bitumen. Laser diffraction was chosen as the PSD analytical method over a hydrometer procedure because it is widely used in the oil sands industry (Scott and Jeeravipoolvarn, 2004). This method uses smaller sample size, and gives a better resolution.

A 50 g sample was taken from the bulk MFT and placed in a 50 mL Teflon centrifuge tube. First, the pore-water was removed by centrifuging at 12,100 g at 4^oC for 30 minutes in a Sorvall RC 5B Superspeed centrifuge using a SS-34 rotor. The supernatant was decanted and discarded. The solid was divided into eight equal-size samples and placed in 50 mL Teflon centrifuge tubes. To remove the bitumen, the tubes were filled with toluene, capped, and placed in a reciprocal shaker for 2 hours. The samples then were centrifuged and the

extractants were decanted and discarded. This was repeated until the toluene was clear with no dissolved bitumen. Next, any remaining organic matter was removed from solid in a 70°C water bath and reacting with hydrogen peroxide. Finally, the solid was washed with distilled water. For analysis, a 0.1 % suspension was required; the suspension was prepared by adding 0.5 g of solid to 500 mL of distilled water and sonicated.

The analysis was performed using a Mastersizer 2000 equipped with a Hydro SM sample dispersion unit (Malvern Instruments, USA). The sample dispersion unit was set at 1800 rpm and flushed three times with distilled water. Immediately after sonication, 2 mL of the suspension was added to the dispersion for analysis. The sample was run in triplicate.

3.3.6.3. In situ Measurement of pH

Similar to section 3.3.6.3, the in situ pH of the MFT was determined with an ISFET pH electrode. To take the measurement, the electrode was first inserted into the pH port, the port valve opened and then the electrode was fully inserted into the MFT to take the reading. After taking the reading, the electrode was partially retracted from the pH port and the valve closed to prevent MFT from escaping.

3.3.6.4. Determination of Cations by Atomic Absorption Spectroscopy

In some cases, soluble cations such as Na⁺, K⁺, Ca²⁺, Mg²⁺, Al³⁺ and Fe²⁺, were determined by Atomic Absorption Spectroscopy in the NRAL. The pore-water was separated from the MFT by centrifugation as described in 3.2.6.4. The samples were analyzed on a SPECTRA 880 atomic absorption spectrometer equipped with an SIPS-20 Sample Introduction Pump System and a SPS-5 autosampler.

3.3.6.5. Determination of Headspace Gases in 50 L Columns

In the mesocolumns, the headspace gas was analyzed for volume of gas produced and its composition. The volume of gas produced during the incubation

was measured by a NaCl-citric acid brine gas trap (Boone 1982). The gas trap was constructed by a 4 L glass beaker filled with approximately 3 L of brine (200 g L⁻¹ NaCl and 5 g L⁻¹ citric acid). A 2 L graduate cylinder with a vacuum hose inserted is inverted and placed in the beaker and held 3 cm from the bottom by a retort stand. A vacuum was used to remove the air trapped in the cylinder and pull up the brine. The vacuum hose was removed. A 1/16 inch stainless steel tube was attached to a bore-through fitting in the top plate of column and the other end of the tube was hooked into the submerged end of the graduate cylinder in the brine. As gas was produced by the column, it was collected in the graduated cylinder displacing brine solution. This displacement was measured to determine the volume of gas produced by the column.

The composition of produced gas was analyzed for O₂, N₂, CH₄ and CO₂ by Eleisha Underwood of the Department of Civil and Environmental Engineering, University of Alberta. A Varian CP-2003 portable micro-GC equipped with a GMT-2HP moisture trapped and with two channels of A and B was used for the analysis. Channel A was installed with CP-Mole Sieve column and a TCD detector. This channel was used for the analysis of O₂, N₂ and CH₄. Channel B was installed with the HayeSep column and a TCD detector. This channel was used to measure CO₂. Helium (He) was used as the carrier gas for both channels.

The mirco-GC had an internal sampling pump to automatically retrieve the gas samples therefore no syringe injection was required. The top plate of the mesocolumns had a bore-through fitting with a tube of 1/16 inch stainless steel tubing attached. This tubing was connected to the sample injection port of the mirco-GC. A suitable sampling time was set to flush out the dead space volume in the gas route between the GC and the column. The injection time was set to 40 minutes and injection volume to 200 nL. The flow rate of the carrier gas was set with a 552 kPa outlet pressure. The minimum detection limit of this GC was 50 ppm.

3.3.6.6. Determination of Carbonate minerals in MFT

The carbonate mineral content of MFT solid was determined using acid digestion followed by GS-MS analysis for CO₂ formation. After centrifuging the MFT, the pore-water was removed (Section 3.2.6.4.) and discarded; then the solids were washed with methanol to remove residual pore-water. One to two grams of MFT sample was placed in a N₂ flushed 250 mL serum bottle, and then the bottle was tightly sealed with a rubber cap. With a N₂ flushed syringe and needle, 20 mL of 1 M HCl was added. The HCl reacts with carbonate minerals to produce CO₂. The headspace of the serum bottle was sampled with a N₂ flushed syringe. This sample was analyzed by GC (section 3.2.6.10) to determine the quantity CO₂, which in turn is used to determine the amount of carbonates in the sample.

4. Results

4.1. 2L Settling Columns

To investigate the chemical changes of MFT undergoing methanogenic accelerated dewatering, fourteen 2 L settling column were filled with SCL MFT of which 7 were amended with $\sim 1400 \text{ mg L}^{-1}$ sodium acetate and the other 7 were unamended controls. The columns were analyzed for water release and MFT settling (Section 4.1.1.), pH (Section 4.1.2), Eh (Section 4.1.3), pore-water concentrations of HCO_3^- (Section 4.1.4), pore-water cations (Section 4.1.5), exchangeable cations (Section 4.1.6.), chemistry of released cap water (Section 4.1.7.) and composition of entrained biogenic gases (Section 4.1.8.).

4.1.1. Water Release, Settling and Densification of MFT

The production of biogases in the acetate amended columns began after approximately 10 d of incubation. At this point, the methane being produced started creating biogas bubbles entrained in the MFT. At this time, cap water began to accumulate at the surface of the columns. The production of biogas bubbles caused the surface of the MFT (solid-liquid interface) to rise in the column until approximately 22 d of incubation. Then the MFT collapsed, resulting in rapid release of pore-water. The columns continued to release pore-water until approximately 50 to 55 d of incubation (Figures 4-1, B-1 and B-2). Using Equation 3-2, it was calculated that, by the end of the 82 d of incubation, the acetate amended columns released 31 % of their initial pore-water, while the baseline control only released 3 %.

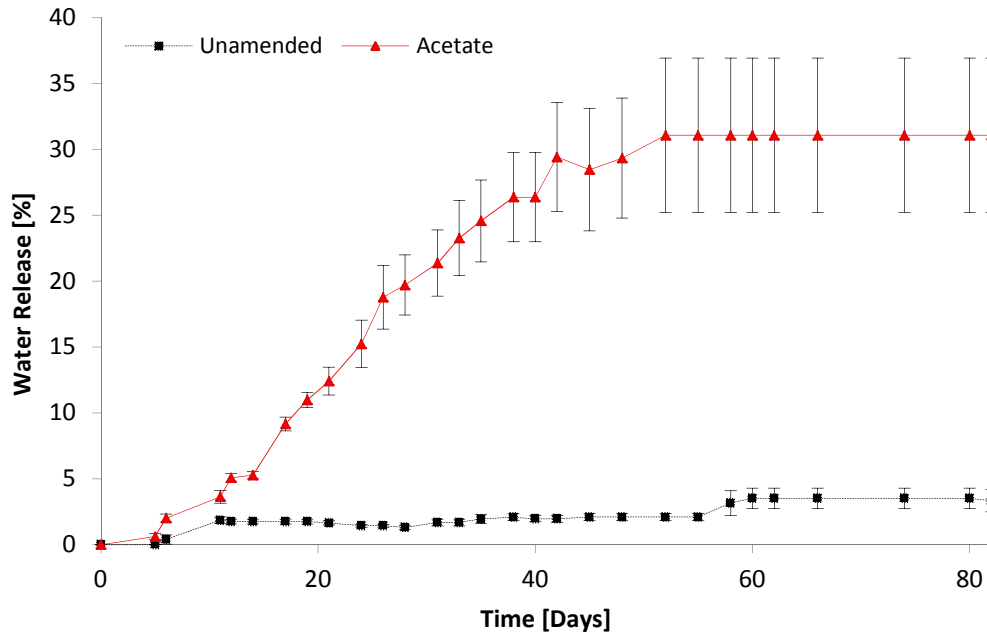


Figure 4-1. Water release from 2L settling columns of Syncrude MFT. Water release is calculated in volumetric percentage of the initial pore-water contents. Error bars show Standard Error (S.E.); days 0-21 n=5, days 22-42 n=4, days 43-82 n=3.

The settling of the MFT during incubation of the 2L settling columns was measured as a decrease in the MFT-cap water (solid-liquid) interface (Figures 4-2, B-3, B-4). Initially during the incubation, the MFT volume of acetate amended columns increased as the gas bubbles formed in the MFT. On 21 d, the MFT in the acetate amended columns began to collapse, and the interface dropped 5.6 cm from its initial height, whereas the unamended MFT experienced little settling. There was high variation in the settling in the acetate amended columns.

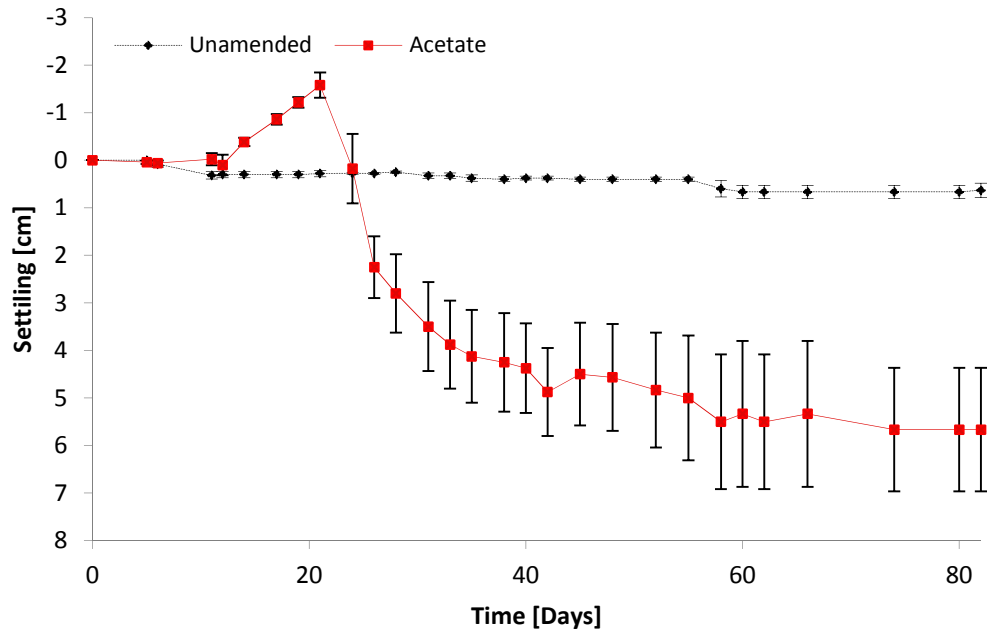


Figure 4-2. Settling of 2L settling columns of Syncrude MFT. Settling is reported as a decrease in solids-cap water interface in cm from initial height. Error bars represent S.E.; days 0-21 n=5, days 22-42 n=4, days 43-82 n=3.

The biogas production and dewatering resulted in a colour change in the acetate amended MFT. The MFT surrounding collapsed former biogas bubbles turned into a lighter grey than the original MFT. This corresponded with an accumulation of separated bitumen at the surface of the settling column that attached to the column wall as the MFT-cap-water interface fluctuated vertically. (Figure 4-3). The colour of unamended MFT remained unchanged during the incubation.

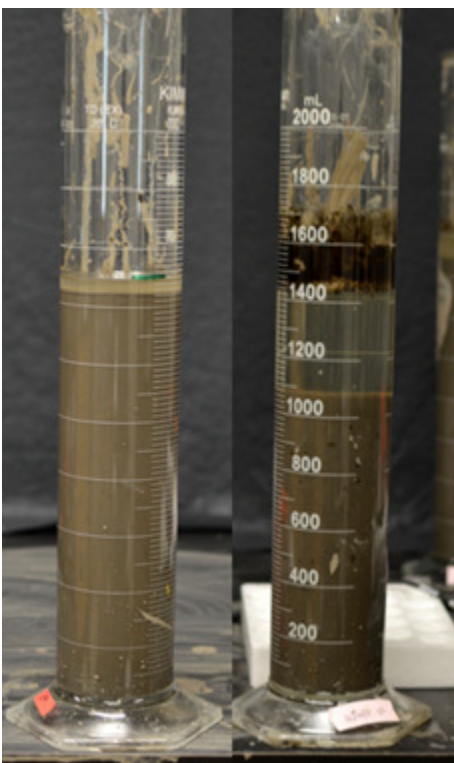


Figure 4-3. 2 L settling columns of Syncrude MFT after 82 days of incubation. Unamended (left) Acetate amended (right).

Table B-1 shows the solids content (μ_s) of the initial MFT material prepared for filling the columns, as well as top and bottom of each column at their respective time of decommissioning. The solids content of the acetate treated columns increased during the incubation period, while the solids content of the unamended control columns remained unchanged. The acetate columns solids content increased from the initial 29.0 % to a mean of 35.5 % (bottom) and 31.1 % (top).

4.1.2. pH change in 2L columns

At time zero, the pH of the acetate amended columns had a slightly higher pH than the unamended columns, 7.64 and 7.32 respectively (Table B-2). Over the 82 d of incubation of the acetate amended columns (A3, A6) reserved for pH measurements, the pH first increased slightly from the initial value of 7.62 to 7.96 (Figure 4-4). Then the pH remained relatively unchanged until 35 d when it declined to a low of 7.21 by 42 d. From 42 d to the end of incubation the pH

varied between 7.13 and 7.62. The pH of unamended control columns (U6-7) remained unchanged during incubation, hovering around 7.7.

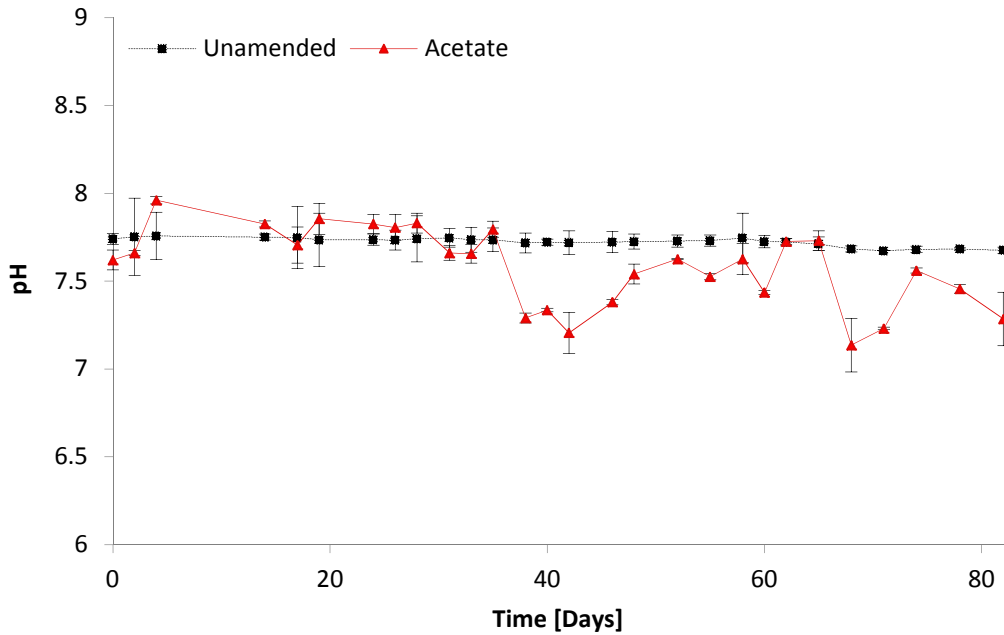


Figure 4-4. pH of 2L settling columns of Syncrude MFT by treatment during 82 days of incubation. Error bars show S.E., n=2.

The pH of the MFT was also determined in the columns, that were designated to monitor other experimental parameters, at time zero, and at their respective time of decommissioning (Figure 4-5). At time zero, the acetate amended and unamended MFTs had pHs of 7.52 and 7.32, respectively. Over the incubation period, the pH of the acetate amended columns decreased while the pH of the unamended control columns increased slightly (Figure 4-5), the amended column decommissioned on 21 d, had exceptionally low lower zone pH of 5.34, and an upper zone pH of 6.61. The amended column decommissioned on 42 d, had similar upper and lower pH of 6.90. Acetate amended columns decommissioned on 82 d had mean upper and lower pHs of 7.14 and 7.35.

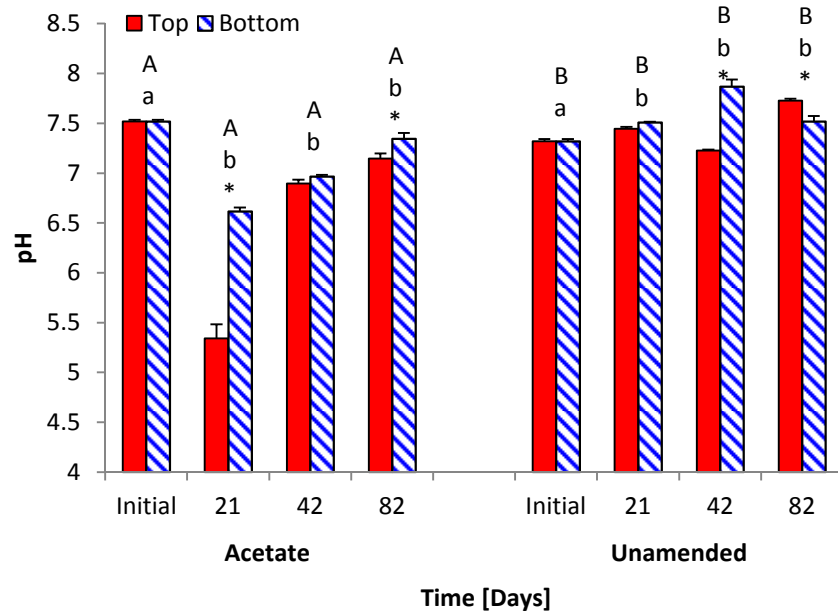


Figure 4-5. pH of 2L settling columns of Syncrude MFT by treatment and incubation time. Error bars show S.E.; n=2 for Initial, 21 d and 42 d, and n=6 for 82 d. (A) signifies a significant difference between the treatments (B), (b) signifies a significant difference within a treatment from initial values (a), and (*) signifies a significant difference between top and bottom values.

4.1.3. Eh change in 2L columns

The Eh of the MFT was determined in the MFT prepared for the columns at time zero, and in the top and bottom of the settling columns at their respective time of decommissioning (Figure 4-6). At time zero, the acetate amended and unamended MFTs had similar Eh values -25 mV and -30.5 mV, respectively. Over the incubation period, the Eh of the acetate amended columns decreased while the Eh of unamended control columns increased. For the acetate columns at three different decommissioning times, there was a significant difference of Eh between top and bottom of the columns. On d 42 and 82, the bottom Ehs were lower, indicating a possible vertical Eh gradient. However, in the column decommissioned on d 21, the top of the column had a lower Eh. The Eh of the unamended control columns increased over time.

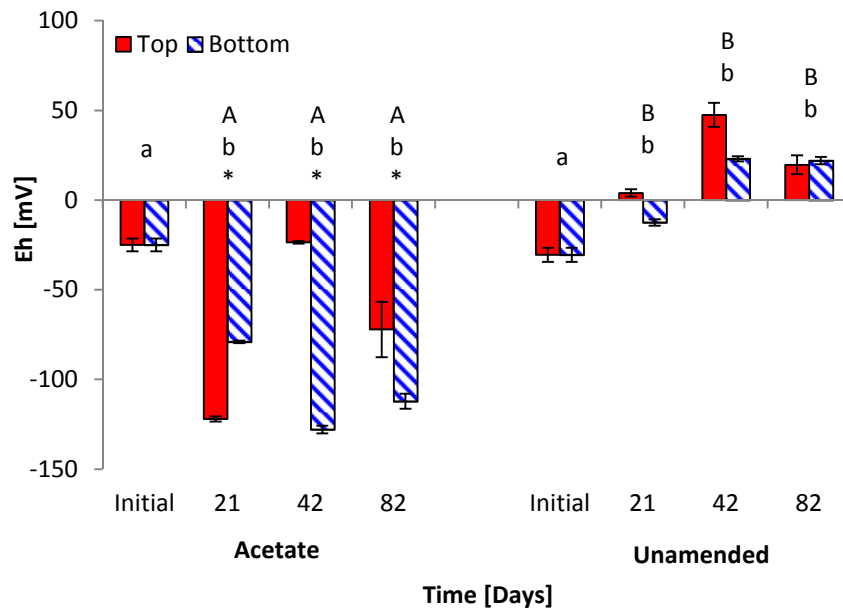


Figure 4-6. Eh of 2L settling columns of Syncrude MFT by treatment and incubation time. Error bars show S.E.; n=2 for Initial, 21 d and 42 d, and n=6 for 82 d. (A) signifies a significant difference between the treatments (B), (b) signifies a significant difference within a treatment from initial values (a), and (*) signifies a significant difference between top and bottom values.

4.1.4. Pore-water HCO_3^- in 2L columns

The concentration of HCO_3^- was determined in the MFT prepared for the columns at time zero, and in the top and bottom MFT of the settling columns at their respective time of decommissioning (Figure 4-7). At time zero, the acetate amended and unamended MFTs had similar HCO_3^- concentrations 1599.6 mg L^{-1} and $1620.57 \text{ mg L}^{-1}$, respectively. Over the incubation period, HCO_3^- concentrations of the acetate amended columns increased while the unamended control columns remained constant. None of the columns had significant differences between the bottom and top samples. In the acetate amended columns, the mean HCO_3^- concentration increased overtime with the columns having HCO_3^- concentrations of 1926.4 mg L^{-1} for 21 d, 2394.1 mg L^{-1} for 42 d and 2857.4 mg L^{-1} for 82 d. The unamended control columns had HCO_3^- concentrations in the range of 1362.2 mg L^{-1} to 1585.5 mg L^{-1} .

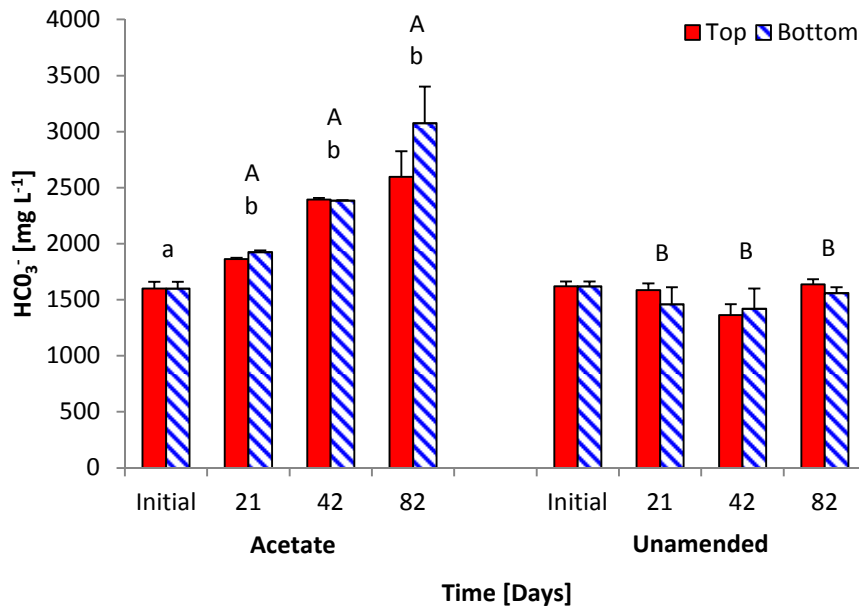


Figure 4-7. Pore-water HCO_3^- of 2 L settling columns of Syncrude MFT by treatment and incubation time. Error bars show S.E.; $n=2$ for Initial, 21 d, and 42 d, and $n=6$ for 82 d. (A) signifies a significant difference between the treatments (B), (b) signifies a significant difference within a treatment from initial values (a), and (*) signifies a significant difference between top and bottom values.

4.1.5. Pore-water Cations in 2L columns

The concentration of Ca^{2+} was determined in the MFT prepared for the columns at time zero, and in the top and bottom MFT of the settling columns at their respective time of decommissioning (Figure 4-8). At time zero, the acetate amended and unamended MFTs had similar Ca^{2+} concentrations 17.1 mg L^{-1} and 18.0 mg L^{-1} , respectively. Over the incubation period, Ca^{2+} concentrations of the MFT in both the acetate amended and unamended control columns increased. In the acetate columns, the top Ca^{2+} concentrations increased to 31.8 mg L^{-1} for 21 d, 27.1 mg L^{-1} for 42 d and 28.3 mg L^{-1} for 82 d. Likewise, Ca^{2+} in the bottom samples increased from the initial concentration to 33.2 mg L^{-1} for 21 d, 38.8 mg L^{-1} for 42 d and 29.2 mg L^{-1} for 82 d. In the unamended control columns, the top Ca^{2+} concentrations increased to 19.9 mg L^{-1} for 21 d, 26.3 mg L^{-1} for 42 d and 29.3 mg L^{-1} for 82 d. Likewise, Ca^{2+} in the bottom samples increased from the initial concentration to 32.1 mg L^{-1} for 21 d, 31.7 mg L^{-1} for 42 d and 27.9 mg L^{-1} for 82 d. The differences between treatments were not significant. The changes within treatments were significant in the acetate columns on 21, 42 and 82 d and in the unamended columns on 42 d and 82 d.

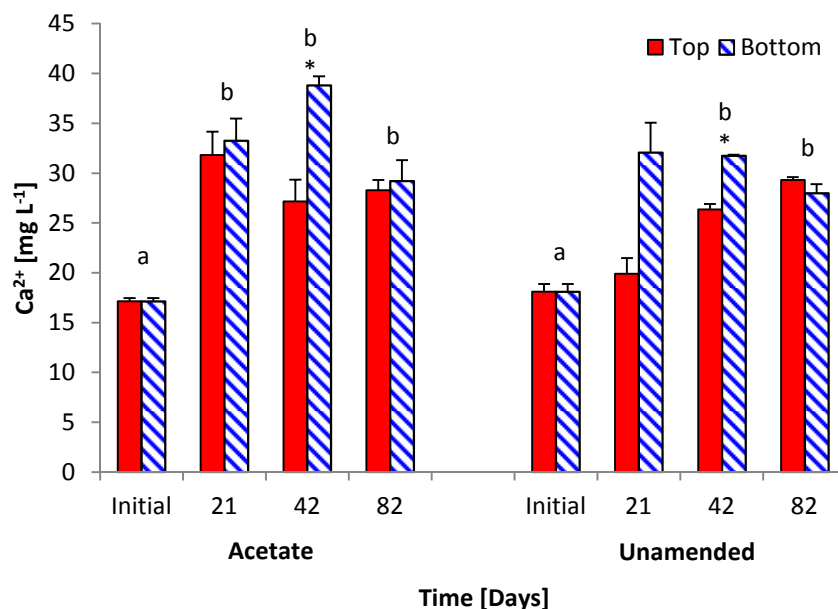


Figure 4-8. Pore-water Ca^{2+} of 2L settling columns of Syncrude MFT by treatment and incubation time. Error bars show S.E.; $n=2$ for Initial, 21 d, and 42 d, and $n=6$ for 82 d. (A) signifies a significant difference between the treatments (B), (b) signifies a significant difference within a treatment from initial values (a), and (*) signifies a significant difference between top and bottom values.

The concentration of Mg^{2+} was determined in the MFT prepared for the columns at time zero, and in the top and bottom MFT of the settling columns at their respective time of decommissioning (Figure 4-9). At time zero, the acetate amended and unamended MFTs had similar Mg^{2+} concentrations 17.7 mg L^{-1} and 16.6 mg L^{-1} , respectively. Over the incubation period, Mg^{2+} concentrations of the acetate amended columns increased and the concentrations in the unamended control columns remained unchanged. In the acetate columns, the top Mg^{2+} concentrations increased to 60.26 mg L^{-1} for 21 d, 34.7 mg L^{-1} for 42 d and 23.9 mg L^{-1} for 82 d. Likewise, Mg^{2+} in the bottom samples increased from the initial concentration to 46.0 mg L^{-1} for 21 d, 47.1 mg L^{-1} for 42 d and 34.8 mg L^{-1} for 82 d. The unamended control columns had Mg^{2+} concentrations in the range of 17.7 mg L^{-1} to 26.6 mg L^{-1} . The changes within the acetate columns were significant and the differences between treatments on 21, 42 and 82 d were significant.

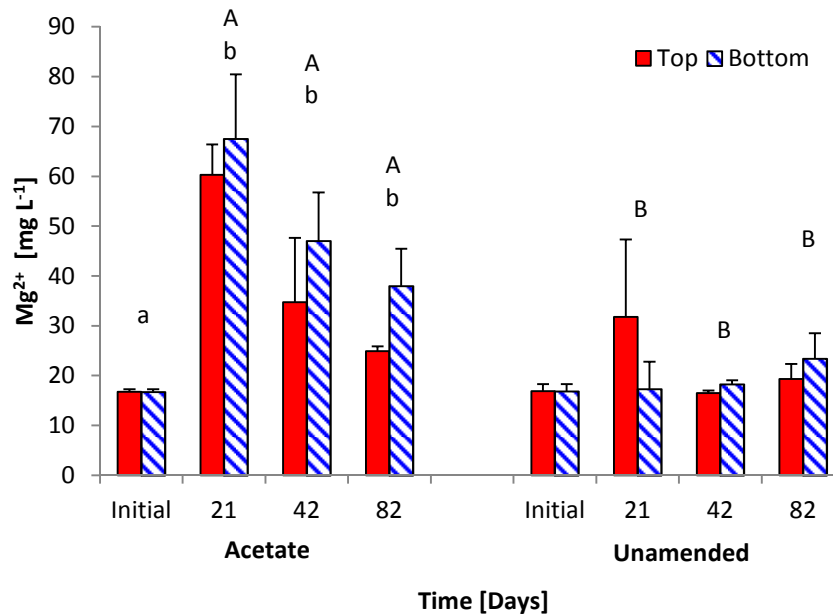


Figure 4-9. Pore-water Mg^{2+} of 2L settling columns of Syncrude MFT by treatment and incubation time. Error bars indicate S.E.; n=2 for Initial, 21 d, and 42 d, and n=6 for 82 d. (A) signifies a significant difference between the treatments (B), (b) signifies a significant difference within a treatment from initial values (a), and (*) signifies a significant difference between top and bottom values.

The concentration of Na^+ was determined in the MFT prepared for the columns at time zero, and in the top and bottom MFT of the settling columns at their respective time of decommissioning (Figure 4-10). The Na^+ concentrations were corrected for the Na^+ added in the form of sodium acetate. At time zero, the acetate amended and unamended MFTs had similar Na^+ concentrations 745.73 mg L^{-1} and 737.8 mg L^{-1} , respectively. Over the incubation period, Na^+ concentrations increased in both the acetate amended columns and the unamended control columns. In the acetate columns, the top Na^+ concentrations increased to 888.6 mg L^{-1} for 21 d, 881.1 mg L^{-1} for 42 d and 1214.8 mg L^{-1} for 82 d. Likewise, Na^+ in the bottom samples increased, from the initial concentration, to 967.7 mg L^{-1} for 21 d, 1163.3 mg L^{-1} for 42 d and 1215.9 mg L^{-1} for 82 d. The unamended control columns increased in the range of 999.81 mg L^{-1} to 1104.5 mg L^{-1} . In both

treatments the changes in pore-water Na^+ over time were significant. The differences between treatments were not significant, except between the 21 d columns.

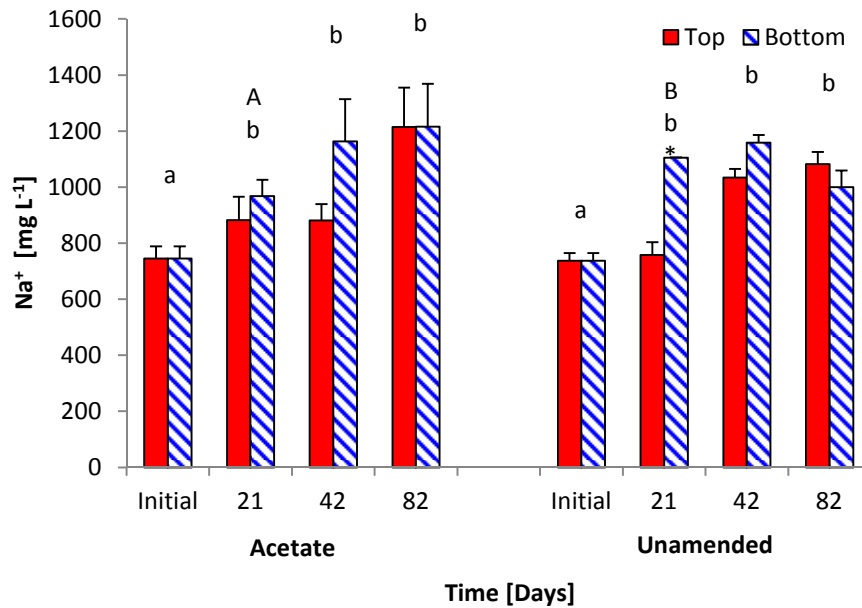


Figure 4-10. Pore-water Na^+ of 2L settling columns of Syncrude MFT by treatment and incubation time. Error bars represent S.E.; $n=2$ for Initial, 21 d, and 42 d, and $n=6$ for 82 d. (A) signifies a significant difference between the treatments (B), (b) signifies a significant difference within a treatment from initial values (a), and (*) signifies a significant difference between top and bottom values.

Over the incubation period, the concentration of K^+ remained stable in both the amended and unamended columns in the range of 26.12 to 32.47 mg L^{-1} (Figure 4-11), except for on 21 d the bottom MFT in the unamended columns had high K^+ concentration.

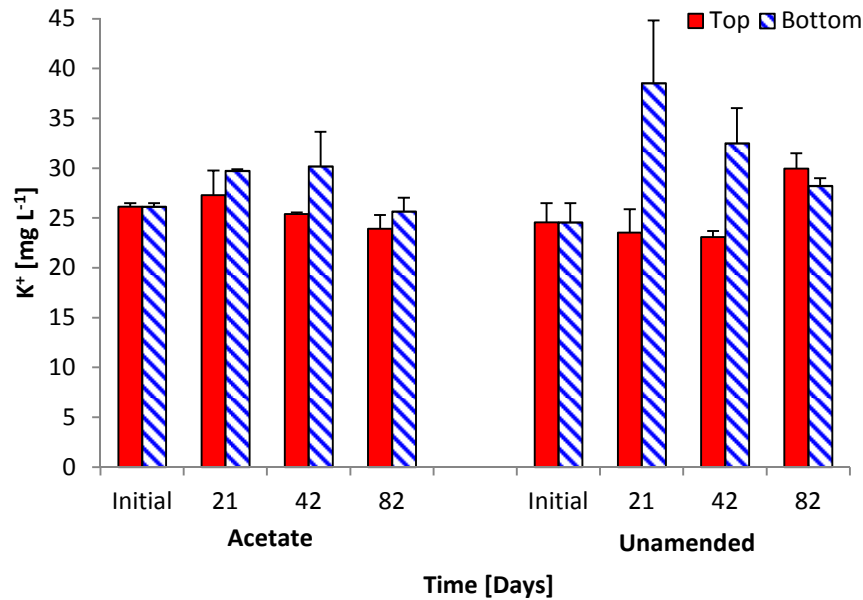


Figure 4-11. Pore-water K⁺ of 2L settling columns of Syncrude MFT by treatment and incubation time. Error bars show S.E.; n=2 for Initial, 21 d, and 42 d, and n=6 for 82 d. (A) signifies a significant difference between the treatments (B), (b) signifies a significant difference within a treatment from initial values (a), and (*) signifies a significant difference between top and bottom values.

Additional pore-water chemical analyses for trace additional elements includes: Al, Fe, B Al, Si, K, Cr, Fe, Mn, Ni, Co, Cu, Zn, Se, Sr, Mo, Cs, Ba, Pb and U. There were no apparent changes or trends in the concentrations during the incubation of the columns (Tables B-4 to B-9).

4.1.6. Exchangeable Cations in 2L columns

The exchangeable cations were determined for the acetate amended and unamended MFTs at time zero, and in the MFT sampled from the top and bottom of the columns at their respective time of decommissioning.

The initial exchangeable Ca in the acetate amended and the unamended MFTs were similar at 2.42 cmol_c kg⁻¹ and 2.61 cmol_c kg⁻¹, respectively (Figure 4-12). The exchangeable Ca increased to 3.64 cmol_c kg⁻¹ in the top MFT and 4.41 cmol_c kg⁻¹ in the bottom MFT in the acetate amended columns after 82 d. In all other columns, the exchangeable Ca remained unchanged. Within treatments only

the changes in the acetate 82 d columns were significant. The only significant difference between treatments were in the 82 d columns.

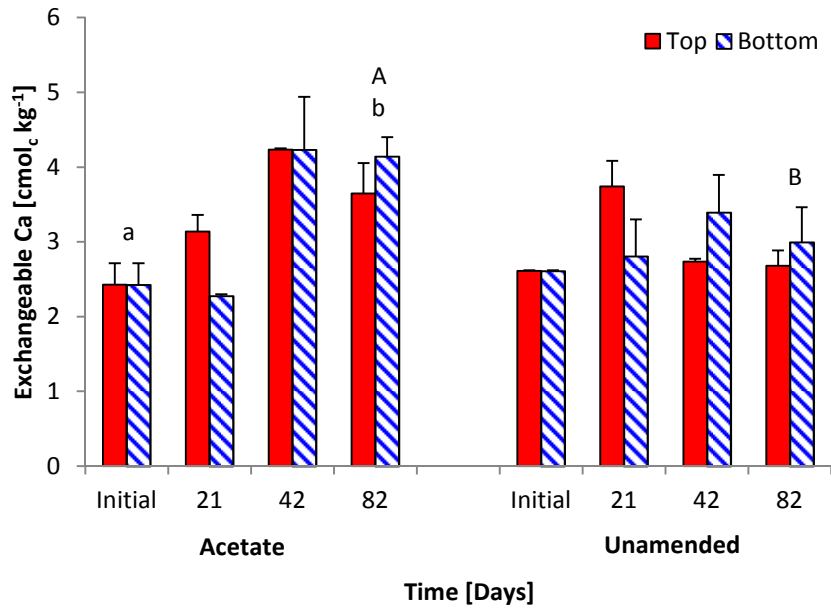


Figure 4-12. Exchangeable Ca of 2 L settling columns of Syncrude MFT by treatment and incubation time. Error bars show S.E.; n=2 for Initial, 21 d, and 42 d, and n=6 for 82 d. (A) signifies a significant difference between the treatments (B), (b) signifies a significant difference within a treatment from initial values (a), and (*) signifies a significant difference between top and bottom values.

The initial exchangeable Mg in the acetate amended and the unamended MFTs were similar at 1.41 cmol_c kg⁻¹ and 1.66 cmol_c kg⁻¹, respectively (Figure 4-13). The exchangeable Mg increased to 2.91 cmol_c kg⁻¹ in the top MFT and 3.61 cmol_c kg⁻¹ in the bottom MFT in the acetate amended columns at 82 d. In all other columns, the exchangeable Mg remained unchanged. Within treatments only the changes in the acetate 82 d columns were significant. The only significant difference between treatments were in the 82 d columns.

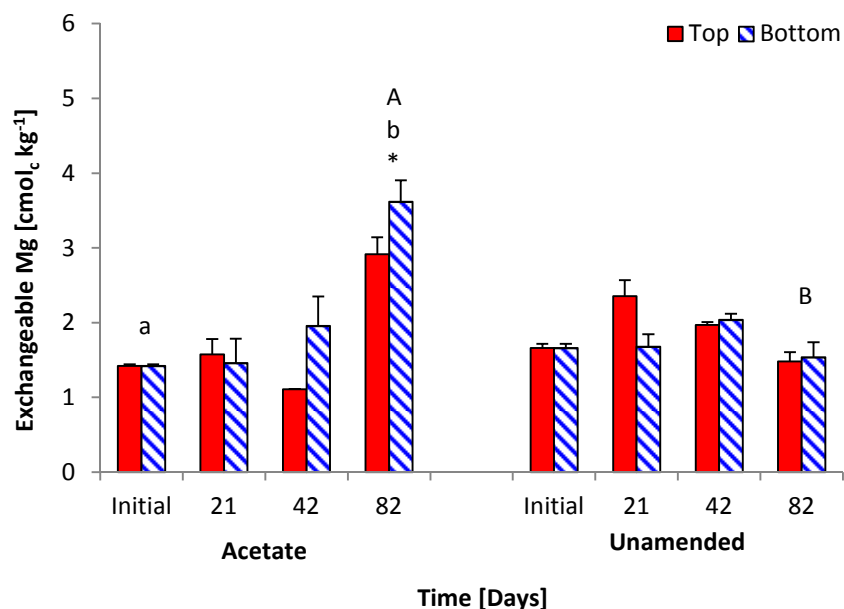


Figure 4-13. Exchangeable Mg of 2 L settling columns of Syncrude MFT by treatment and incubation time. Error bars show S.E.; n=2 for Initial, 21 d, and 42 d, and n=6 for 82 d. (A) signifies a significant difference between the treatments (B), (b) signifies a significant difference within a treatment from initial values (a), and (*) signifies a significant difference between top and bottom values.

The initial exchangeable Na in the amended columns (4.11 cmol_c kg⁻¹) was higher than unamended MFT (3.60 cmol_c kg⁻¹) (Figure 4-13). In both the acetate amended and unamended control columns, the exchangeable Na generally remained unchanged. Only the columns decommissioned on 21 d had significant changes in the exchangeable Na. The 21 d acetate column had a decrease to 2.56 cmol_c kg⁻¹ in the top MFT and 2.04 cmol_c kg⁻¹ in the bottom MFT compared to the 21 d unamended column where 4.08 cmol_c kg⁻¹ exchangeable Na was present in top zone of MFT. The change in exchangeable Na was only significant in both treatments in the 21 d columns. Between treatments, the difference in exchangeable Na was significant for the initial MFTs and the 21 day columns.

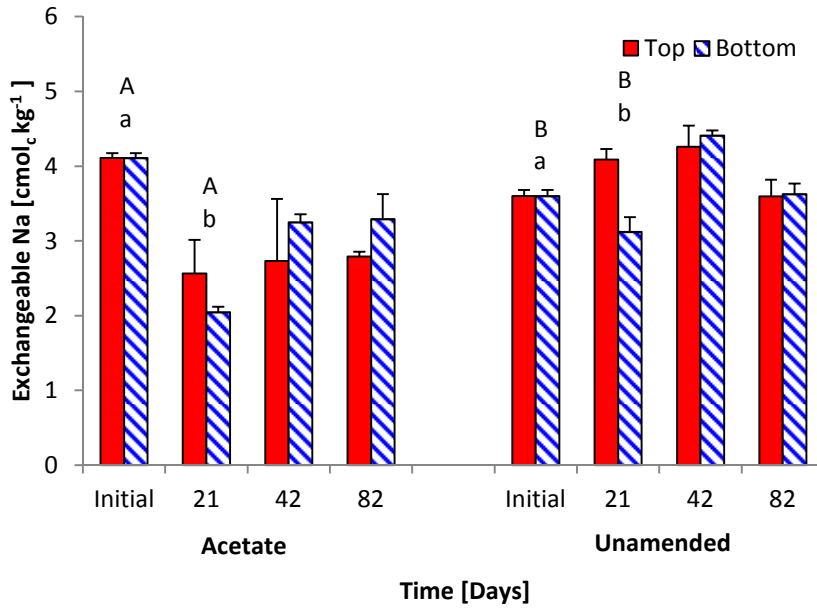


Figure 4-14. Exchangeable Na of 2 L settling columns of Syncrude MFT by treatment and incubation time. Error bars show S.E.; n=2 for Initial, 21 d, and 42 d, and n = 6 for 82 d. (A) signifies a significant difference between the treatments (B), (b) signifies a significant difference within a treatment from initial values (a), and (*) signifies a significant difference between top and bottom values.

The initial exchangeable K in the acetate amended and the unamended MFTs were similar, i.e., 0.54 cmol_c kg⁻¹ and 0.58 cmol_c kg⁻¹, respectively (Figure 4-15). Over the incubation period, the exchangeable K remained unchanged in all columns, in the range 0.40 to 0.82 cmol_c kg⁻¹.

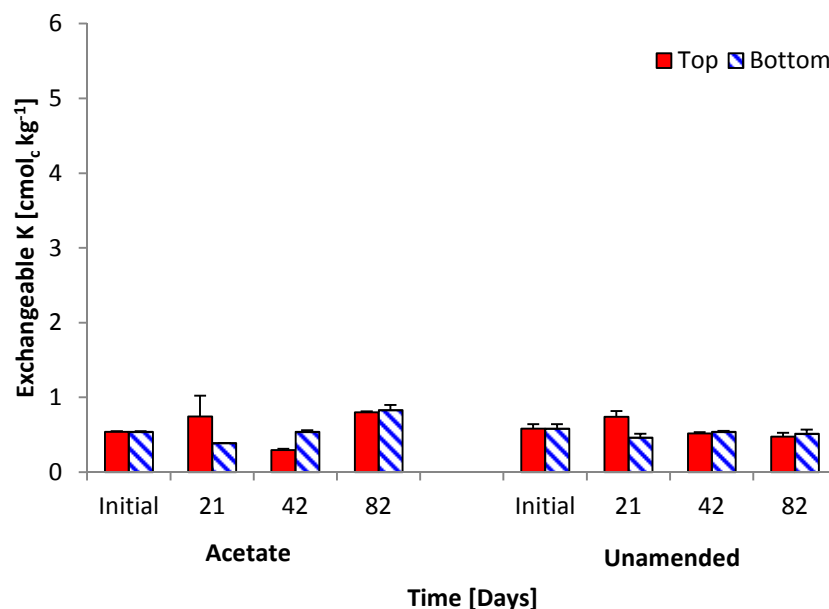


Figure 4-15. Exchangeable K of 2L settling columns of Syncrude MFT by treatment and time. Error bars show S.E.; n=2 for Initial, 21 d, and 42 d and n=6 for 82 d. (A) signifies a significant difference between the treatments (B), (b) signifies a significant difference within a treatment from initial values (a), and (*) signifies a significant difference between top and bottom values..

4.1.7. Chemical Analysis of Released Cap-Water in 2L column

Only the acetate amended columns generated enough cap-water to enable chemical analysis, thus no meaningful comparison between treatments could be made. The cap-water chemistry is found in Appendix B, Tables B-10 to B-14 and Figure B-6 to B-16.

4.2. 50L Settling Columns

Two 50 L settling column were filled with SCL MFT, one amended with hydrolyzed canola and the other as unamended control to investigate the chemical changes in the MFT undergoing methanogenic conditions. The columns were analyzed for gas production (Section 4.2.1.), water release and settling of MFT (Section 4.2.2.), pH (Section 4.2.3), pore-water concentrations of HCO_3^- and other anions (Section 4.2.4), pore-water cations (Section 4.2.5) and the carbonate content of the MFT solids (Section 4.2.6).

4.2.1. Gas Production in 50L columns

The column C (amended one) produced substantively more biogenic gases than the control UM (Figure 4-16). Over the incubation period the volume of gas produced by UM was 110 mL and C produced 4040 mL. In column C, gas began to be released by 6 d and increased in volume to 2800 mL by 35 d, then leveled off until 45 d. The volume of gas increased again from 2800 mL to 4000 mL by day 72 d. When biogas was produced in the MFT, it formed bubbles which remained entrained in MFT. This gas volume was not measured in the gas traps until the bubbles were released into the headspace through the MFT. The entrained gas increased the volume of the MFT. Over the first 50 d, the MFT in column C increased significantly in volume as biogas bubbles generated during metabolism of canola. At approximately 50 d, the MFT collapsed releasing significant pore-water and causing the second increase of captured biogenic gas. From 80d through 213 d, the column was visibly still producing gas bubbles without any corresponding increase of volume in the trap suggesting that the gas trap under-measure the true gas production.

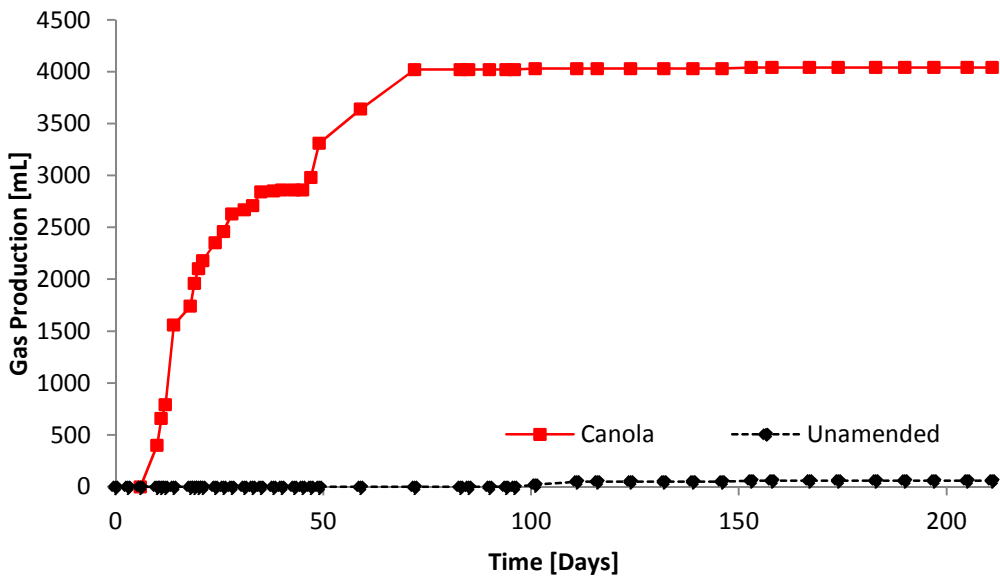


Figure 4-16. Volume of biogenic gases produced over 213 d of incubation in 50 L Syncrude MFT settling columns: canola amended and unamended control.

The analysis of headspace from the 50L columns by GC is presented in Figure 4-17. In column C, the concentration of CH₄ increased exponentially to 70% by 45 d and the concentration of CO₂ increases to a maximum of 11 % by 68 d and hovers around 10 % for the remainder of incubation. The decrease in CH₄ concentration after the peak was a result of disturbance caused by refilling the gas trap. The gas trap had a capacity of less than 2 L and when it was filled, it was reset by removing the entrapped gas by vacuum. In the control, the levels of CH₄ and CO₂ remained a constant 1.5 % and 3.3 % throughout the incubation, respectively.

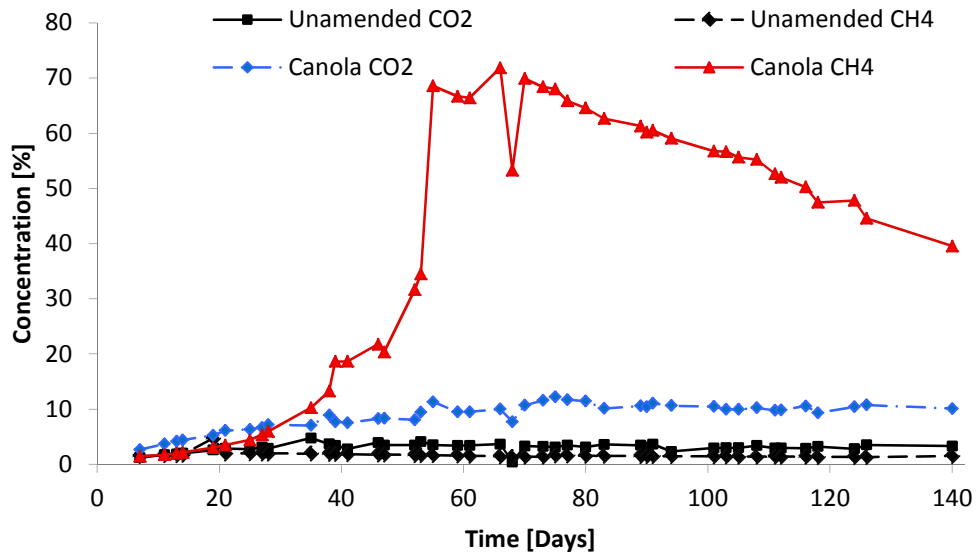


Figure 4-17. Composition of biogenic gases produced over 213 d of incubation in 50L Syncrude MFT settling columns: canola amended and unamended control.

4.2.2. Water Release and Settling of MFT in 50L columns

During the first phase of incubation from 0 d to 47 d, both column C and UM had similar water release behavior (Figure 4-18). During this phase, both columns released approximately 13.3 % of their initial pore-waters. At day 47 d, the large gas bubbles in column C began to collapse resulting in significant pore-water release and settling. The collapse event occurred over a 14 day period, after which the water release rate of column C remained steady. By 212 d of

incubation, columns C and UM release 34.3 % and 25.6 % of their initial pore-waters, respectively.

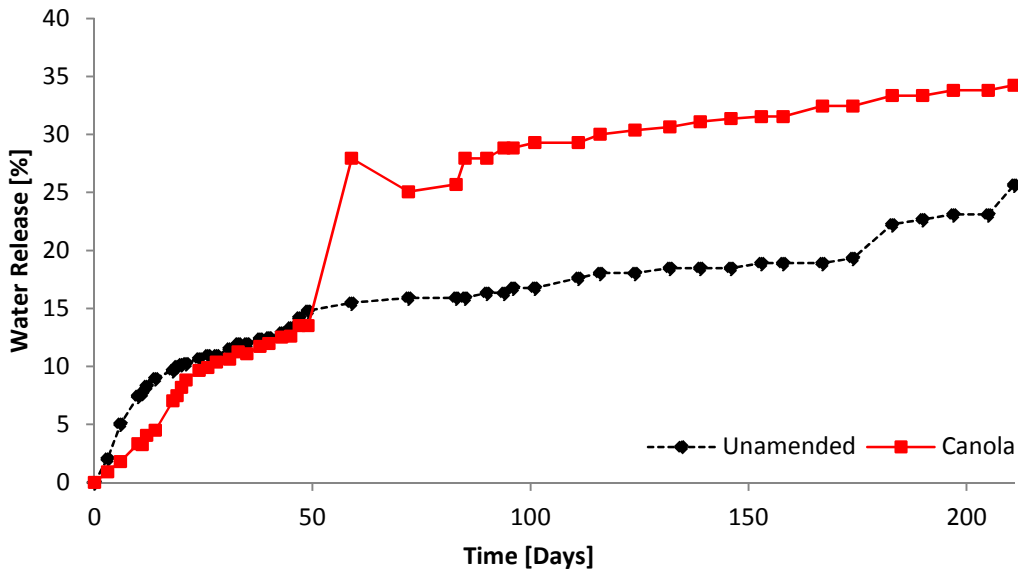


Figure 4-18. Water Release during 213 d incubation from 50 L Syncrude MFT settling columns: canola amended and unamended control. Release water is reported in volumetric percentage of initial pore-water.

The settling behavior of the columns differed substantively between treatments (Figure 4-19). UM began to settle quickly during the first 50 d, then the rate of settling slowed, remaining constant until 213 d. The settling rate of UM coincided with its water release rate. That was not the case for C. Initially the MFT in C increased in volume as biogenic gas was produced and entrained in the MFT. The largest observable bubbles reached a height of approximately 3 cm (Figure 4-20). On 47 d, the entrained gas bubbles began to collapse resulting in rapid settling over a 14 d period. The MFT in C subsequently settled at a constant rate. At day 21 both columns settled 26.2 cm, even though C had more water release. This is explained by the fact the C still had substantial amounts of entrained biogenic gases which increased the volume of the MFT.

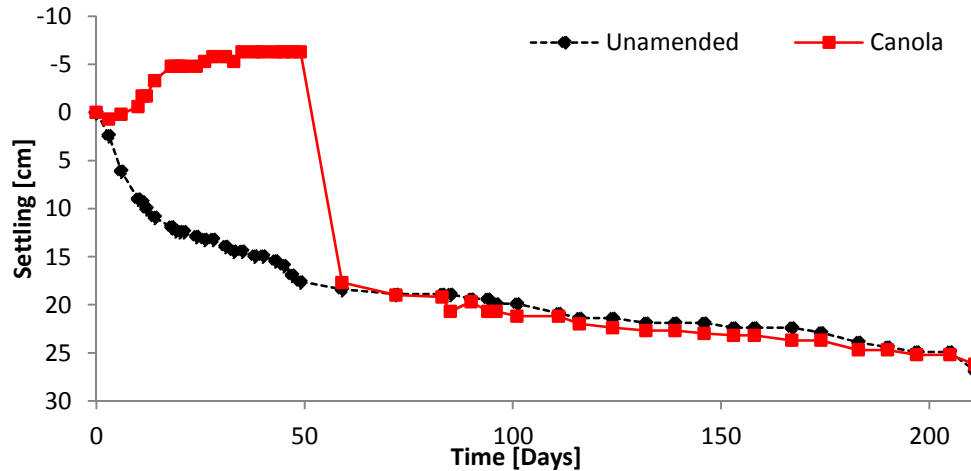


Figure 4-19. Settling of 50L Syncrude MFT settling columns: canola amended and unamended control. Settling reported as a decrease in solids-cap water interface in cm from initial height.



Figure 4-20. Formation of a large biogas bubble after 46 d of incubation in the 50L settling column amended with canola meal.

Colour changes occurred in the MFT in C during the production and collapse of biogenic gas bubbles (Figure 4-21). The MFT around a collapsed bubble turned into a lighter grey colour than the original MFT, creating a marbling pattern in the column. This was accompanied by an accumulation of bitumen on the surface of the cap-water and around the walls of the settling column. The colour of the MFT in the unamended control UM remained unchanged during incubation and had no accumulation of separated bitumen.

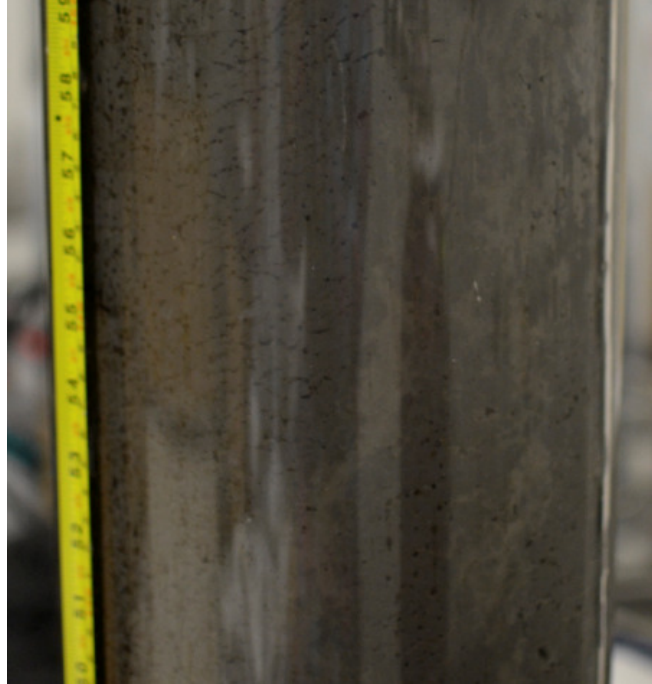


Figure 4-21. Appearance of lighter coloured MFT material marbled throughout the 50L settling column amended with canola meal after 62 d of incubation.

4.2.3. pH change in 50L columns

At time zero, the pH of the MFT in both C and UM columns had the same pH of 7.6 (Figure 4-22). Over the first 40 d of incubation, both pH varied considerably and increased to a maximum of 8.6. After 40 d, the pH of columns began to decline. UM decreased and approached its initial value of 7.6. After 40 d, the pH of C decreased more rapidly reaching minimums of 6.6 at 102 d and 6.5 at day 141. By 213 d the pH stabilized just below 7.

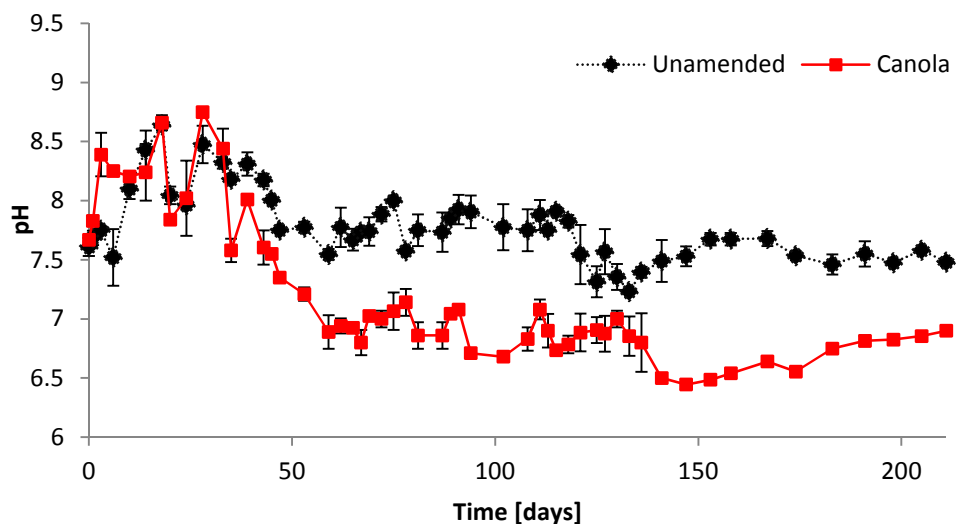


Figure 4-22. pH of 50 L Syncrude MFT settling columns: canola amended and unamended control. Values are mean pH of middle and bottom ports. Errors bars show S.E. with n=2.

4.2.4. HCO_3^- , SO_4^{2-} and Cl^- in 50L columns

On 213 d of incubation, samples from each of the ports on both columns were withdrawn to determine concentrations of anions (HCO_3^- , SO_4^{2-} , Cl^-). All the anion concentrations in column C were corrected for anions contributed by the canola amendment itself (Table C-1) to isolate the chemical changes caused by methanogenesis.

Column C had elevated concentrations HCO_3^- compared to column UM (Figure 4-23). The concentrations of HCO_3^- of the MFT in column C was 1499.1 mg L^{-1} in the middle port and 1487.1 mg L^{-1} in the bottom port while the concentrations of HCO_3^- of the MFT in column UM was 1406.7 mg L^{-1} in the middle port and 1387.8 mg L^{-1} in the bottom port. In both columns, there appeared to be no vertical gradient in HCO_3^- . In both columns, there was less HCO_3^- in the cap-water than the MFT pore-water.

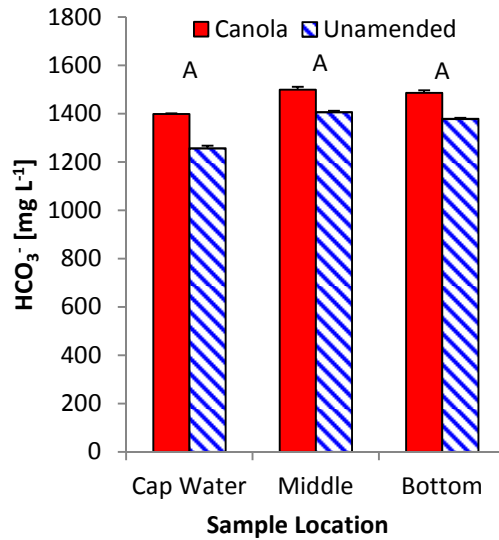


Figure 4-23. HCO_3^- concentrations in the cap-water and MFT pore-water collected from top, middle and bottom ports, respectively at canola amended and unamended control 50L settling columns. Incubation time was 213 at time of sampling. Error bars show S.E. with $n=2$. (A) Signifies a significant difference between the treatments.

The concentrations of PO_4^- , SO_4^{2-} and Cl^- MFT in samples withdrawn from the columns on day 213 of incubation were also determined. In all samples the concentration of PO_4^- was under detectable limits. The concentrations of SO_4^{2-} was negligible in the MFT samples and were in the range of 28.1 to 34.8 mg L^{-1} in the cap-water (Figure C-2).

4.2.5. Pore-Water Cations in 50L columns

On 212 d of incubation, samples from each of the ports on both columns were withdrawn to determine concentrations of cations (Ca^{2+} , Mg^{2+} , Na^+ , and K^+). All the cation concentrations in column C were corrected for cations contributed by the canola amendment itself (Table C-1), to isolate the chemical changes caused by methanogenesis.

Column C had elevated concentrations Ca^{2+} compared to column UM (Figure 4-24). The pore-water concentrations of Ca^{2+} of the MFT in column C was 26.7 mg L^{-1} in both the middle and lower port compared to 16.0 mg L^{-1} in UM. In both columns, the cap-water had similar concentrations of Ca^{2+} as their respective MFT pore-water had and there was no vertical gradient in Ca^{2+} in the MFT.

Similarly, the concentrations of Mg^{2+} was higher in columns C than in column UM, with 18.8 mg L^{-1} in both the middle and lower ports of C compared to 11.1 mg L^{-1} in UM. In both columns, the cap-water had similar concentrations of Mg^{2+} as their respective MFT had and there was no vertical gradient in Mg^{2+} concentration in the MFT.

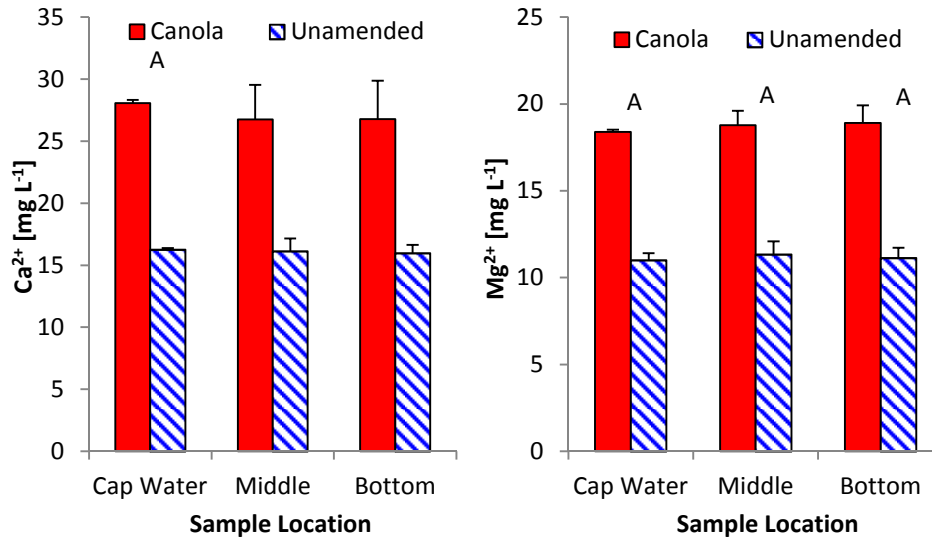


Figure 4-24. Ca²⁺ and Mg²⁺ concentrations of MFT pore-water and cap-water samples collected from top, middle and bottom ports of canola amended and unamended control 50 L MFT settling columns. Incubation time was 213 at time of sampling. Error bars show S.E., n=2. (A) Signifies a significant difference between the treatments.

The concentration of monovalent cations Na⁺ and K⁺ were similar in both columns (Figure 4-25). The concentrations of Na⁺ in the MFT were in the range of 825.4 to 837.0 mg L⁻¹ in the columns. The concentrations of K⁺ in the MFT were in the range of 14.0 to 14.7 mg L⁻¹. Neither column had a gradient in Na⁺ and K⁺ concentrations, and in both columns the cap-water had similar concentrations as the MFT.

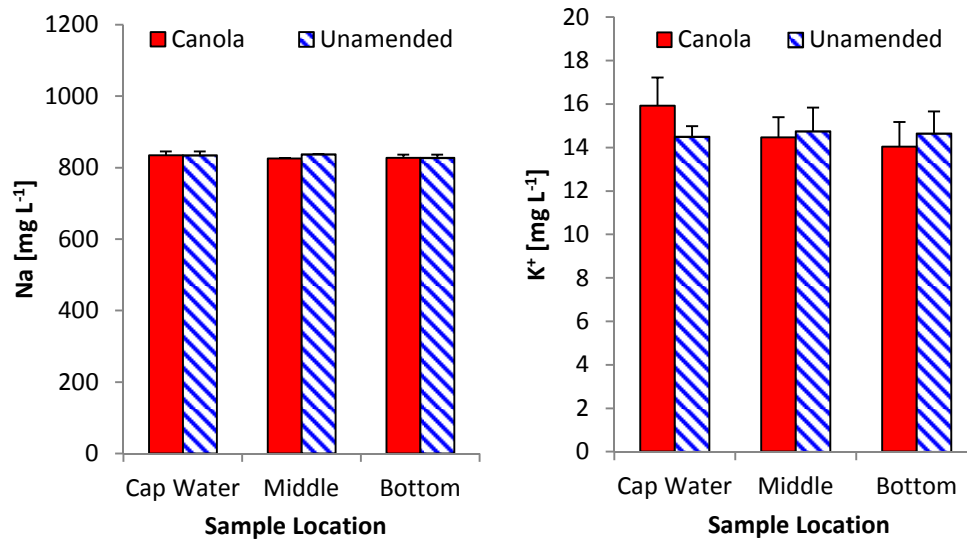


Figure 4-25. Na⁺ and K⁺ concentrations of MFT pore-water and cap-water samples collected from top, middle and bottom ports of canola amended and unamended control 50 L MFT settling columns. Incubation time was 213 at time of sampling. Error bars show S.E., n=2. (A) Signifies a significant difference between the treatments.

4.2.6. MFT Solids Carbonate Content in 50L columns

On 212 d of incubation, MFT samples were withdrawn from the middle and bottom port on both the columns to determine the carbonate contents of the MFT solids. In the middle port, column C had a lower carbonate content than column UM, 1.91 % and 2.73 %, respectively (Figure 4-26). In the bottom port, the difference between the columns was less, columns C and UM having carbonate contents of 2.51 % and 2.76 %, respectively. This suggests that there is a vertical gradient of carbonate content in the column C whereas the UM carbonate content appears to be uniform.

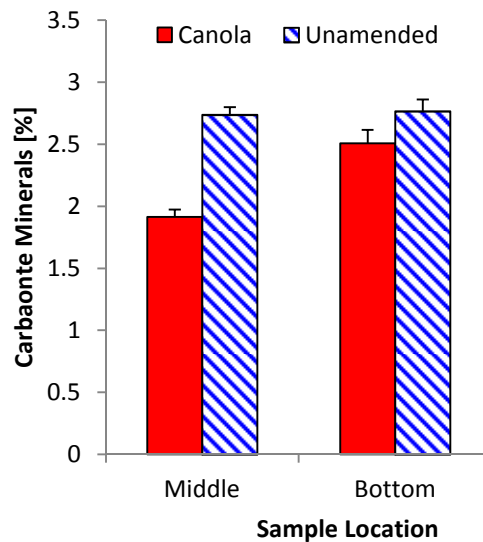


Figure 4-26. Carbonate contents of MFT solid fraction in samples collected from middle and bottom ports of canola amended and unamended control 50 L MFT settling columns. Incubation time was 213 at time of sampling. Error bars show S.E., n=2.

5. Discussion

5.1. Water Release and Settling

In both the experiments, the amended MFT released significantly more pore-water to the surface as cap-water than the unamended control MFT. In Experiment 1 over a period of 82 d of incubation, the acetate amended columns released about 28% more pore-water compared to the unamended control. In Experiment 2 after 213 d of incubation, amended column C released about 9 % more water compared to the unamended control. The majority of the water released from the amended MFT occurred within 40 d for Experiment 1 and 50 d for Experiment 2. It was expected that the methanogenic accelerated-dewatering would occur much faster in Experiment 1, because the amended canola Experiment 2 has to first be converted to acetate prior to acetoclastic or hydrogenotrophic methanogenesis (Section 2.2.4.).

The water release and settling behaviors of the unamended control MFT differed significantly between Experiment 1 and Experiment 2 (Figures 4-1, 4-2, 4-17 and 4-18). In Experiment 1, the unamended control MFT did not settle or release any significant amount of pore-water (less than 3.33 % of its initial pore-water), whereas in Experiment 2, the unamended control MFT had significant water recovery, releasing 25.6 % of its initial pore-water. The MFT received from SCL used in this research had a gravimetric water content of 60.89 %, which was adjusted to 75.00 % by adding cap-water before filling up the 50L columns. If the physical and chemical characteristics of this batch of MFT are such that the original solids content naturally densifies, the added cap-water would release into the surface during the settling, which would correspond to water release of 18.8 %. This accounts for the majority of the water release in the 50L unamended control MFT and would account for approximately half of the water release in the canola amended MFT.

There was a large variation in water release and settling of the acetate amended MFT in Experiment 2, probably due to incomplete mixing of the amended sodium acetate during the preparation of the MFT. The adjusted pore-

water concentration of Na^+ varies between 882.1 to 1215.2 mg L^{-1} (Figure 4-10), indicating that the MFT in each column received a different dosage of the amendment. The variation in water release also corresponded with visually observed gas production and with pore-water concentrations of HCO_3^- . The MFT with greater water release, had increased Na^+ (due to more sodium acetate) and HCO_3^- , indicating that they had a higher dosage of amendment and increased levels of methanogenesis.

The settling behavior of the amended MFT was similar in both experiments (Figures 4-2 and 4-18). During the initial period of incubation, the amended MFT increased in height as methanogenesis began to occur. After this increase, the MFT collapsed rapidly, generating the majority of the released water. Even after the collapse, the MFT retained substantial volumes of entrained gas bubbles. Increase in the volume of MFT undergoing methanogenesis has been reported by Fedorak et al. (2000), Li (2010) and Lou (2004). The entrainment of produced biogases causes the measurement of settling to understate the benefits of biodensification. The measurement of released water is a better indicator of biodensification.

5.2. Chemical Changes

5.2.1. Biogenic Gas Production

In both Experiments 1 and 2, the carbon amended MFT produced more biogenic gases than the unamended control MFT. In Experiment 2, the amended MFT produced 36.7 times the amount of biogenic gases as the unamended control produced (Figure-16). In Experiment 1, the volume of biogenic gases was not directly quantified. However, the acetate amended MFT visibly generated significant entrained gas bubbles as seen in the photographs, whereas the unamended control MFT did not. The amended MFT in Experiment 1 began to produce biogenic gases earlier in incubation than the amended MFT in Experiment 2. This is because the amended canola has to first be activated and fermented into acetate prior to acetoclastic methanogenesis or hydrogenotrophic methanogenesis (Lay et al. 1998).

The composition of the biogenic gases produced was determined in Experiment 2. In Experiment 2, analysis of the released biogases showed that the percentage of CH₄ increased from an initial value of 0 to 70 % within 65 d of incubation and CO₂ increased from 0 to 11 % (Figure 4-17). There is a lag between production of the biogenic gas species in the MFT and their detection on the GC-MS, as when the gases are produced in the MFT they initially remained entrained in the MFT. Then the entrained gas bubbles move to the surface of the MFT and are then released into headspace and analyzed. As a result, chemical changes in the pore-water will appear to occur prior to changes in release gas chemistry, when in fact they occur simultaneously.

When CH₄ is produced via methanogenesis, CO₂ is produced in equal quantity (Equation 2-6). This CO₂ can be reduced hydrogenotrophic methanogenesis (Equation 2-7) or released into the MFT. The theoretical gas production produced via anaerobic methanogenesis can be calculated from the chemical composition of the substrate using the Buswell equation (Roberts 2002). The elemental analysis of the canola used in Experiment 2 (Table C-3) shows the ratio of carbon to hydrogen similar C₇H₁₂. Thus C₇H₁₂ was used as the basis to estimate the theoretical productions of CH₄ and CO₂ from the hydrolyzed canola (Equation 5-1):



The canola column was amended with 64 g of hydrolyzed canola which contained 17.9 g of Carbon and 2.6 g of Hydrogen, which is equivalent to 0.212 mol C₇H₁₂. Eq. 5-1 predicts that this would produce 1.06 mol CH₄ and 0.42 mol CO₂. Assuming that the gases are ideal the theoretical gas volumes are 26.0 L CH₄ and 10.4 L. The volumes collected in the gas traps were 26.2 L CH₄ and 4.08 L CO₂. This suggests that the hydrolyzed canola was completely degraded. The source of the excess CH₄ is from residual processing hydrocarbon in the MFT. The volume of CO₂ produced is 39.2 % of the predicted value. This is because the produced CO₂ released either gas or dissolved as HCO₃⁻ and H⁺ in the pore-water (Equations 2-8 to 2-10). This is evident Experiment 2, as the concentration of

HCO_3^- increased in the amended MFT (4-21). The increased concentration of HCO_3^- in amended MFT was also evident in Experiment 1.

The suitable Eh for methanogenesis is in the range of -150 mV to -220 mV (Fedorak et al. 2000). The measured Eh in the acetate amended MFT in Experiment 1 never reached that range (Figure 4-6). The Eh was determined by first separating the pore-water by centrifugation (Section 3.2.5.6.); this handling of the MFT prior to measurement may have skewed the reading. Also, Fedorak et al. (2000) suggested that microsites with low Eh host pockets of methanogenesis and that the measure Eh is not sensitive to these sites. Lou (2004) reported positive Eh measurements in methanogenic settling columns of MFT and CT.

In Experiment 1, the MFT had concentrations of SO_4^{2-} (Table B-3) in the range of 37.15 to 77.95 mg L^{-1} , and in Experiment 2, amended MFT had a slightly higher level of SO_4^{2-} compared to the unamended MFT (Figure C-2). Theoretically, sulphate reducing bacteria (SRB) should out-compete methanogens for common substrates, such as H_2 and acetate (Lay 1998). Thus, SO_4^{2-} should be depleted before CH_4 production begins (Fedorak et al. 2000). However, methanogenesis has been shown to occur in MFT concurrently with SO_4^{2-} reduction (Salluom et al. 2002; Fedorak et al. 2003). During sample preparation performed under normal atmosphere, sulfide exposed to air could produce SO_4^{2-} .

5.2.2. Pore-Water HCO_3^- and pH

The enhanced microbial activity detailed above induces chemical changes in the MFT. As the microbial consortium in the MFT produces CO_2 , some of the CO_2 dissolves as carbonic acid, lowering the pH and increasing the concentration of HCO_3^- . This process is fully evident in Experiment 2 and partially in Experiment 1.

In Experiment 1, there is a clear increase in pore-water HCO_3^- in the amended MFT compared to the unamended control MFT (Figure 4-7). However, there is no clear accompanying decrease in pH in the amended MFT. The pH of the acetate amended MFT was measured *in situ* during incubation and only a

decrease from the initial 7.62 to a minimum of 7.13 (Figure 4-4) was observed. The pH measured during the decommissioning of the acetate amended columns showed a slight decrease from 7.50 to 7.14 for 82 d of incubation (Figure 4-5). One column, (A4) decommissioned at 21 d of incubation, had an exceptionally low pH of 5.3 in top MFT and 6.6 in the MFT collected from the bottom of the column. The pH measured *in situ* during incubation may be higher than the actual value. This is because the measurement was taken by vertically inserting the probe through the cap-water into the MFT, mixing in some cap-water to where the measurement was taken. The cap-water has a significantly higher pH than the MFT (Figure B-6).

In Experiment 2, the pH of amended MFT decreased significantly compared to unamended control (Figure 4-20). The decrease in pH in amended MFT coincides with the increase in biogas production in the MFT as discussed above. As the biogas production levels off in amended MFT, the pH stabilizes. At 213 d of incubation, the columns in Experiment 2 were sampled and analyzed for concentration of HCO_3^- in the MFT and amended MFT showed elevated levels of HCO_3^- compared to unamended MFT column (Figure 4-21).

Li (2010) performed a similar analysis of pH and HCO_3^- concentrations in settling columns of Shell Albian MFT, treated with 200 mg L^{-1} citrate and incubated for 10 months. Li (2010) found elevated concentrations of HCO_3^- in the citrate amended MFT compared to the unamended control MFT, increasing from an initial value of 500 mg L^{-1} to a final value of 550 mg L^{-1} , along with a decrease in pH from 7.7 to a minimal value of 6.6 in the citrate amended MFT after 30 d of incubation. By 150 d of incubation, the pH returned to alkaline conditions of 8.10 to 8.25 for the remainder of the incubation. Fedorak et al. (2003) reported an increase in HCO_3^- , from 1600 mg L^{-1} to 2500 mg L^{-1} in SO_4^{-2} amended SCL methanogenic MFT that was incubated for 350 d. Similarly, Salloum et al. (2002) reported an increase in HCO_3^- in SCL MFT amended with SO_4^{-2} that was also methanogenic, from 1700 mg L^{-1} to 1250 mg L^{-1} over an incubation period of 65 d.

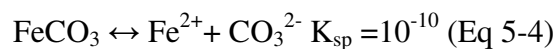
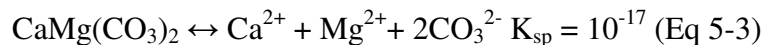
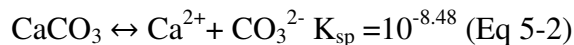
As discussed in Section 2.2.2., MFT contains carbonate minerals and as discussed in Section 2.3, carbonate minerals can be a possible source and sink of pore-water HCO_3^- because carbonate minerals can dissolve and precipitate under changing environmental conditions, especially changing pH. This couples HCO_3^- to changes in pore-water cations, which is discussed in the next section.

5.2.3. Pore-Water Cations and Carbonate Minerals

In both experiments, during incubation there were changes in the composition of pore-water cations in the amended MFT, including increases in divalent cations Ca^{2+} and Mg^{2+} . In Experiment 1, the pore-water concentration of Ca^{2+} increased in both the amended and unamended control MFT during incubation (Figure 4-8). In Experiment 1, the pore-water concentration of Mg^{2+} increased in the amended MFT and remained unchanged in the unamended control MFT (Figure 4-9). In Experiment 2, the pore-water Ca^{2+} and Mg^{2+} concentrations elevated in column C as to column UM.

The source of the increased pore-water concentrations of Ca^{2+} and Mg^{2+} might be the dissolution of carbonate minerals in the MFT caused by microbial activity inducing a lower pH, as discussed above. The dissolution of carbonate minerals was evident in Experiment 2; the carbonate content determined for the solids fraction of MFT was lower in Column C than in Column UM (Figure 4-26).

As discussed in section 2.2.2., MFT contains carbonates such as CaCO_3 , $\text{CaMg}(\text{CO}_3)_2$ and FeCO_3 (Kaminsky 2008). The solubility equations for these species are shown in Equations 5-2, 5-3 and 5-4 with their solubility product at 25°C (Tan 2010):



As the pH in the MFT lowers, CaCO_3 is the first mineral to begin to dissolve followed by $\text{CaMg}(\text{CO}_3)_2$ and FeCO_3 . The solution chemistry of $\text{CaMg}(\text{CO}_3)_2$ is not well understood (Luttge et al. 2003). $\text{CaMg}(\text{CO}_3)_2$ undergoes incongruent dissolution where more Mg^{2+} dissolves than Ca^{2+} . The crystalline structure of $\text{CaMg}(\text{CO}_3)_2$ has alternating sheets of Mg^{2+} and Ca^{2+} with CO_3 in between. It is speculated that incongruent dissolution occurs because as $\text{CaMg}(\text{CO}_3)_2$ dissolves, pits are formed in the surface allowing access to the Mg^{2+} sheets (Luttge et al. 2003). This may explain the elevated levels of Mg^{2+} in the amended MFT in Experiment 1.

The high levels of Mg^{2+} compared to Ca^{2+} in the amended MFT pore-water may also be explained by the precipitation behavior of CaCO_3 and $\text{CaMg}(\text{CO}_3)_2$. High concentrations of dissolved HCO_3^- precipitate with pore-water cations in alkaline conditions to form carbonates. Calcite is the dominant carbonate formed during precipitation (Blusset and Plumber 1982). This is because when dolomite dissolves, it does not precipitate as $\text{CaMg}(\text{CO}_3)_2$ but CaCO_3 . As the pH varies in the MFT, the carbonates minerals are dissolved and precipitated.

The solution chemistry of carbonates is usually studied in single species systems using crystalline samples. The MFT contains amorphous as well as crystalline minerals (Luttge et al. 2003). Amorphous minerals are more readily dissolved, which may explain why CaCO_3 and $\text{CaMg}(\text{CO}_3)_2$ could be dissolved at higher pH than expected in the methanogenic MFT, which could explain the significant increase in Mg^{2+} in the amended MFT in both Experiment 1 and 2.

5.2.4. Exchangeable Cations

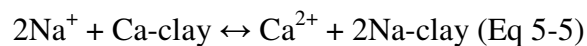
The pore-water chemical changes occurring during methanogenesis lead to changes in the exchangeable cations in the MFT. In Experiment 1, the exchangeable Ca^{2+} changed from the initial value of $2.41 \text{ cmol}_c \text{ kg}^{-1}$ to $4.41 \text{ cmol}_c \text{ kg}^{-1}$ after 82 d of incubation (Figure 4-13). Similarly, the exchangeable Mg^{2+} changed from the initial value of $1.41 \text{ cmol}_c \text{ kg}^{-1}$ to $3.61 \text{ cmol}_c \text{ kg}^{-1}$ after 82 d of incubation (Figure 4-14). The changes in exchangeable Na^+ decreased slightly,

however the decrease was not significant (Figure 4-15). The exchangeable K^+ remained unchanged throughout the incubation.

The exchangeable cations in MFT, or any oil sands processing streams, have never been previously determined. It is assumed that the exchange surfaces of the clays are dominated by Na^+ (Kaminski 2011; Omotoso 2011). This assumption is based on the pore-water chemistry of the MFT: Na^+ is the dominant pore-water cation (approximately 1000 mg L^{-1}), having concentrations of two orders of magnitude higher than divalent cations Mg^{2+} and Ca^{2+} (approximately 10 to 20 mg L^{-1}). The analysis of exchangeable cations in the MFT (Figures 4-13 to 4-16) show that Na^+ comprises the majority of the exchangeable cations, followed by Ca^{2+} and Mg^{2+} . The difference between Na^+ and the divalent cations is not nearly as large as the difference in concentrations in the pore-water.

The composition of exchangeable cations in MFT is similar to the composition of river and terrestrial clays treated with sea water (Sayles and Mangeldorf 1977). Sea water has a Na^+ concentration of $\sim 10000 \text{ mg L}^{-1}$, which is an order of magnitude higher than MFT pore-water. Sayles and Mangeldorf (1997) found that Na^+ comprised 24 to 55 % of the exchangeable cations, Mg^{2+} comprised 22 % to 40 % and Ca^{2+} comprised 1 % to 26 %.

Since the exchangeable cations are in equilibrium with the pore-water cations, changes in exchangeable cations should be reflective of changes in pore-water chemistry. Cation exchange reactions occur according to the law of mass action, for the exchange reaction of heterovalent system (such as Ca^{2+} and Na^+) is expressed (Tan 2010):



The cation exchange equilibrium of two species in a heterovalent salt solution is shown with the Gapon equation (Tan 2010):

$$\frac{[Na^+]\sqrt{[Ca^{2+}]}}{[Na^+]\sqrt{[Ca^{2+}]}} = \sqrt{K} \text{ (Eq 5-6)}$$

Where K is the exchange equilibrium constant and $[]$ denote exchangeable concentration and $()$ denote pore-water concentration. The application of the Gapon equation for oil sands clays is not well understood because of a lack of laboratory exchangeable cation investigation on oil sands clays (Holden et al. 2011), though it still gives a framework to interpret changes in exchangeable cations during methanogenesis.

In Experiment 1 for the 82 d amended columns, the increase in pore-water concentrations of Mg^{2+} and Ca^{2+} in the MFT did lead to an increase in exchangeable Mg^{2+} and Ca^{2+} . However, the 82 d unamended control MFT also had an increase of pore-water Ca^{2+} which did not result in an increase in exchangeable Ca^{2+} .

From Equation 5-4, the increase in exchangeable Mg^{2+} and Ca^{2+} in the 82 d acetate amended columns in Experiment 1 should have resulted in an equivalent decrease in exchangeable Na^+ . This was not the case, as exchangeable Na^+ did not decrease significantly. This might be due to either the limitation of the method used because soluble cations need to be subtracted from the total extractable cations to calculate exchangeable cations, and already very high concentration of Na^+ was present in the pore-water that could mask the differences between the treatments. Also, the sum of measured cation in exchange, known as effective cation exchange capacity (CECe) (Tan 2010), increased during the incubation period.

The increase of CECe was unexpected, as CEC should decrease as pH decreases, as discussed in Section 2.2.2.1. The increase in CECe in the amended MFT may be explained by the apparent separation of bitumen from the solids which could expose more clay surfaces to the pore-water. Kaminski (2008) found that when determining CEC of MFT using the Methyl Blue Index (MBI), removing the bitumen from the solids did not affect the CEC. The MBI method gives the maximum CEC possible of a sample. The results of the MBI do not give you the CEC of a sample under anaerobic conditions as it involves sonicating the sample in a solution to fully disperse all the peds of MFT solids, which

effectively removes the bitumen from the sample. Increase in CECE might be due to the formation of new minerals during the incubation.

A limitation in the determination exchangeable cations was that the extractant used was a mixture of 0.1 M BaCl₂/0.1 M NH₄Cl (Section 3.2.6.9.) contained cations (Ba²⁺ and NH₄⁺) that probably exist on the exchange surfaces of the MFT. The MFT pore-water concentrations were 0.00 to 1.79 mg L⁻¹ for Ba²⁺ and 3.92 to 10.55 for NH₄⁺ (Tables B-3 and B-8). At these pore-water concentrations, the exchangeable Ba and NH₄ is probably low, but could be accounted for by using a different extractant.

The increase in divalent exchangeable cations in the amended MFT contributes to flocculation, enhancing settling and accelerated dewatering of MFT (Tan 2010). As divalent cations replace monovalent cations, it increases the mean counter charge (Z_{μ}) which influence the colloidal properties of the suspended clays in the MFT.

5.2.5. Diffuse Double Layer and Water Release

The mechanism that links the changes in the pore-water chemistry during methanogenesis to changes in the flocculation and settling of the MFT is the DDL surrounding the suspended clay particles in the MFT (as discussed in Section 2.2.2.3.). The DDL thickness can be suppressed by increasing the ionic strength of the pore-water and by increasing the valence of exchangeable cations. When the DDL thickness is decreased, it promotes flocculation of the clay particles suspended in the MFT.

In both experiments the ionic strength of the pore-water fluid increased in the amended columns during incubation. Ionic strength was calculated from the concentrations of pore-water species (Figures 4-7 to 4-11, Tables B-3 to B-9) using Equation 5-7 (Tan 2010):

$$I = \frac{1}{2} \sum Z_j^2 c_j \text{ (Eq 5-7)}$$

where, I is the ionic strength, Z is the charge of the j^{th} species and c is the molar concentration j^{th} species. In Experiment 1, the ionic strength in the acetate amended MFT increased from an initial value of 0.051 M to 0.065 by 21 d, to 0.073 M by 42 d and to 0.078 M by 82 d (Figure 5-1). The ionic strength in the unamended control MFT remained unchanged in the 0.051 M to 0.062 M range. The increase in pore-water HCO_3^- accounts for the majority of the increase in ionic strength in the acetate amended MFT. Similarly in Experiment 2, the ionic strength of the pore-water was elevated in amended MFT compared to unamended MFT (Figure C-3) after 213 d of incubation. The thickness of the DDL is proportional to the inverse square of ionic strength (Equation 2-5).

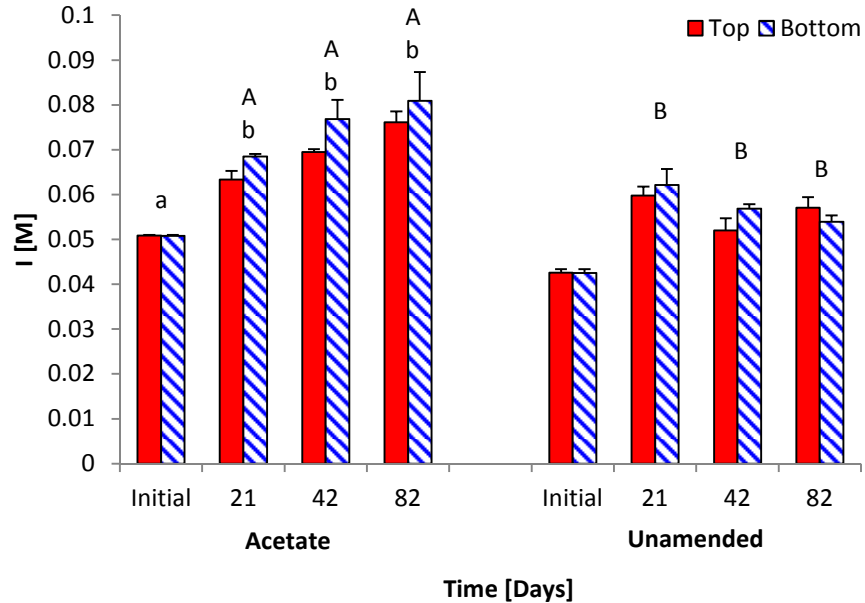


Figure 5-1. Ionic Strength (I) of 2L settling columns of Syncrude MFT by treatment and time. Error bars show S.E., $n=2$ for Initial, 21 d, and 42 d, and $n=6$ for 82 d. (A) signifies a significant difference between the treatments (B), (b) signifies a significant difference within a treatment from initial values (a), and (*) signifies a significant difference between top and bottom values.

In Experiment 1, the measured composition of exchangeable cations showed an increase in exchangeable divalent cations, Ca^{2+} and Mg^{2+} , in the 82 d acetate amended MFT (Figures 4-13 and 4-14). The valence of the exchangeable cations is inversely proportional to the thickness of the DDL (Equation 2-5).

Normally, colloidal systems are studied with monovalent electrolyte systems and the Z is an integer: $Z = 1,2,3\dots$ (Tan 2010). The colloidal system in MFT is heterovalent with monovalent species (Na^+ , K^+) and divalent species (Ca^{2+} , Mg^{2+}), thus using an integer as a Z gives a poor representation of the charge of the exchangeable cations on the clays surfaces in MFT. The value for charge representative of the suspended clay particles in the MFT was determined by taking the weighted average of the charges of the exchangeable cations (Equation 5-8):

$$Z_{\mu} = \sum_{i=1}^j \chi_j Z_j \text{ (Eq 5-8)}$$

Where Z_{μ} is the average charge, and χ_j is the molar fraction of the j^{th} exchangeable cation. With this approximation, the Z_{μ} of the acetate amended MFT increases from an initial value of $1.29 \text{ cmol}_c \text{ kg}^{-1}$ to $1.49 \text{ cmol}_c \text{ kg}^{-1}$ in the 82 d columns (Figure 5-2). The Z_{μ} of the unamended control MFT remained unchanged.

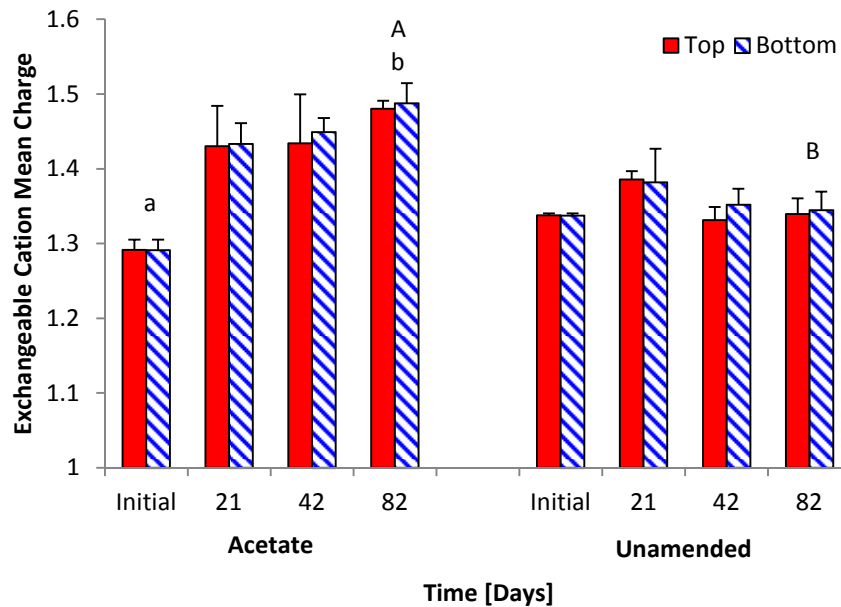


Figure 5-2. Exchangeable cations mean charge on clays in the MFT of 2L settling columns by treatment and time. Error bars show S.E.; $n=2$ for Initial, 21 d, and 42 d and $n=6$ for 82 d. (A) signifies a significant difference between the treatments (B), (b) signifies a significant difference within a treatment from initial values (a), and (*) signifies a significant difference between top and bottom values.

Using equation 2-5 with ionic strength and Z_{μ} , the DDL thickness was estimated for the columns in Experiment 1 (Figure 5-3). The estimated DDL decreases by more than half in the acetate amended MFT from 9.10×10^{-8} m at time zero to 3.49×10^{-8} at 82 d of incubation. The DDL thickness of the unamended control MFT remained unchanged during incubation.

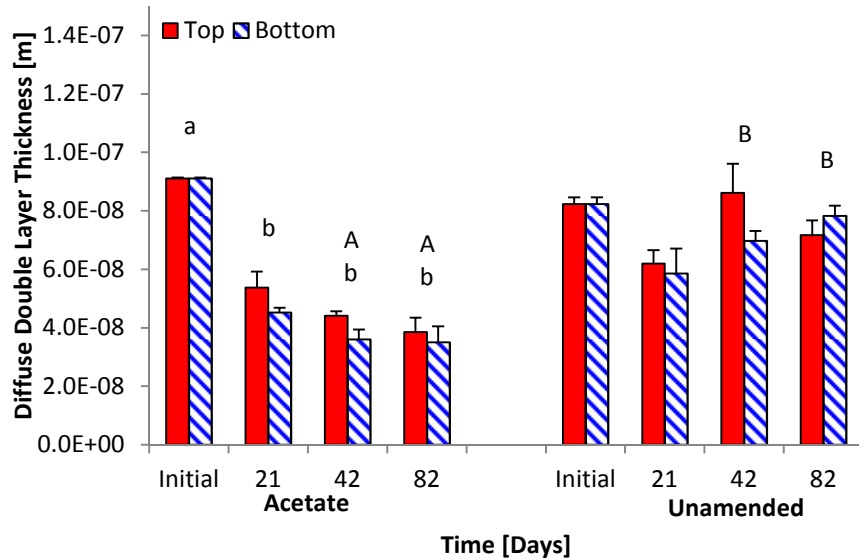


Figure 5-3. Estimated DDL thickness of clays in the MFT of 2L settling columns by treatment and time. Error bars indicate S.E.; n=2 for Initial, 21 d, and 42 d, and n=6 for 82 d. (A) signifies a significant difference between the treatments (B), (b) signifies a significant difference within a treatment from initial values (a), and (*) signifies a significant difference between top and bottom DDL.

The variation in water release and changes in chemistry in Experiment 1 allow for simple linear regression to evaluate the relationship between water release and the estimated DDL thickness. There is a strong negative linear relationship between the estimated DDL thickness and water release, with an R^2 of 0.83 (Figure 5-4) (R-Project, version 2.14.1). There is an even stronger linear relationship between square-root of ionic strength and water release with R^2 of 0.89 (Figure 5-5) (R-Project, version 2.14.1). The square-root of ionic strength was used because the DDL thickness is proportional to the inverse-square-root of ionic strength (Equation 2-5). This shows that there is a strong relationship between the chemical changes in the MFT during methanogenesis and the water

released from the MFT. It is unclear if these chemical changes are the only factor explaining the settling mechanism of accelerated dewatering of MFT, or other pathways are also on work.

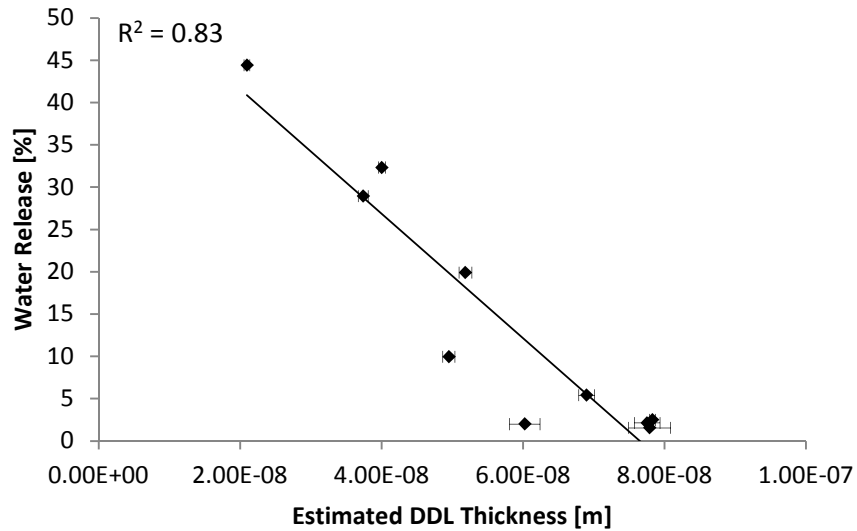


Figure 5-4. Water release versus estimated diffuse double layer thickness of clay in the MFT of 2L settling columns. Error bars indicate S.E., n=4.

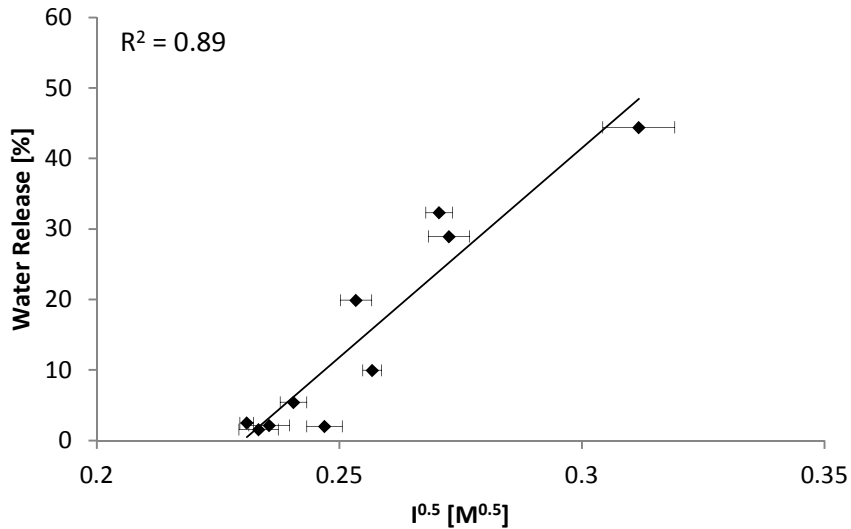


Figure 5-5. Water release versus square root of pore-water ionic strength in the MFT of 2L settling columns. Error bars show S.E., n=4.

If the relationship between water release and estimated DDL thickness was stronger than the relationship between water release and ionic strength, it would be clear that the changes in colloidal chemistry were the driver of settling and dewatering of MFT. As MFT is an aqueous colloidal suspension, clay particles are stabilized by repulsion in the particles due to the clay surface charge potential in the DDL; expanded DDL causes dispersion. Destabilization of colloid suspension can be achieved by increasing ionic strength and increasing the valence of the cations in the DDL which cause the DDL to be suppressed, which allows the clays to flocculate and settle. The valence of the cations in the DDL should have a greater effect on flocculation than ionic strength (Morrison and Ross 2002).

The difference in the strength of relationship of the water release and estimated DDL thickness, and water release and ionic strength may be due to shortcomings in the estimation of the DDL. First, the DDL flocculation theory assumes a constant surface charge on the colloid surface (Morrison and Ross 2002). In Experiment 1, the CECe increases in the amended MFT with increased water release. Second in DDL flocculation theory, the models assume homovalency of the cations (Morrison and Ross 2002), whereas the MFT is a system with a heterovalency. The Z of the DDL of the MFT was assumed to be the mean Z of the exchangeable cations, this assumption maybe a source of error in the estimation of the DDL thickness. The variance in CECe and the estimation of Z may explain why Ionic strength alone had a stronger relationship with water release than the estimated DDL thickness.

5.3. Evaluation of the Proposed Chemical Pathway for Accelerated Dewatering of MFT

The results of the investigation show that the microbial community in the MFT induces chemical changes during methanogenesis. The chemical changes in the MFT, in most cases, supports the hypothesized chemical pathway of accelerated dewatering of MFT (Figure 2-4). The changes in chemistry of the

amended MFT along with their support for the chemical pathway are summarized below.

The first step in the pathway is the enhanced production of biogenic gases by the microbial community. This step was evident in the experiments performed in this investigation. This result is not surprising as methanogenesis coupled to densification of MFT has been previously reported (Fedorak et al. 2000, Foght et al. 2010, and Li 2010).

The second step in the pathway is dissolution of CO₂ produced by the microbial community resulting in an increase in pore-water HCO₃⁻ and lowering of the pH. In Experiment 1 during incubation, there was an increase in pore-water HCO₃⁻, and a smaller than expected decrease in pH. In Experiment 2, there were both an increase in pore-water HCO₃⁻ and a corresponding decrease in pH. An increase in HCO₃⁻ in MFT undergoing methanogenesis coupled to densification has been previously reported (Fedorak et al. 2000; Li 2010). Li (2010) also reported a decrease in pH.

Zhu et al. (2011) reported increased densification of CNRL and Sycrude tailings with the addition of CO₂. The direct addition of CO₂ induced similar pore-water chemical changes as methanogenesis, lowering of pH and increase concentrations. Suggesting similar accelerated dewatering could be achieved without methanogenesis. It is difficult compare the effectiveness of CO₂ treatment to methanogenic accelerated dewatering because the Zhu et al. 2011 experiment was performed using whole tailings and methanogenic accelerated dewatering was performed on MFT.

The third step is the dissolution of carbonate minerals, resulting in the release of Ca²⁺ and Mg²⁺ in the MFT pore-water. In Experiment 2, the dissolution of carbonate minerals was evident, and in Experiment 1 the carbonate mineral content was not determined. In both Experiments 1 and 2, there was a clear increase in pore-water Mg²⁺. Pore-water Ca²⁺ increased in Experiment 2, while in

Experiment 1, the pore-water Ca^{2+} increased in both the amended MFT and the unamended control.

In the fourth step, the released Ca^{2+} and Mg^{2+} replaced Na^+ on the exchange surfaces in the MFT through exchange reactions. In Experiment 1, the exchangeable cations were determined showing that the exchangeable Ca^{2+} and Mg^{2+} did increase, however there was not a corresponding decrease in exchangeable Na^+ . This lead to an unexpected increase in CECe.

In the fifth step, the increase in exchangeable divalent cations, Ca^{2+} and Mg^{2+} , along with an increase in pore-water ionic strength leads to a suppression of the DDL thickness causing flocculation, settling and dewatering of MFT. The increase in ionic strength was evident in both experiments. While in Experiment 1, there was an increase in divalent exchangeable cations resulting in an increase in Z_{μ} . The increase in ionic strength and Z_{μ} resulted in a significant decrease in DDL thickness.

6. Conclusion

To meet tailings management goals, the oil sand industry needs new technologies and processes to treat the fluid fine tailings. Methanogenic accelerated dewatering is a potential process to recover entrained pore-water from fluid fine tailings to be recycling back into processing operations and densify tailings for reclamation activities. The changes in chemistry in MFT undergoing methanogenic accelerated dewatering were analyzed in 2L bench scale settling columns (Experiment 1) and 50L settling columns (Experiment 2). Carbon amendments sodium acetate (Experiment 1) and hydrolyzed canola meal (Experiment 2) were used to enhance microbial activity and methanogenesis as the experimental treatment, and in both experiment unamended columns were used as baseline controls.

In Experiment 1, the acetate amended columns over 82 day incubation recovered a mean of 31.07 % of initial pore-water as released cap-water, versus a mean of 3.33% for the unamended control. Over the incubation period, the acetate columns had slight decrease in pore-water pH and a significant increase in pore-water HCO_3^- , and the unamended control remained unchanged. The acetate columns had an increase in pore-water Ca^{2+} and Mg^{2+} . The exchangeable cations in the acetate columns also change during incubation, with an increase in exchangeable Ca^{2+} and Mg^{2+} and a decrease in exchangeable Na^+ . The unamended control has no significant changes in pore-water chemistry nor in exchangeable cations. The increase in pore-water ionic strength and the changing composition of exchangeable cations during methanogenesis causes the double diffusion layer of the suspended fines to shrink, which leads to flocculation and settling, which in turns, leads to the water recovery.

In experiment 2, after 212 days of incubation the canola amended column released 34.55 % of its initial pore-water as cap water, versus 25.44 % for unamended control. During incubation, there was a significant decrease in pH in the canola columns versus the unamended control. At day 212 the columns were sampled for chemical analysis showing that the canola columns had higher pore-

water HCO_3^- , Ca^{2+} and Mg^{2+} . Analysis of the solids showed that the canola amended column had a lower carbonate content than the unamended column, suggesting that dissolving carbonates is the source of the pore-water Ca^{2+} and Mg^{2+} .

The hypothesized chemical mechanism of methanogenic dewatering involves five steps, each step with the evidence supporting evidence summarized below:

- 1) Biodegradation of an organic substrate leading to acetoclastic methanogenesis. The GC analysis of the release biogases produced in Experiment 2 confirmed the production of CH_4 and CO_2 .
- 2) Dissolution of the biogenic CO_2 as carbonic acid producing HCO_3^- and H^+ , lowering the pH of the pore-water and increasing its ionic strength. The step was evident as both experiments had significant increases in pore-water HCO_3^- . Experiment 2 had a significant decrease in pH in the canola amended column. Experiment 1 only had a slight decrease in pH in the acetate treated column.
- 3) The lowering pH of the pore-water causes dissolution of carbonate minerals such as calcite (CaCO_3) and dolomite ($\text{CaMg}(\text{CO}_3)_2$) releasing Ca^{2+} and Mg^{2+} into solution. The decrease in carbonate minerals was evident in experiment 2. The increase in Ca^{2+} and Mg^{2+} was evident in both experiments.
- 4) The release Ca^{2+} and Mg^{2+} exchange with Na^+ in the cation exchange complex of the clays. This was evident in experiment 2, as exchangeable Ca^{2+} and Mg^{2+} increased and Na^+ decreased in the acetate amended columns over the 82 day incubation period.
- 5) The changing composition of cations in the exchange complex and the increased ionic strength of the pore-water cause a decrease in the double diffusion layer of the suspended clay particles in the MFT leading to flocculation, settling and water release. In experiment 1, the estimated double diffusion layer thickness of the acetate amended MFT decreased

significantly over the 82 day incubation period. In experiment 1, there was a strong correlation between water release and estimated double diffusion layer thickness and a very strong correlation between water release and ionic strength.

These results indicate that the chemical changes in the MFT during methanogenic accelerated dewatering contribute to the enhanced settling and water release. This indicates that methanogenic accelerated dewatering is a beneficial process that can improve tailings management in the oil sands industry. The two main goals of tailings management is to densify the MFT and recover water from the MFT to recycling back into oil sands processing. Methanogenic accelerated dewatering can be a technology that contributed to the achievement of both goals. In comparison to other current dewatering processes methanogenic accelerated dewatering is a better option because it produces water suitable for reuse unlike chemical flocculent additives, it is less energy intensive than centrifuge based processes and addresses both tailing management challenges unlike processes like thin layer disposal. Another potential densification process is treating tailings with CO₂ injection; this process relies on similar chemical changes as methanogenic accelerated dewatering (Zhu et al. 2011). CNRL at the Horizon Oil Sand Mine is currently undertaking a pilot project using CO₂ injection. At this time is not clear which would be the better option. The negative externality of methanogenic accelerated dewatering, production of methane, can be mitigated by performing this process in a bioreactor to capture methane to be recycled into the natural gas generators used on site. Methanogenic accelerated dewatering is not a totally solution for tailings management, but would integrate into the suite of tailings management technologies that will be needed for the future of oil sands tailings management.

7. References

- Adeyinka, O. B., Samiei, S., Xu, Z., and Masliyah, J. H. (2009). Effect of particle size on the rheology of Athabasca clay suspensions. *The Canadian Journal of Chemical Engineering*, 87, 3, 422-34.
- Alberta Energy. (2011). About Oil Sands. Alberta Energy, Edmonton Alberta. www.energy.gov.ab.ca
- Bailey, S. W. (1980). Summary of recommendations of AIPEA Nomenclature Committee. *Clay Minerals*, 15(1), 85-93.
- Bayliss, P., and Levinson, A.A. (1976). Mineralogical review of the Alberta oil sand deposits (Lower Cretaceous, Mannville Group). *Bulletin of Canadian Petroleum Geology*, 24 (2): 211–224.
- Boone, D. R. (1982). Terminal Reactions in the Anaerobic Digestion of Animal Waste. *Applied Environmental Microbiology*, 43(1), 57-64.
- BGC Engineering Inc. (2010). Oil Sands Tailings Technology Review. Oil Sands Research and Information Network, University of Alberta, School of Energy and the Environment, Edmonton, Alberta. OSRIN Report No. TR-1. 1-136.
- Burdige, D. J. (1993). The biogeochemistry of manganese and iron reduction in marine sediments. *Earth Science Review*, 35, 249-284.
- Bordenave, S., Ramos, E., Lin, S., Voordouw, G., Gieg, L., Guo, C., and Wells, S. (2009). Use of Calcium Sulfate to Accelerate Densification while Reducing Greenhouse Gas Emissions from Oil Sands Tailings Ponds. *Proceedings of the Canadian International Petroleum Conference*, 1-5.
- Canadian Association of Petroleum Producers (2010). About Canada's Oil Sands. Calgary Canada. www.capp.ca
- Carter, M.R. (1993). *Soil sampling and Methods of Analysis*. Canadian Society of Soil Science. Lewis Publicers, Canada.
- Chalaturnyk, R. J., Don Scott, J., and Özüim, B. (2002). Management of Oil Sands Tailings. *Petroleum Science and Technology*, 20(9-10), 1025-1046.

- Dean, E.W. and Stark D.D. (1920). A Convenient Method for the Determination of Water in Petroleum and Other Organic Emulsions. *Industrial and Engineering Chemistry*, 12(5).
- Dusseault, M.B, Sacfe D.W., and Scott, J.D. (1989). Oil sands mine waste management: Clay mineralogy, moisture transfer and disposal technology, *AOSTRA Journal of Reaearch*, 5, 303-320.
- Energy Resource Conservation Board. (2009). Directive 074: Tailings performance criteria and requirements for oil sands mining schemes. Energy Resource Conservation Board, Calgary, Canada.
- Eckert, W. F., Masliyah, J. H., Gray, M. R., and Fedorak, P. M. (1996). Prediction of sedimentation and consolidation of fine tails. *AIChE Journal*, 42(4), 960-972.
- Fedorak P.M., Coy D.L., Dudas M.J., Renneberg A.J., and Salloum M.J., 2000. Role of Microbiological Processes on Sulfate-enriched Tailings Deposits. Department of Biological Sciences. University of Alberta. Edmonton. Alberta.
- Fedorak, P., Coy, D., and Dudas, M. (2003). Microbially-mediated fugitive gas production from oil sands tailings and increased tailings densification rates. *Journal of Environmental Engineer Science*, 2, 199-211.
- Foght, J.M., Fedorak, P.M., Westlake, D.W.S., and Boerger, H.J. 1985. Microbial content and metabolic activities in the Syncrude tailings pond. *AOSTRA J. Res.*, 1, 139- 146.
- Foght, J.M., Bressler, D., Cardenas, M., Fedorak, P.M., Guigard, S., Gupta, R., and Siddique, T. (2010). Microorganisms in oil sands tailings pond influence the properties and behavior of mature fine tailings (MFT). *Proceedings of the International Oil Sands Tailings Conference*, 393-396.
- Fine Tailings Fundamentals Consortium (1995). *Advances in Oil Sands Tailings Research*. Alberta Department of Energy. Oil Sands and Research Division. Edmonton. Alberta.
- Holden, A., Donahue, R. B., and Ulrich, A.C. (2011). Geochemical interactions between process-affected water from oil sands tailings ponds and North Alberta surficial sediments. *Journal of contaminant hydrology*, 119(1-4), 55-68.

- Holowenko, F. M., MacKinnon, M. D., and Fedorak, P. M. (2000). Methanogens and sulfate-reducing bacteria in oil sands fine tailings waste. *Canadian journal of microbiology*, 46(10), 927-937.
- Horn, M. A., Matthies, C., Kusel, K., Schramm, A., and Drake, H. L. (2003). Hydrogenotrophic Methanogenesis by Moderately Acid-Tolerant Methanogens of a Methane-Emitting Acidic Peat. *Applied and Environmental Microbiology*, 69(1), 74-83.
- Kaminsky, H. W., Etsell, T. H., Ivey, D. G., and Omotoso, O. (2009). Distribution of clay minerals in the process streams produced by the extraction of bitumen from Athabasca oil sands. *The Canadian Journal of Chemical Engineering*, 87(1), 85-93.
- Kaminsky, H.W. (2008). Characterization of an Athabasca oil sands ore and process streams. Ph.D. Thesis. University of Alberta, Canada.
- Kaminsky, H.W. (2011). Introduction to clay mineralogy in oil sands. 2nd CONRAD Clay Workshop, Edmonton, AB.
- Kasperski, K.L. (1992) A review of properties and treatments of oil sands tailings. *AOSRTA Journal of Research*, 8, 11-53.
- Kopittke, P. M., So, H. B., and Menzies, N. W. (2006). Effect of ionic strength and clay mineralogy on Na:Ca exchange and the SAR:ESP relationship. *European Journal of Soil Science*, 57(5), 626-633.
- Kusel, K., and Drake, H. L. (1994). Acetate Synthesis in Soil from a Bavarian Beech Forest. *Applied Environmental Microbiology*, 60(4), 1370-1373
- Lay, J. J., Li, Y. Y., and Noike, T. (1998). Interaction between homoacetogens and methanogens in lake sediments. *Journal of Fermentation and Bioengineering*, 86(5), 467-471
- Li, C. (2010). Methanogenesis in oil sands tailings: An analysis of the microbial community involved and its effects on tailings densification. M.Sc. Thesis. University of Alberta, Canada.
- List, B. R., and Lord, E. R. F. (1997). Syncrude's tailings management practices from research to implementation. *CIM Bulletin*, 90, 39-44.
- Mikula, R. J., Zrobok, R., and Omotoso, O. (2004). The Potential for Carbon Dioxide Sequestration in Oil Sands Processing Streams. *Journal of Canadian Petroleum Technology*, (3), 48-52.

- Lou, Gengxin. (2004). Investigation of CT Beneath MFT Deposition for Oils Sands Tailings Disposal. M.Sc. Thesis. University of Alberta, Canada.
- Mitchell, J. K. (1976). Fundamentals of soil behaviors. John Wiley and Sons Inc, New York, USA.
- Morrison, I.D., and Ross, S. (2002). Colloidal Dispersions.
- Omotoso, O. (2011). Characterization of clays in oil sands. 2nd CONRAD Clay Workshop, Edmonton, AB.
- Penner, T. J., and Foght, J. M. (2010). Mature fine tailings from oil sands processing harbour diverse methanogenic communities. Canadian Journal of Microbiology, 56, 459-470.
- R-Project (2011). R Statistical Language (Version 2.14.1). Toronto, Canada.
- Rayment, G. E. and Lyons, D. J. (2010). Soil Chemical Methods: Australasia. CSIRO Publishing Collingwood, Australia.
- Roberts, D.J. (2002). Methods for assessing anaerobic biodegradation potential. Manual of Environmental Microbiology, 2ed. ASM Press, Washington USA, 1008-1017.
- Salloum, M. J., Dudas, M. J., and Fedorak, P. M. (2002). Microbial reduction of amended sulfate in anaerobic mature fine tailings from oil sand. Waste Management and Research, 20(2), 162-171.
- Sayles, F. L., and Mangelsdorf, P. C. (1977). The equilibration of clay minerals with seawater : exchange reactions. Geochimica et Cosmochimica Acta, 41, 951-960.
- Schramm, L. L., Stasiuk, E. N. and MacKinnon, M. (2000). Surfactants: Fundamentals and Applications in the Petroleum Industry. Press Syndicate of the University of Cambridge, Cambridge, UK.
- Scott, J.D. and Jeeravipoolvarn, S. (2004) Evaluation of particle size distribution test methods for Albian Sands tailings. Albian Sands Energy Inc, Calgary, Canada.
- Siddique, T., Penner, T., Semple, K., and Foght, J. M. (2011). Anaerobic biodegradation of longer-chain n-alkanes coupled to methane production in oil sands tailings. Environmental science and technology, 45(13), 5892-9.

- Siddique, T., Gupta, R., Fedorak, P. M., MacKinnon, M. D., and Foght, J. M. (2008). A first approximation kinetic model to predict methane generation from an oil sands tailings settling basin. *Chemosphere*, 72(10), 1573-80.
- Siddique, T., Fedorak, P. M., MacKinnon, M. D., and Foght, J. M. (2007). Metabolism of BTEX and naphtha compounds to methane in oil sands tailings. *Environmental science and technology*, 41(7), 2350-6.
- Siddique, T., Fedorak, P. M., and Foght, J. M. (2006). Biodegradation of short-chain n-alkanes in oil sands tailings under methanogenic conditions. *Environmental science and technology*, 40(17), 5459-64.
- Srodon, J. (1999). Nature of mixed-layer clays and mechanisms of their formation and alteration. *Annual Review of Earth and Planetary Sciences*, 27, 19-53.
- Suthaker, N.N. (1995). *Geotechnics of Oil Sand Fine Tailings*. Ph.D. Thesis. University of Alberta, Canada.
- Tan, K.H. (2010). *Principals of Soil Chemistry*. 4th ed. CRC Press Boca Raton, USA.
- Tang, J. (1997) *Fundamental Behavior of Composite Tailings*. M.Sc. Thesis. University of Alberta, Edmonton, Canada.
- Tucker, B. (1985). A proposed new reagent for the measurement of cation exchange properties of carbonate soils. *Australian Journal of Soil Research*, 23, 633-42.
- Wu, S., Feng, X., and Wittmeier, A. (1997). Microwave Digestion of Plant and Grain Reference Materials in Nitric Acid or a Mixture of Nitric Acid and Hydrogen Peroxide for the Determination of Multi-elements by Inductively Coupled Plasma Mass Spectrometry. *Journal of Analytical Atomic Spectrometry*, 12, 797-806.
- Zhao, H., Dang-Vu, T., Long, J., Xu, Z., and Masliyah, J. H. (2009). Role of Bicarbonate Ions in Oil Sands Extraction Systems with a Poor Processing Ore. *Journal of Dispersion Science and Technology*, 30(6), 809-822.
- Zhu, R., Liu, Q., Xu, Z., and Masliyah, J. (2011). Role of Dissolving Carbon Dioxide in Densification of Oil Sands Tailings. *Energy and Fuels*, 25, 2049-2057.

Appendix A: AWRI 2 L Settling Columns

Table A-1. Composition of clay minerals in Syncrude MFT clay fractions (<2.0 μm) (Kaminsky et al. 2009).

Clay Mineral	Composition (%)	
	<0.2 μm	0.2-2.0 μm
Chlorite	0	7
Kaolinite-smectite	19	8
Kaolinite	15	34
Illite-smectite	54	25
Illite	13	26

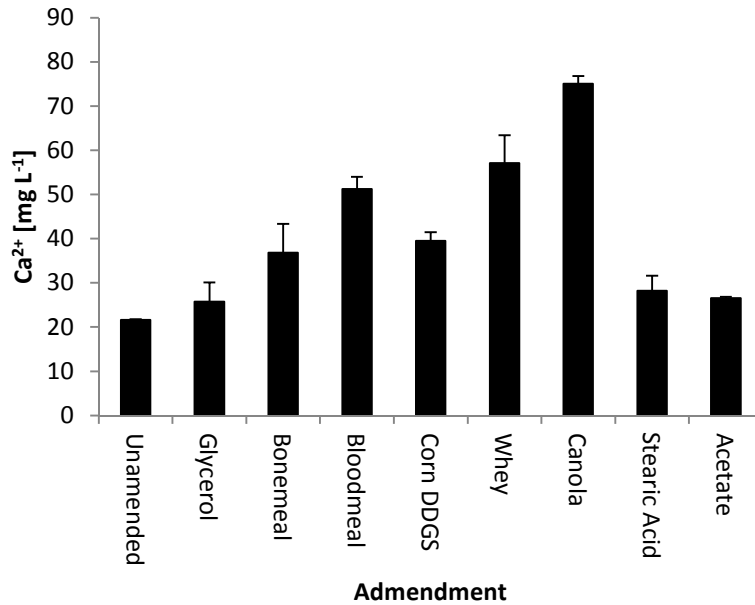


Figure A-1. Pore-water Ca^{+2} of 2L settling columns of Syncrude MFT amended with various carbon substrates at 40 mg L^{-1} , on carbon bases. The columns were incubated for 168 days. Error bars show S.E., $n=2$.

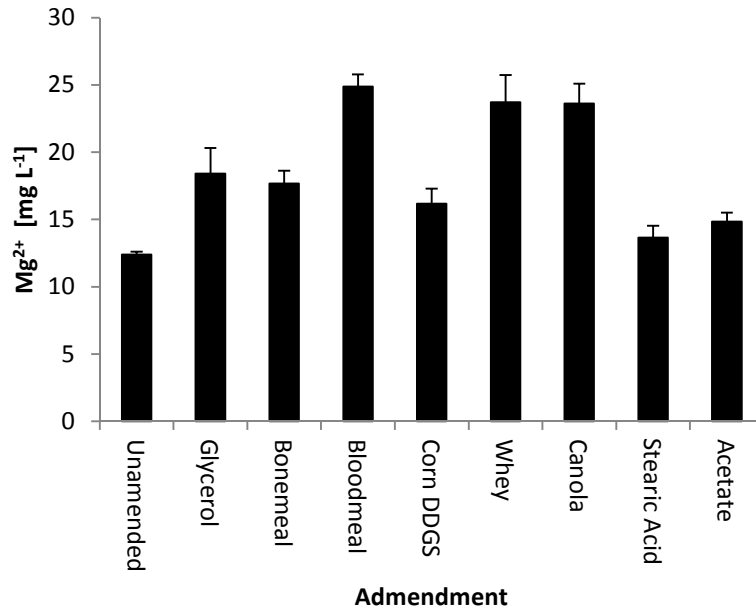


Figure A-2. Pore-water Mg²⁺ of 2L settling columns of Syncrude MFT amended with various carbon substrates at 40 mg L⁻¹, on carbon bases. The columns were incubated for 168 days. Error bars show S.E., n=2.

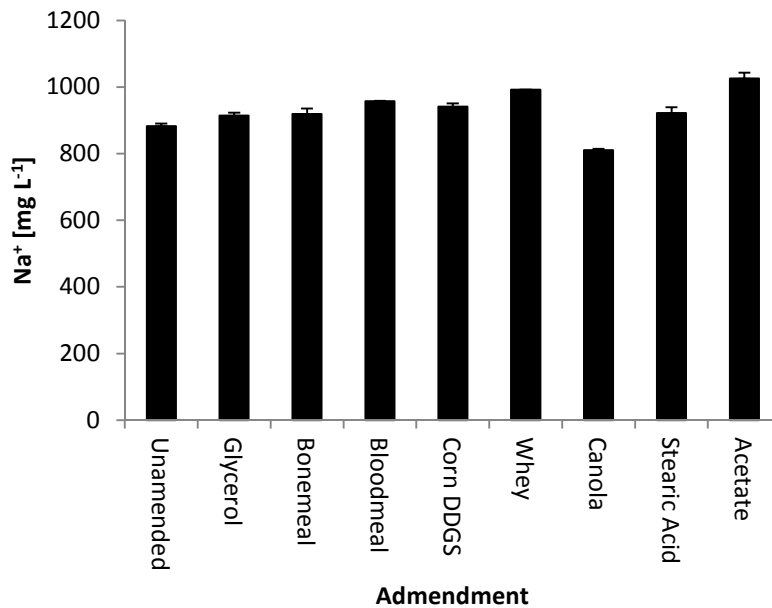


Figure A-3. Pore-water Na⁺ in 2L settling columns with Syncrude MFT amended with various carbon substrates at 40 mg L⁻¹, on carbon bases. The columns were incubated for 168 days. Error bars show S.E., n=2.

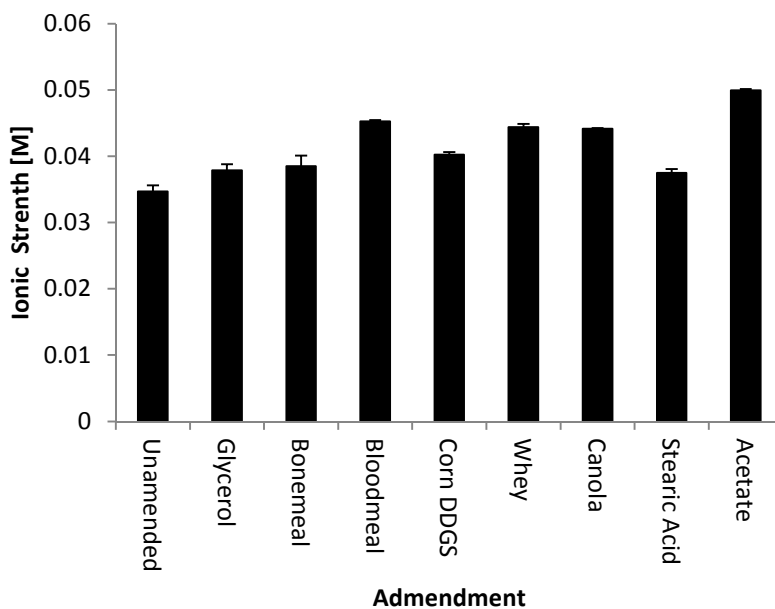


Figure A-4. Pore-water ionic strength of 2 L settling columns of Syncrude MFT amended with various carbon substrates at 40 mg L^{-1} , on carbon bases. The columns were incubated for 168 days. Error bars show S.E., $n=2$.

Appendix B: 2L Settling Columns

Table B-1. Solids Content of samples withdrawn from 2L settling columns of Syncrude MFT.

Column	Solids Content [%]	
	Bottom	Top
Acetate Initial	29.00	
Unamended Initial	25.22	
A2	35.18	28.60
A4	35.18	32.81
A1	33.18	28.02
A5	39.42	35.00
A7	35.45	31.37
U2	27.47	26.45
U4	24.37	18.20
U1	25.21	24.06
U3	37.00	25.31
U5	25.59	27.08

Table B-2. Initial pH of 2L settling columns of Syncrude MFT.

Column	pH
A2	7.68
A4	7.62
A1	7.67
A5	7.61
A7	7.64
U2	7.86
U4	7.02
U1	7.01
U3	7.32
U5	7.33

Table B-3. Pore-water SO_4^{-2} , Cl^- and NH_4^+ concentrations of 2L settling columns of Syncrude MFT.

Time [Days]	Column	Sample Location	Pore-water Concentration [mg L ⁻¹]					
			SO_4^{-2}		Cl^-		NH_4^+	
			Mean	SD	Mean	SD	Mean	SD
0	Amended	Bulk	21.43	0.33	576.00	20.00	9.48	3.16
21	A4	Top	52.98	5.83	493.75	2.25	6.81	1.54
	A4	Bottom	57.90	0.70	529.50	8.75	10.55	5.44
42	A2	Top	59.75	1.20	601.25	7.88	5.01	0.09
	A2	Bottom	57.65	1.15	573.75	1.88	9.75	0.11
82	A1	Top	54.88	1.17	510.13	5.50	5.53	0.72
	A1	Bottom	66.69	1.26	569.00	7.38	9.46	6.80
	A5	Top	56.78	0.13	626.00	23.88	4.65	0.08
	A5	Bottom	65.85	10.45	583.75	26.63	11.24	6.70
82	A7	Top	64.05	15.15	651.00	4.88	11.00	4.45
	A7	Bottom	63.00	1.80	620.00	2.50	9.55	0.02
0	Unamended	Bulk	20.55	1.20	606.00	13.63	6.33	4.60
21	U4	Top	37.15	22.90	770.75	99.50	6.23	0.94
	U4	Bottom	75.93	14.48	893.75	260.64	5.46	0.42
42	U2	Top	22.48	5.63	585.25	2.25	5.56	1.37
	U2	Bottom	12.20	0.20	633.50	3.00	6.17	0.00
82	U1	Top	77.95	25.70	564.23	154.64	7.10	2.10
	U1	Bottom	59.78	6.42	476.00	2.50	3.92	1.11
	U3	Top	55.35	8.15	610.75	28.25	4.83	0.11
	U3	Bottom	25.95	2.50	580.50	47.13	6.64	0.82
82	U5	Top	51.28	1.23	671.75	9.50	5.67	0.38
	U5	Bottom	46.45	8.85	639.75	25.75	6.24	1.50

Table B-4. Pore-water B, Al and Si concentrations of 2L settling columns of Syncrude MFT.

Time [Days]	Column	Sample Location	Pore-water Concentration [mg L ⁻¹]					
			B		Al		Si	
			Mean	SD	Mean	SD	Mean	SD
0	Amended	Bulk	1.523	0.066	1.804	0.060	4.807	0.836
21	A4	Top	8.289	0.158	1.629	0.128	16.326	1.528
	A4	Bottom	8.303	0.189	1.549	0.124	18.010	0.674
42	A2	Top	9.007	0.110	2.803	0.062	24.536	0.082
	A2	Bottom	8.405	0.151	3.190	0.192	24.466	0.155
82	A1	Top	9.042	0.129	1.977	0.050	18.824	0.056
	A1	Bottom	8.523	0.106	1.794	0.009	17.939	0.016
	A5	Top	7.738	0.090	1.986	0.531	18.961	1.430
	A5	Bottom	7.577	0.121	1.716	0.068	20.575	2.535
82	A7	Top	6.616	0.226	1.473	0.051	16.474	0.348
	A7	Bottom	6.929	0.073	1.668	0.219	16.685	0.742
0	Unamended	Bulk	1.516	0.266	1.493	0.128	4.776	1.734
21	U4	Top	2.752	2.171	12.287	3.161	42.916	6.493
	U4	Bottom	6.224	0.360	5.912	3.378	24.843	1.864
42	U2	Top	6.575	0.078	1.987	0.316	20.651	3.103
	U2	Bottom	7.000	0.129	2.002	0.055	22.574	1.400
82	U1	Top	7.391	0.118	3.160	0.023	21.646	0.234
	U1	Bottom	7.174	0.335	4.410	1.272	24.755	3.343
	U3	Top	6.027	0.023	1.866	0.683	5.530	0.007
	U3	Bottom	6.374	0.280	1.032	0.261	18.850	1.976
82	U5	Top	7.509	0.709	5.310	3.989	31.273	6.442
	U5	Bottom	6.176	0.112	1.643	0.026	18.120	0.113

Table B-5. Pore-water Cr, Fe and Mn concentrations of 2L settling columns of Syncrude MFT.

Time [Days]	Column	Sample Location	Pore-water Concentration [mg L ⁻¹]					
			Cr		Fe		Mn	
			Mean	SD	Mean	SD	Mean	SD
0	Amended	Bulk	0.033	0.000	1.178	0.042	0.037	0.002
21	A4	Top	0.015	0.006	1.065	0.113	0.037	0.002
	A4	Bottom	0.026	0.006	0.365	0.317	0.134	0.090
42	A2	Top	0.016	0.002	0.497	0.122	0.056	0.008
	A2	Bottom	0.029	0.009	0.596	0.167	0.060	0.004
82	A1	Top	0.007	0.002	0.940	0.044	0.047	0.000
	A1	Bottom	0.015	0.001	1.277	0.040	0.048	0.013
	A5	Top	0.044	0.001	1.053	0.126	0.047	0.002
	A5	Bottom	0.036	0.005	0.844	0.044	0.042	0.003
82	A7	Top	0.014	0.006	1.229	0.045	0.038	0.006
	A7	Bottom	0.014	0.010	1.095	0.087	0.053	0.008
0	Unamended	Bulk	0.022	0.008	1.280	0.245	0.085	0.005
21	U4	Top	0.013	0.004	2.237	1.428	0.083	0.031
	U4	Bottom	0.036	0.036	0.368	0.043	0.735	0.652
42	U2	Top	0.007	0.004	1.021	0.103	0.066	0.006
	U2	Bottom	0.002	0.002	0.969	0.153	0.083	0.007
82	U1	Top	0.000	0.000	0.997	0.180	0.065	0.004
	U1	Bottom	0.000	0.000	0.965	0.212	0.072	0.012
	U3	Top	0.006	0.005	0.719	0.420	0.097	0.004
	U3	Bottom	0.002	0.002	0.894	0.145	0.080	0.005
82	U5	Top	0.009	0.002	1.119	0.924	0.120	0.048
	U5	Bottom	0.004	0.000	0.665	0.248	0.089	0.011

Table B-6. Pore-water Ni, Co and Cu concentrations of 2L settling columns of Syncrude MFT.

Time [Days]	Column	Sample Location	Pore-water Concentration [mg L ⁻¹]					
			Ni		Co		Cu	
			Mean	SD	Mean	SD	Mean	SD
0	Amended	Bulk	0.014	0.002	0.004	0.001	0.023	0.009
21	A4	Top	0.006	0.000	0.008	0.000	0.028	0.004
	A4	Bottom	0.003	0.000	0.008	0.006	1.404	1.370
42	A2	Top	0.001	0.001	0.003	0.000	0.038	0.004
	A2	Bottom	0.002	0.002	0.019	0.014	0.032	0.004
82	A1	Top	0.000	0.000	0.003	0.000	0.026	0.002
	A1	Bottom	0.000	0.000	0.000	0.000	0.024	0.001
	A5	Top	0.007	0.000	0.002	0.000	0.031	0.003
	A5	Bottom	0.004	0.001	0.032	0.001	1.106	0.648
82	A7	Top	0.004	0.001	0.002	0.001	0.020	0.003
	A7	Bottom	0.003	0.003	0.002	0.000	0.023	0.000
0	Unamended	Bulk	0.001	0.001	0.000	0.000	0.019	0.006
21	U4	Top	0.003	0.001	0.006	0.002	0.025	0.003
	U4	Bottom	0.017	0.013	0.012	0.010	0.045	0.012
42	U2	Top	0.007	0.001	0.002	0.000	0.025	0.001
	U2	Bottom	0.001	0.001	0.003	0.000	0.026	0.000
82	U1	Top	0.000	0.000	0.002	0.002	0.023	0.000
	U1	Bottom	0.000	0.000	0.002	0.002	0.024	0.001
	U3	Top	0.002	0.002	0.002	0.000	0.022	0.000
	U3	Bottom	0.006	0.000	0.002	0.000	0.022	0.002
82	U5	Top	0.008	0.003	0.005	0.001	0.024	0.000
	U5	Bottom	0.003	0.001	0.003	0.001	0.021	0.000

Table B-7. Pore-water Zn, Se and Sr concentrations of 2L settling columns of Syncrude MFT.

Time [Days]	Column	Sample Location	Pore-water Concentration [mg L ⁻¹]					
			Zn		Se		Sr	
			Mean	SD	Mean	SD	Mean	SD
0	Amended	Bulk	0.186	0.184	0.058	0.005	0.528	0.003
21	A4	Top	1.785	0.315	0.023	0.001	0.707	0.080
	A4	Bottom	0.656	0.632	0.115	0.086	0.443	0.437
42	A2	Top	0.817	0.064	0.023	0.003	0.572	0.023
	A2	Bottom	2.087	1.466	0.019	0.000	0.920	0.078
82	A1	Top	0.569	0.017	0.022	0.003	0.544	0.021
	A1	Bottom	0.706	0.264	0.023	0.004	0.785	0.045
	A5	Top	0.208	0.081	0.027	0.000	0.969	0.003
	A5	Bottom	0.001	0.000	0.024	0.000	0.018	0.001
82	A7	Top	0.201	0.075	0.021	0.001	0.679	0.123
	A7	Bottom	0.147	0.010	0.026	0.001	0.958	0.092
0	Unamended	Bulk	0.000	0.000	0.028	0.003	0.443	0.053
21	U4	Top	0.960	0.818	0.025	0.002	0.229	0.184
	U4	Bottom	2.324	0.591	0.025	0.000	0.755	0.089
42	U2	Top	0.250	0.110	0.026	0.001	0.600	0.027
	U2	Bottom	0.238	0.129	0.021	0.002	0.818	0.017
82	U1	Top	0.099	0.001	0.024	0.003	0.735	0.063
	U1	Bottom	0.151	0.051	0.022	0.001	0.793	0.005
	U3	Top	0.492	0.178	0.024	0.002	0.843	0.000
	U3	Bottom	0.749	0.477	0.022	0.002	0.722	0.040
82	U5	Top	7.758	0.027	0.036	0.001	0.697	0.059
	U5	Bottom	3.723	2.896	0.024	0.004	0.632	0.072

Table B-8. Pore-water Mo, Cs and Ba concentrations of 2L settling columns of Syncrude MFT.

Time [Days]	Column	Sample Location	Pore-water Concentration [mg L ⁻¹]					
			Mo		Cs		Ba	
			Mean	SD	Mean	SD	Mean	SD
0	Amended	Bulk	0.048	0.001	0.129	0.006	1.792	0.559
21	A4	Top	0.015	0.001	0.005	0.000	1.250	0.050
	A4	Bottom	0.022	0.000	0.024	0.019	1.364	0.007
42	A2	Top	0.020	0.001	0.004	0.000	1.387	0.019
	A2	Bottom	0.018	0.003	0.022	0.019	1.655	0.136
	A1	Top	0.015	0.001	0.002	0.000	1.327	0.016
	A1	Bottom	0.007	0.000	0.002	0.000	1.485	0.043
82	A5	Top	0.017	0.000	0.002	0.000	1.364	0.015
	A5	Bottom	0.000	0.000	1.335	0.071	0.000	0.000
	A7	Top	0.023	0.010	0.002	0.000	1.146	0.046
	A7	Bottom	0.028	0.004	0.000	0.000	0.002	0.001
0	Unamended	Bulk	0.030	0.012	0.103	0.005	1.439	0.400
21	U4	Top	0.009	0.001	0.005	0.000	0.661	0.031
	U4	Bottom	0.018	0.003	0.006	0.003	0.990	0.184
42	U2	Top	0.003	0.000	0.000	0.000	0.003	0.000
	U2	Bottom	0.014	0.000	0.003	0.000	1.302	0.017
	U1	Top	0.010	0.001	0.003	0.000	1.170	0.032
	U1	Bottom	0.009	0.002	0.003	0.000	1.247	0.045
82	U3	Top	0.008	0.000	0.004	0.000	0.945	0.003
	U3	Bottom	0.012	0.001	0.000	0.000	0.004	0.000
	U5	Top	0.017	0.004	0.002	0.002	0.940	0.047
	U5	Bottom	0.011	0.001	0.003	0.000	0.806	0.034

Table B-9. Pore-water Pb and U concentrations of 2L settling columns of Syncrude MFT.

Time [Days]	Column	Sample Location	Pore-water Concentration [mg L ⁻¹]			
			Pb		U	
			Mean	SD	Mean	SD
0	Amended	Bulk	0.000	0.000	0.007	0.000
21	A4	Top	0.002	0.002	0.001	0.001
	A4	Bottom	0.004	0.000	0.005	0.000
42	A2	Top	0.005	0.000	0.018	0.015
	A2	Bottom	0.005	0.000	0.003	0.000
82	A1	Top	0.000	0.000	0.000	0.000
	A1	Bottom	0.001	0.001	0.001	0.001
	A5	Top	0.002	0.001	0.005	0.000
	A5	Bottom	0.005	0.000	0.005	0.000
82	A7	Top	0.002	0.000	0.004	0.002
	A7	Bottom	0.002	0.000	0.005	0.001
0	Unamended	Bulk	0.000	0.000	0.004	0.002
21	U4	Top	0.013	0.008	0.002	0.000
	U4	Bottom	0.014	0.011	0.003	0.001
42	U2	Top	0.003	0.003	0.005	0.000
	U2	Bottom	0.005	0.000	0.002	0.000
82	U1	Top	0.000	0.000	0.000	0.000
	U1	Bottom	0.000	0.000	0.000	0.000
	U3	Top	0.003	0.000	0.001	0.000
	U3	Bottom	0.000	0.000	0.002	0.000
82	U5	Top	0.004	0.001	0.001	0.000
	U5	Bottom	0.002	0.000	0.001	0.000

Table B-10. Cap-water concentrations of B, Al, Si and Cr in 2L setting columns of Syncrude MFT amended with sodium acetate.

Time [Days]	Column	Cap-water Concentration [mg L ⁻¹]							
		B		Al		Si		Cr	
		Mean	SD	Mean	SD	Mean	SD	Mean	SD
21	A4	1.258	0.097	0.942	0.078	0.896	0.032	0.009	0.001
42	A2	2.860	0.156	5.074	0.287	6.807	2.558	0.036	0.005
	A1	2.838	0.066	2.696	0.024	4.418	0.169	0.013	0.002
82	A5	2.427	0.022	1.118	0.037	4.387	0.295	0.032	0.001
	A7	1.507	0.268	3.148	0.355	5.323	1.007	0.020	0.003

Table B-11. Cap-water concentrations of Fe, Mn, Ni and Co in 2L setting columns of Syncrude MFT amended with sodium acetate.

Time [Days]	Column	Cap-water Concentration [mg L ⁻¹]							
		Fe		Mn		Ni		Co	
		Mean	SD	Mean	SD	Mean	SD	Mean	SD
21	A4	5.113	0.286	0.008	0.007	0.007	0.007	0.002	0.001
42	A2	2.567	0.715	0.007	0.002	0.001	0.001	0.009	0.000
	A1	4.232	0.278	0.010	0.010	0.388	0.380	0.009	0.001
82	A5	4.840	0.380	0.016	0.016	0.008	0.008	0.007	0.001
	A7	5.083	0.319	0.036	0.005	0.003	0.001	0.007	0.001

Table B-12. Cap-water concentrations of Cu, Zn, Se and Sr in 2L setting columns of Syncrude MFT amended with sodium acetate.

Time [Days]	Column	Cap-water Concentration [mg L ⁻¹]							
		Cu		Zn		Se		Sr	
		Mean	SD	Mean	SD	Mean	SD	Mean	SD
21	A4	0.009	0.008	4.116	2.494	0.030	0.004	0.283	0.022
42	A2	0.016	0.005	2.262	0.609	0.057	0.001	0.572	0.006
	A1	0.010	0.000	1.555	0.020	0.026	0.026	0.244	0.221
82	A5	0.037	0.010	7.675	1.764	0.074	0.014	0.625	0.054
	A7	0.004	0.000	1.755	0.302	0.050	0.006	0.387	0.034

Table B-13. Cap-water concentrations of Mo, Cs and Ba in 2L setting columns of Syncrude MFT amended with sodium acetate.

Time [Days]	Column	Cap-water Concentration [mg L ⁻¹]					
		Mo		Cs		Ba	
		Mean	SD	Mean	SD	Mean	SD
21	A4	0.004	0.000	0.156	0.066	28.063	21.708
42	A2	0.007	0.000	0.054	0.019	11.577	6.019
	A1	0.010	0.003	0.025	0.014	5.081	0.034
82	A5	0.007	0.000	0.119	0.046	80.679	30.888
	A7	1.511	1.505	0.101	0.101	12.099	4.663

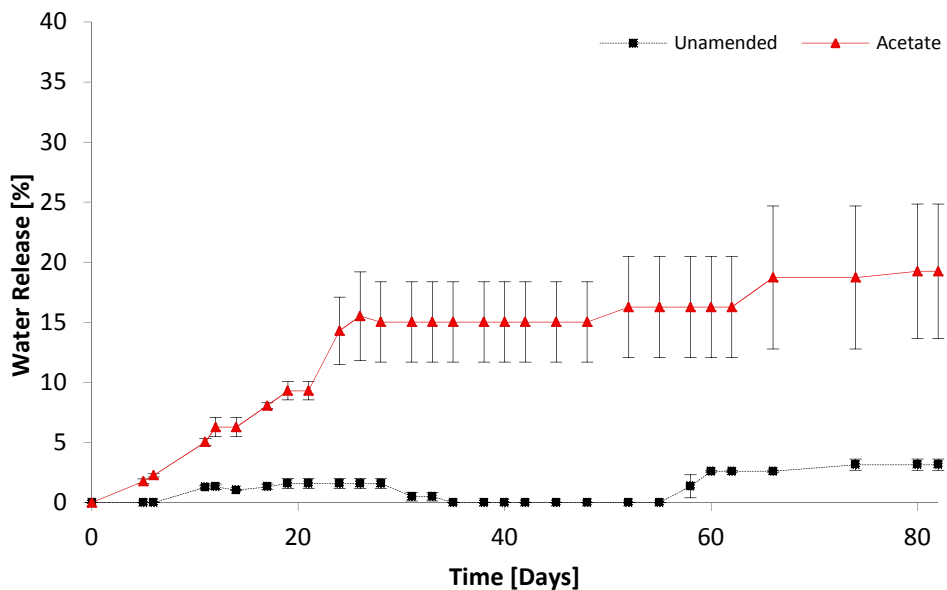


Figure B-1. Water Release of 2 L settling columns of Syncrude MFT by time. pH columns Settling reported as a decrease in solids-cap-water interface in cm from initial height.

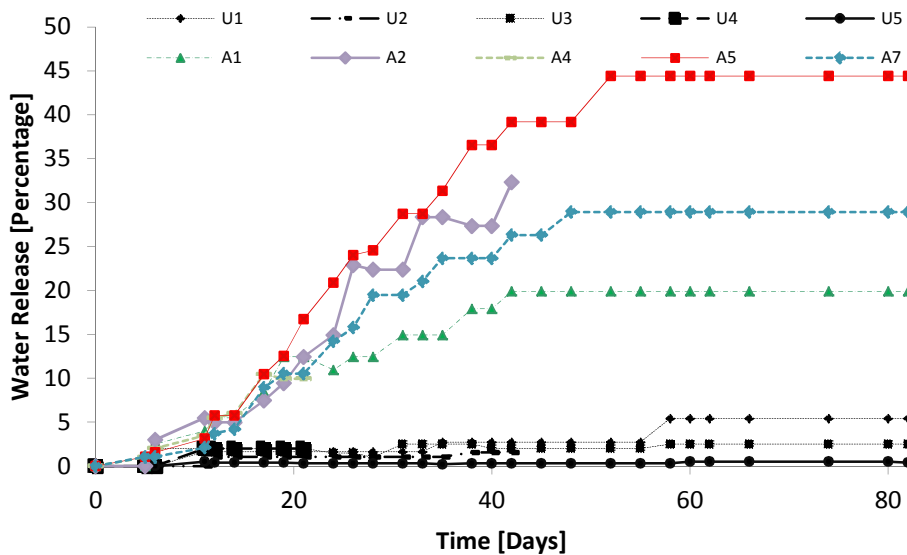


Figure B-2. Water release of 2 L settling columns of Syncrude MFT by time. Settling reported as a decrease in solids-capwater interface in cm from initial height.

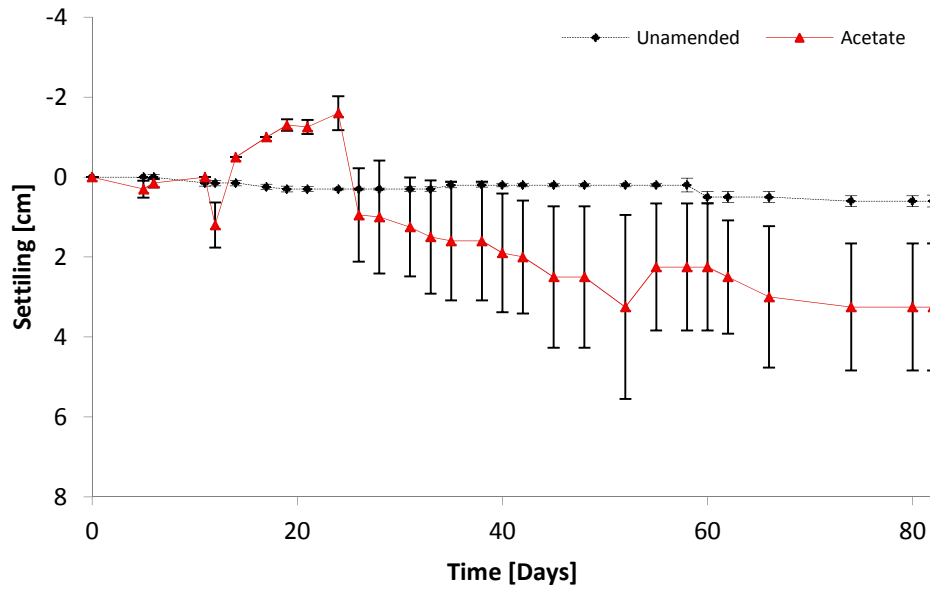


Figure B-3. Settling of 2L settling columns of Syncrude MFT reserved for measurement of in situ pH. Settling is reported as a decrease in solids-cap water interface in cm from initial height. Error bars represent S.E., n=2.

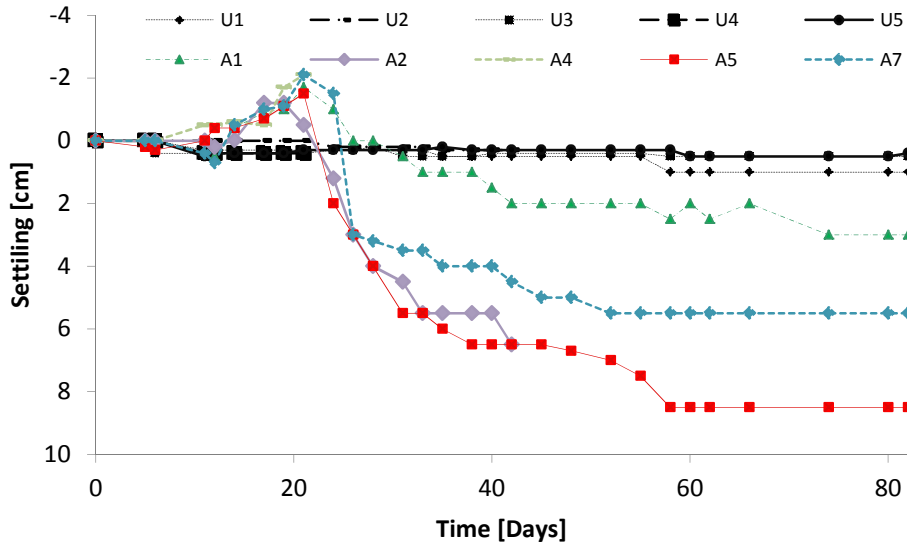


Figure B-4. Settling of 2L settling columns of Syncrude MFT. Settling is reported as a decrease in solids-cap water interface in cm from initial height.

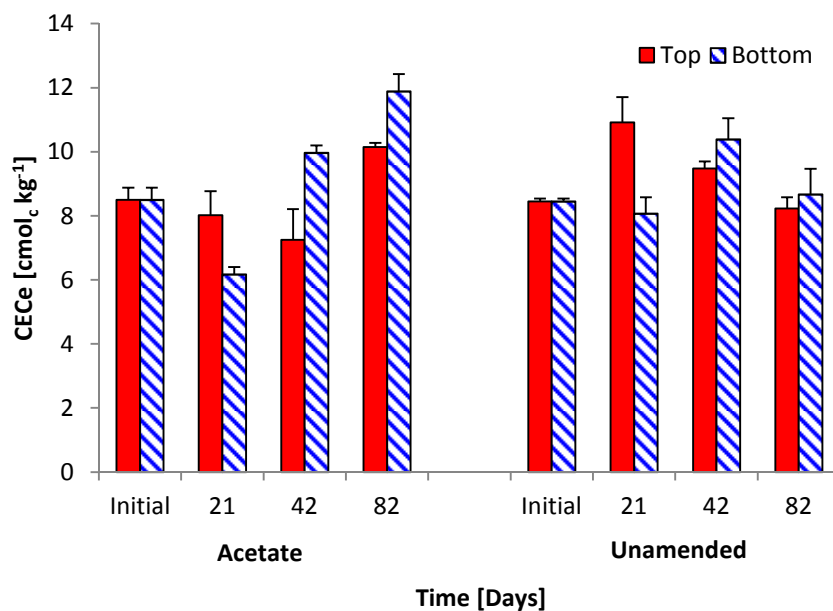


Figure B-5. CEC_e of 2 L settling columns of Syncrude MFT by treatment and time. Error bars show S.E., n=2 for Initial, 21 d, 42 d and n=6 for 82 d.

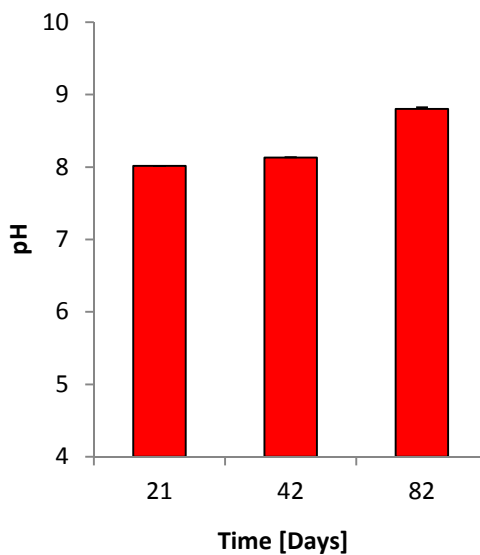


Figure B-6. pH of cap-water released in 2L settling columns of Syncrude MFT amended with sodium acetate. Error bars show S.E., n=2 for Initial, 21 d, 42 d and n=6 for 82 d.

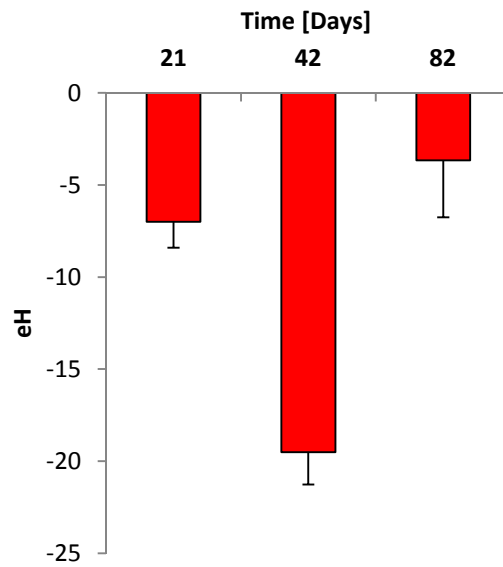


Figure B-7. Eh of cap-water released in 2L settling columns of Syncrude MFT amended with sodium acetate. Error bars show S.E., n=2 for Initial, 21 d, 42 d and n=6 for 82 d.

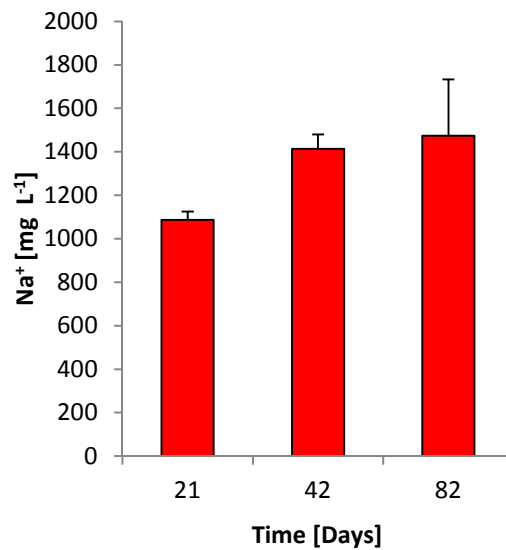


Figure B-8. Na⁺ concentration in cap-water released in 2L settling columns of Syncrude MFT amended with sodium acetate. Error bars show S.E., n=2 for Initial, 21 d, 42 d and n=6 for 82 d.

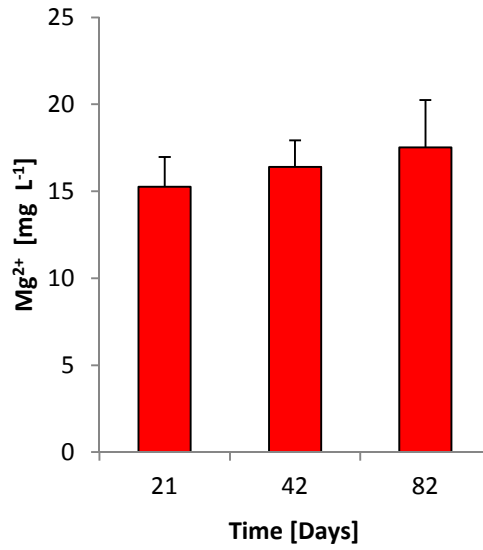


Figure B-9. Mg²⁺ concentration in cap-water released in 2L settling columns of Syncrude MFT amended with sodium acetate. Error bars show S.E., n=2 for Initial, 21 d, 42 d and n=6 for 82 d.

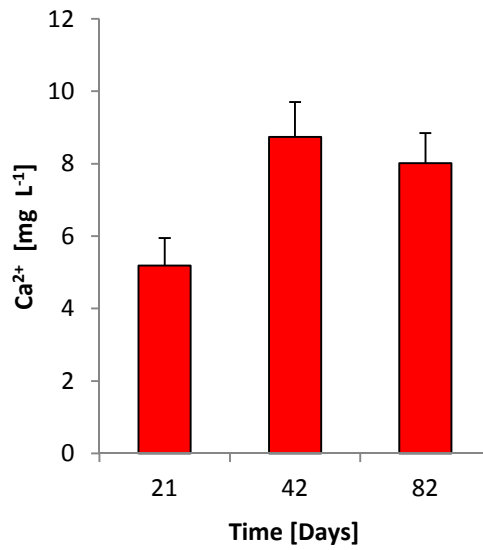


Figure B-10. Ca²⁺ concentration in cap-water released in 2L settling columns of Syncrude MFT amended with sodium acetate. Error bars show S.E., n=2 for Initial, 21 d, 42 d and n=6 for 82 d.

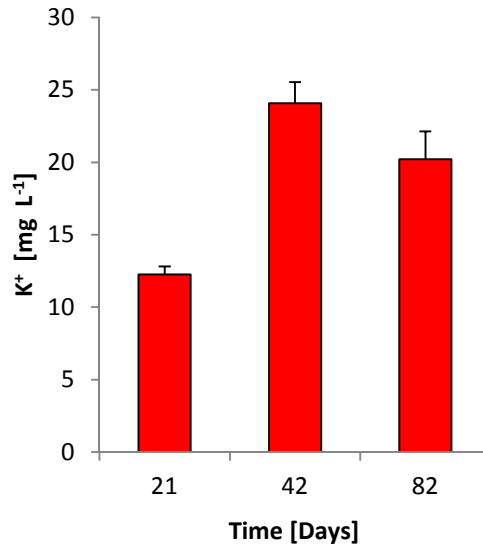


Figure B-11. K⁺ concentration in cap-water released in 2L settling columns of Syncrude MFT amended with sodium acetate. Error bars show S.E., n=2 for Initial, 21 d, 42 d and n=6 for 82 d.

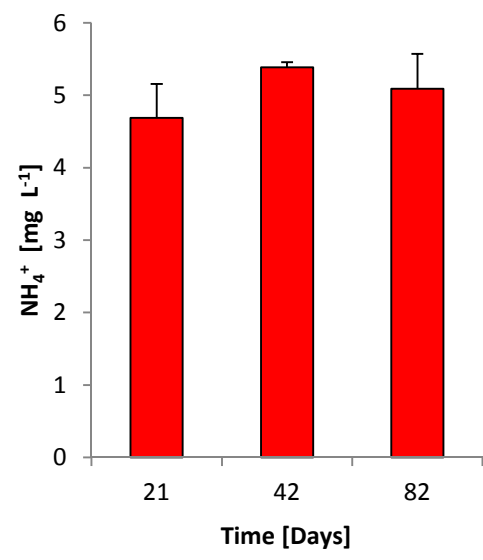


Figure B-12. NH₄⁺ concentration in cap-water released in 2L settling columns of Syncrude MFT amended with sodium acetate. Error bars show S.E., n=2 for Initial, 21 d, 42 d and n=6 for 82 d.

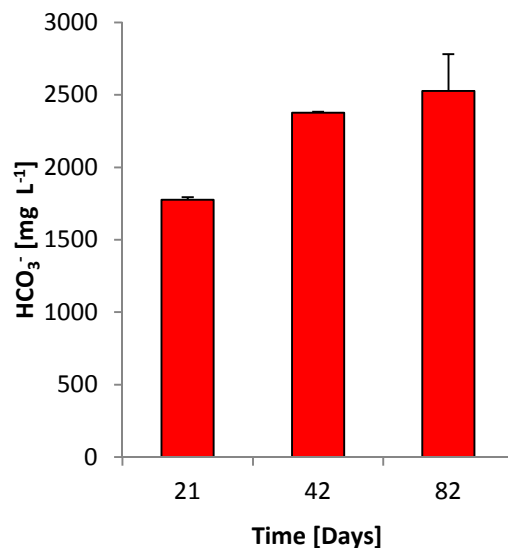


Figure B-13. HCO₃⁻ concentration in cap-water released in 2L settling columns of Syncrude MFT amended with sodium acetate. Error bars show S.E., n=2 for Initial, 21 d, 42 d and n=6 for 82 d.

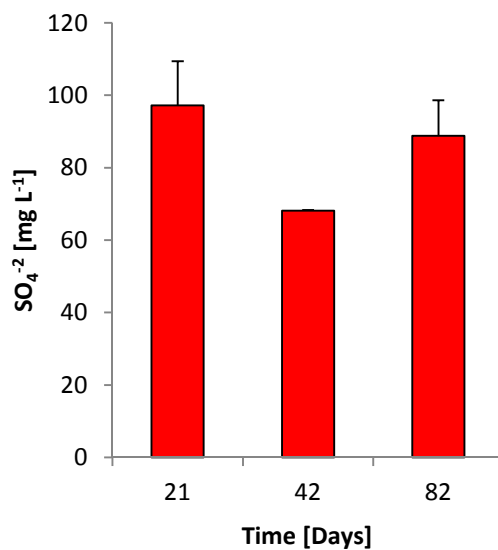


Figure B-15. SO₄⁻² concentration in cap-water released in 2L settling columns of Syncrude MFT amended with sodium acetate. Error bars show S.E., n=2 for Initial, 21 d, 42 d and n=6 for 82 d.

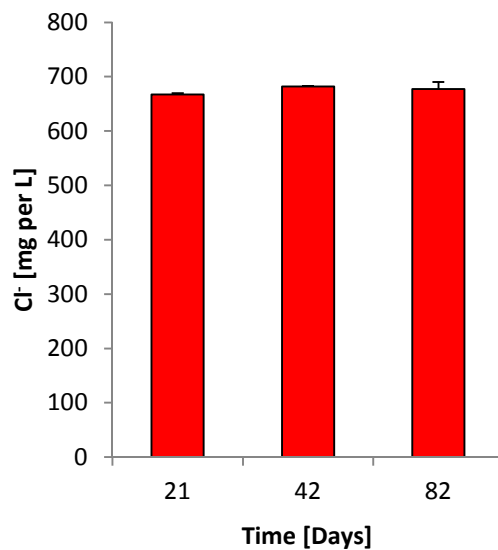


Figure B-15. Cl⁻ concentration in cap-water released in 2L settling columns of Syncrude MFT amended with sodium acetate. Error bars show S.E., n=2 for Initial, 21 d, 42 d and n=6 for 82 d.

Appendix C: 50 L Settling Columns

Table C-1. Select chemical composition of hydrolyzed canola and its contribution to pore-water chemistry in the 50L settling column.

Species	Soluble Fraction of Canola		Contribution to Pore-water	
	Meal [% Mass]	SD	[mg L ⁻¹]	SD
Na ⁺	10.232	1.739	194.029	32.979
K ⁺	0.766	0.014	14.519	0.273
Mg ²⁺	0.105	0.003	1.990	0.062
Ca ²⁺	0.039	0.001	0.735	0.026
Cl ⁻	19.350	0.591	366.925	11.203
SO ₄	0.120	0.007	2.274	0.125
HCO ₃ ⁻	11.245	0.470	213.247	8.918

Table C-2. Elemental analysis of hydrolyzed canola

Element	Percentage Composition
N	4.3
C	27.9
H	4.0
S	0.4

Table C-3. Oil-Water-Solids Content of Syncrude MFT received May 2011 by Dean-Stark analysis

Sample	Content [%]		
	Water	Oil	Solids
Syncrude 2011	60.89	2.46	36.13

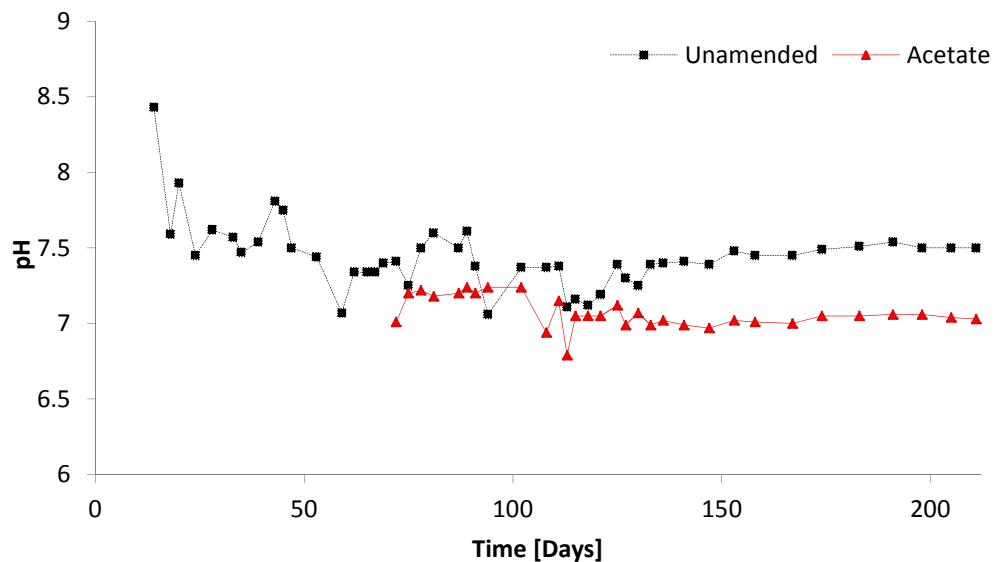


Figure C-1. Cap water pH of 50L Syncrude MFT settling columns. Measured in the top pH port in canola amended and unamended control columns. Incubation time of 213 d.

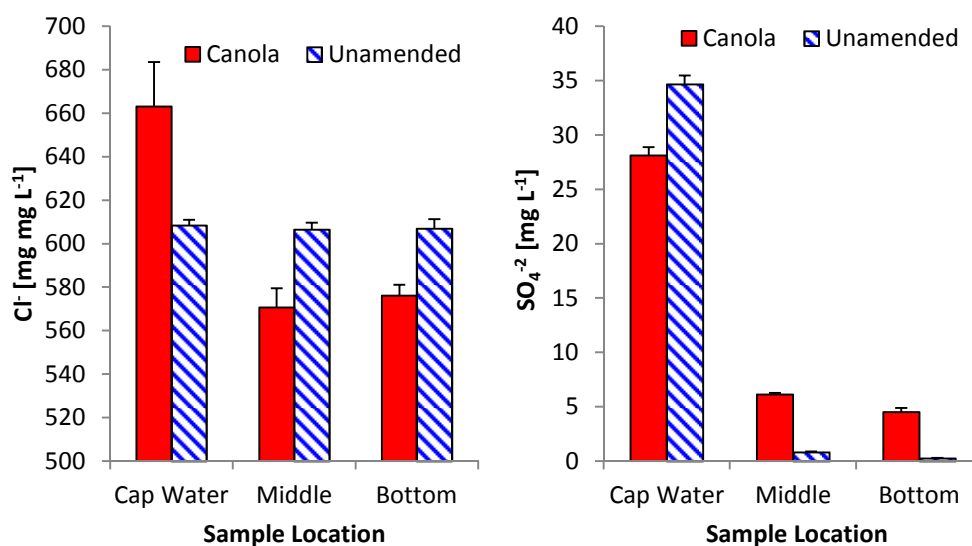


Figure C-2. Cl⁻ and SO₄²⁻ concentrations of MFT pore-water and cap water samples collected from top, middle and bottom ports of canola amended and unamended control 50L MFT settling columns. Incubation time was 212 at time of sampling. Error bars show S.E., n=2.

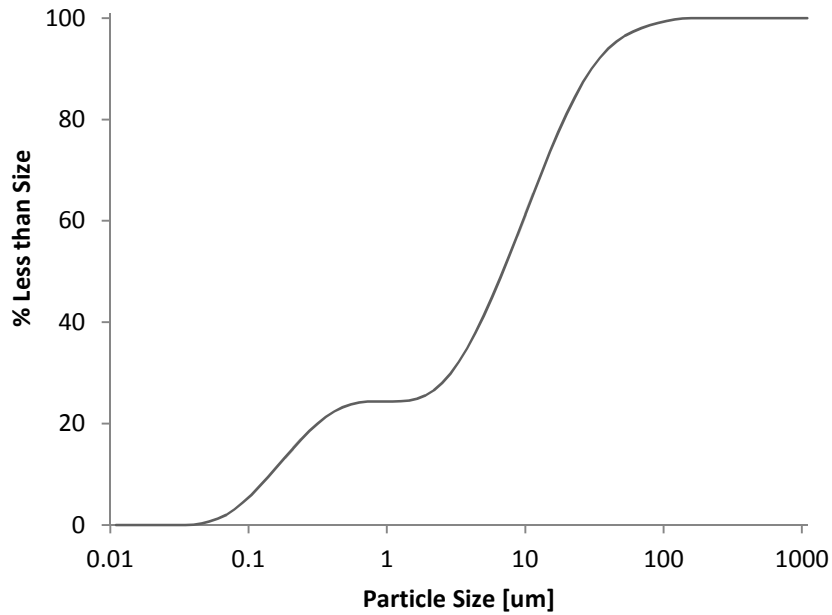


Figure C-3. Particle Size Distribution of Syncrude MFT.

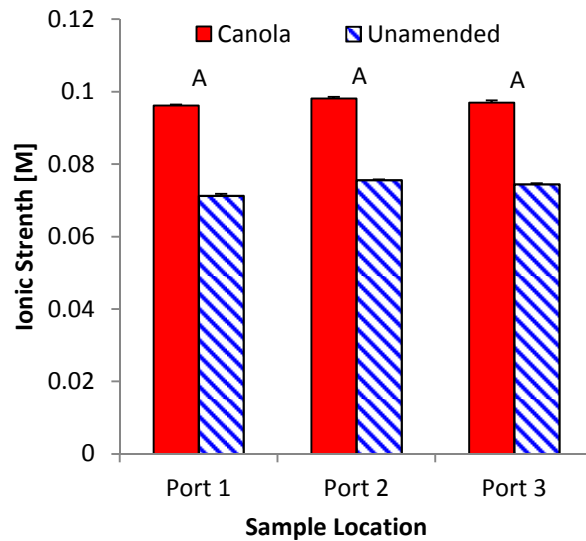


Figure C-4. Ionic Strength of MFT pore-water and cap water samples collected from top, middle and bottom ports of canola amended and unamended 50 L MFT settling columns. Incubation time was 213 d at time of sampling. Error bars show S.E., n=2.